2 mip

139008

THE OPTICAL PUMPING OF ALKALI ATOMS USING COHERENT RADIATION FROM SEMI-CONDUCTOR INJECTION LASERS AND INCOHERENT RADIATION FROM RESONANCE LAMPS

Final Report
July 1, 1973

Partially Supported By

THE GODDARD SPACE FLIGHT CENTER - ADVANCED DEVELOPMENT DIVISION
NATIONAL AERONAUTICS AND SPACE ADMINISTRATION
Contract No. NGR 21-002-218

Prepared By

Gurbax Singh
Associate Professor of Physics
University of Maryland, Eastern Shore
Princess Anne, Maryland

Principal Investigator:

Carroll O. Alley
Professor of Physics
University of Maryland
College Park, Maryland

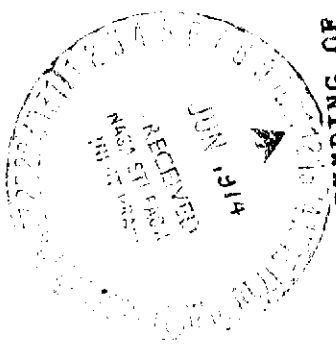

UNIVERSITY OF MARYLAND
DEPARTMENT OF PHYSICS AND ASTRONOMY
COLLEGE PARK, MARYLAND

THE OPTICAL PUMPING OF ALKALI ATOMS USING COHERENT RADIATION FROM SEMI-CONDUCTOR INJECTION LASERS AND INCOHERENT RADIATION FROM RESONANCE LAMPS

Final Report
July 1, 1973

Partially Supported By

THE GODDARD SPACE FLIGHT CENTER - ADVANCED DEVELOPMENT DIVISION
NATIONAL AERONAUTICS AND SPACE ADMINISTRATION
Contract No. NGR 21-002-218

Prepared By

Gurbax Singh
Associate Professor of Physics
University of Maryland, Eastern Shore
Princess Anne, Maryland

Principal Investigator:

Carroll O. Alley
Professor of Physics
University of Maryland
College Park, Maryland

GENERAL CONTENTS

ABSTRACT iii

LIST OF PUBLICATIONS vi

ACKNOWLEDGMENTS vii

THE REPORT IS ORGANIZED INTO TWO PARTS, EACH PART HAVING ITS OWN DETAILED TABLE OF CONTENTS. ONLY THE TITLES OF THE CHAPTERS CONTAINED IN THE TWO PARTS ARE LISTED BELOW.

PART ONE

STUDY OF GALLIUM ARSENIDE JUNCTION LASERS TO OPTICALLY PUMP THE GROUND STATE HYPERFINE LEVELS OF CESIUM-133

I. General Discussion 1

II. Properties of the GaAs Lasers 11

III. Operation of the GaAs Lasers 21

IV. Observations On The GaAs Laser Induced Population Inversion In The Ground State Hyperfine Levels of Cs^{133} 35

References 47

PART TWO

OPTICAL PUMPING STUDIES OF ALKALI VAPORS AND PHASE DESTRUCTION DETECTION OF GROUND STATE HYPERFINE TRANSITIONS IN CESIUM-133

I. General Discussion 1

II. Theory of Optical Orientation and detection 12

III. Phase Destruction Method and Light Shifts 20

IV. Enhancement of Optical Signals 28

V. Instrumentation 35

VI. Construction of The Pulsed Cesium Resonance Lamp 58

VII. Preparation of Wall-Coated Cesium Vapor Cells 65

VIII. Detection of Hyperfine Resonances of Cs-133 By The Method of Phase Destruction 73

APPENDIX EFFECT OF A ROTATING MAGNETIC FIELD PULSE ON A PURE QUANTUM STATE $|F, \mu\rangle$ 91

REFERENCES 96

REPRINTS OF PUBLISHED PAPERS

ABSTRACT

The motivation of the present investigation was to carry out an experimental study of several different processes with a view toward creating population differences in the ground states of alkali atoms. (Cesium-133 was specifically studied but the techniques developed are equally applicable to other alkali atoms). Such studies may eventually lead to the development of cell-type Cesium atomic frequency standards and cesium masers. Both GaAs diode lasers and RF excited resonance lamps were used for the present work. This report is accordingly divided into two major parts.

Part one describes the details of the studies made on GaAs-junction lasers and the achievement of population inversions among the hyperfine levels in the ground state of Cs^{133} by optically pumping it with radiation from a GaAs diode laser. The laser output was used to monitor the populations in the two ground state hyperfine levels as well as to perform the hyperfine pumping.

By varying the injection current, a GaAs laser, operated CW at about $77^{\circ}K$, was used to scan the $8521^{\circ}A$ line of Cs^{133}. The intensity of the resonance scattering from cesium vapor served as an indicator of the populations of the two levels involved. Experiments were performed both with neon-filled and with paraflint-coated cells containing the cesium vapor. The Doppler broadened and

pressure broadened line width of cesium in the neon-filled vapor cell at 100 Torr was found to be 1300MHz for the D_2-transition.

It was discovered that the diode laser could ealily be tuned by manually adjusting the injection current to match either of the hyperfine components of the D_2 optical transition. The laser mode could be held on either component for up to a few seconds by manually controlling the current. This indicates that automatic locking should be easily possible and practical.

Possible future applications, including a re-study of light shifts, the construction of a cesium maser, and the physics of optical pumping with coherent light are discussed.

Part two describes the details of the investigations which were made for the development of the triple reasoance coherent pulse technique for the creation of population differences among the ground state levels in cesium-133 and for the detection of the microwave induced hyperfine trasistions by destroying the phase relationships between the various ground state levels produced by a radio frequency (Zeeman) pulse.

Using this method we have successfully detected the hyperfine resonances of the ground state of Cs-133. In addition, we have succeeded in making paraflint wall-coated Cs-133 vapor cells with very long relaxation times for optically pumped alkali atoms. (Relaxation

times over 250ms have been observed in 2.5" diameter cells.) Moreover, these cells have been found to be very stable and have not shown any detectable deterioration even after a period of one & a half years.

A 'pulsed Cesium resonance lamp' which was essential for the success of the coherent pulse technique, was also developed. It is well known that the rf discharge in a conventional vapor lamp begins in an unpredictable way some time after the application of the rf power. The resonance lamp designed and operated by us showed very clean and reproducible switching characteristics and the formerly present time lag did not exist.

Publications

1. A Technique for Preparing Wall Coated Cesium Vapor Cells, Gurbax Singh. P. Dilavore and C.O. Alley, Rev. of Scientific Inst. Vol. 43, Number 9, pp. 1388, sep. 1972.

2. GaAs Laser Induced Population Inversion In The Ground State Hyperfine Levels of Cesium-133, Gurbax Singh, P. Dilavore and C.O. Alley, J. Quantum Electronics, QE-7, #5, 196, (1971).

3. A Pulsed Cesium Spectral Lamp For Optical Pumping Studies, Gurbax Singh and P. Dilavore, Rev. Sci. Inst., Vol. 41, #10, 1516 (1970).

Technical Reports

1. Study of Gallium Arsenide Lasers to Optically Pump the Ground State Hyperfine Levels of Cesium-133, Gurbax Singh, Technical Report No. 71-118, Department of Physics, University of Maryland, College Park, Md. (1971).

2. Optical Pumping Studies of Alkali Vapors and Phase Destruction Detection of Ground State Hyperfine Transitions in Cesium-133, Gurbax Singh, Technical Report No. 71-119, Department of Physics, University of Maryland, College Park, Maryland (1971).

ACKNOWLEDGMENTS

I (G. Singh) wish to express sincere appreciation to Professor Carroll O. Alley for his interest and generous support during this research.

I owe an incalculable debt of gratitude to Dr. Philip Dilavore who has been associated, both mentally and physically, with this research since its earliest stages.

I express my sincere thanks to Mr. Charles C. Packard, Dr. H. F. Quinn and Dr. William H. Culver of IBM Federal System Division, who graciously loaned the Gallium Arsenide Lasers.

I am deeply indebted to Dr. D. G. Currie and Dr. S. K. Poultney for many fruitful discussions. Dr. Fuad Major is thanked for his interest and loan of equipment to carry out this work. Professors U. Hochuli and Lester Erich and my other colleagues are specially thanked for countless helpful remarks and discussions which are so beneficial in doing research.

It is with pleasure to acknowledge the help of Mrs. Jeanette Zubkoff on innumerable matters. The help of Mrs. Marcella Walsh, Mrs. Ann U. Frantz, and Mrs. Linda Sabo in typing the final draft of this report and of Mr. Ralph E. Williams in proofreading is thankfully acknowledged.

This work was supported, in part, by the National Aeronautics and Space Administration (Grants NGR 21-002-022), Advanced Research Project Agency (Grant SD101), U. S. Army Research Office (Grant DAHCO 467C0023).

PART ONE

TABLE OF CONTENTS

Chapter		Page
STUDY OF GALLIUM ARSENIDE LASERS TO OPTICALLY PUMP THE GROUND STATE HYPERFINE LEVELS OF CESIUM -133.		
I.	GENERAL DISCUSSION	1
	A. Introduction	2
	B. Tunable Sources of Coherent Light . . .	3
	1. Dye Lasers	3
	2. Parameteric Optical Oscillators . . .	4
	3. Semiconductor Lasers	4
	C. Gallium Arsenide Junction Lasers	7
	1. Diffused Junctions	7
	2. Epitaxial Junctions	8
	3. Hetro Structure Junction Lasers . . .	8
	D. Degradation in GaAs Junction Lasers and Its Physical Basis	9
II.	PROPERTIES OF THE GaAs LASERS	11
	A. Laser Modes	11
	1. Mode Structure of the Laser Output . . .	11
	2. Mode Separation of the Laser Output . . .	11
	B. Efficiency of the Diode Lasers	15
	C. Dependence of the Junction Temperature on the Injection Current in C-W Operated Diode Lasers .	16
	D. Effect of Junction Temperature on the Threshold Current	17

Chapter | Page

E. Shift of the Laser Modes With the Rise in the Junction Temperature 18

F. Line Width of the Mode of a Diode Laser . . . 19

III. OPERATION OF THE GaAs LASERS 21

A. Problems Associated With the Matching of a GaAs Laser Mode With the D_2-transition of Cs-133 . . . 21

B. CW Operation of the GaAs Lasers 23

1. General Discussion 23

2. Construction of the Cryostat . . . 25

3. Output Power Versus Injection Current Characteristics 27

4. Study of the Laser Modes and Selection of the Laser 27

IV. OBSERVATIONS ON THE GaAs LASER INDUCED POPULATION INVERSION IN THE GROUND STATE HYPERFINE LEVELS OF Cs^{133} . 35

A. Experimental Setup 35

B. Modulation of the Injection Current . . . 35

C. Population Inversion in the Ground State of Hyperfine Levels of Cs-133 38

1. Observations With Laser #1 38

2. Observations With Laser #2 41

D. Conclusions 45

REFERENCES 47

CHAPTER I

GENERAL DISCUSSION

A. Introduction.

Applications using laser radiation for optical pumping and the study of atomic states have been very limited in the past because of the lack of available lasers which have output frequency to match the desired atomic transition. Moreover, most laser lines are very narrow and practically untunable. This is true for gas and solid state lasers. Semiconductor lasers, dye lasers, and parameteric oscillators have recently become sources of continuously tunable coherent radiation in some selected regions of the spectrum. Based on recent developments in the field of laser technology, it is quite reasonable to expect that within a few years, narrow band, tunable, coherent sources will be available over the entire spectral range from 0.2 μ to greater than 100 μ, which will provide enough power per mode to do optical pumping, semiconductor studies, spectroscopy, etc. Semiconductor lasers alone are capable of providing radiation at all wave lengths from 0.3 μ to over 60 μ although they have many practical limitations. These difficulties are solvable with future developments in the field of semiconductor material technology. A very recent breakthrough in this field resulted in the development of Gallium-Aluminum-Arsenide heterojunction lasers which operate continuously at room temperature[1].

An outline of some of the possible methods which can be employed

to generate coherent radiation for optical pumping of Rb^{87} and Cs^{133} and the limitations which presently limit their uses are discussed very briefly in this chapter. Gallium arsenide injection lasers which we have used for the optical pumping of Cs^{133}, will be discussed in detail in the rest of the report. In Chapter IV , we describe population inversions among the hyperfine levels in the ground state of Cs^{133} achieved by optically pumping these atoms with radiation from a GaAs diode laser. The laser output was used to monitor the populations in the two ground state hyperfine levels as well as to perform the hyperfine pumping.

The GaAs lasers were operated continuously at about $77^{o}K$. By temperature tuning, the laser mode could be matched to the 8521 A^{o} line of Cs^{133}. The intensity of the resonance radiation scattered from the cesium vapor served as an indicator of the relative populations of the two levels involved. Experiments were performed both with neon-filled and with paraflint-coated cells containing the cesium vapor.

It was also discovered that the diode laser could easily be tuned by manually adjusting the injection current to match either of the hyperfine components of the D_2-optical transition. The laser mode could be held for a few seconds on either component.

Possible future applications including a re-study of the light shifts, the construction of a Cesium laser, and the physics of optical pumping with coherent light are discussed. No laser is yet available to match the Rb-87 optical transitions. However lasers made out of GaAlAs could match the D_1 and D_2 transitions in Rb-87 or Rb-85. Although some GaAlAs lasers have been reported, the art of making them is still

in the developmental stage. Injection lasers offer the advantage of small size, high efficiency, ease of operation and modulation, low cost and continuous coverage of a very wide range of spectral outputs. However the present restrictions to low temperature operation and degradation of output with time, are serious handicaps.

B. Tunable Sources of Coherent Light

1. Dye Lasers

Stimulated emission from a number of solid and liquid solutions of organic dyes has been reported by a number of investigators. Sorokin and Lankard[2] were the first to report laser action from dye solutions excited by a ruby laser pulse and later by a coaxial flash lamp[3]. Laser action in plastic rods (containing organic dyes as the active medium) excited by a flash lamp has been published by Peterson and Snavely[4]. CW operation of an organic dye laser excited by an Argon Ion laser has been achieved for the first time by Peterson et al[5].

The widespread interest in the development of dye lasers is because they can provide simple, high power light sources continuously tunable over a broad frequency range. Furthermore, a large number of dyes with spectral emission in different, overlapping regions have been discovered[6]. In principle, by using a few different diffraction gratings to optimize the output performance and a dozen dyes, the entire spectral range from ultraviolet to the infrared can be spanned. Frequency locking of the dye lasers to specific atomic resonance lines has also been reported[7]. However, the above stipulations are accompanied by serious practical difficulties. It is more true if one desires

to operate a dye laser in the continuous mode and in the far infrared region.

2. Parametric Optical Oscillators

Work on parametric generation of light as sources of tunable coherent radiation began as early as 1961[8]. It was followed by a number of proposals and theoretical studies[9 - 11]. It took almost four years before a successful optical oscillator could be practically realized[12]. Giordmaine and Miller[12] were the first to demonstrate a working parametric oscillator in the optical range. Continuous optical parametric oscillations were first observed by Geusic[13] et al in 1968. Work on parametric oscillators has extended rapidly. It is now possible to tune through most of the visible and near infrared with greater than 50 percent efficiency and thresholds as low as 3mw[14]. It has also been possible to lock an optical parameteric oscillator to an atomic transition[15].

Some preliminary investigations were made on the possibility of using a dye laser or an optical parametric oscillator to optically pump the alkali vapors. However, the project was given up in favor of using semiconductor junction lasers because they seemed to offer less difficulties and more possible applications. One of the most important applications, which we have on the back of our mind, is their use in the making of ultralight weight atomic frequency standards.

3. Semiconductor Lasers

Since the first observation of electroluminescence in GaAs in 1955[16] and followed by the first observation of stimulated emission in

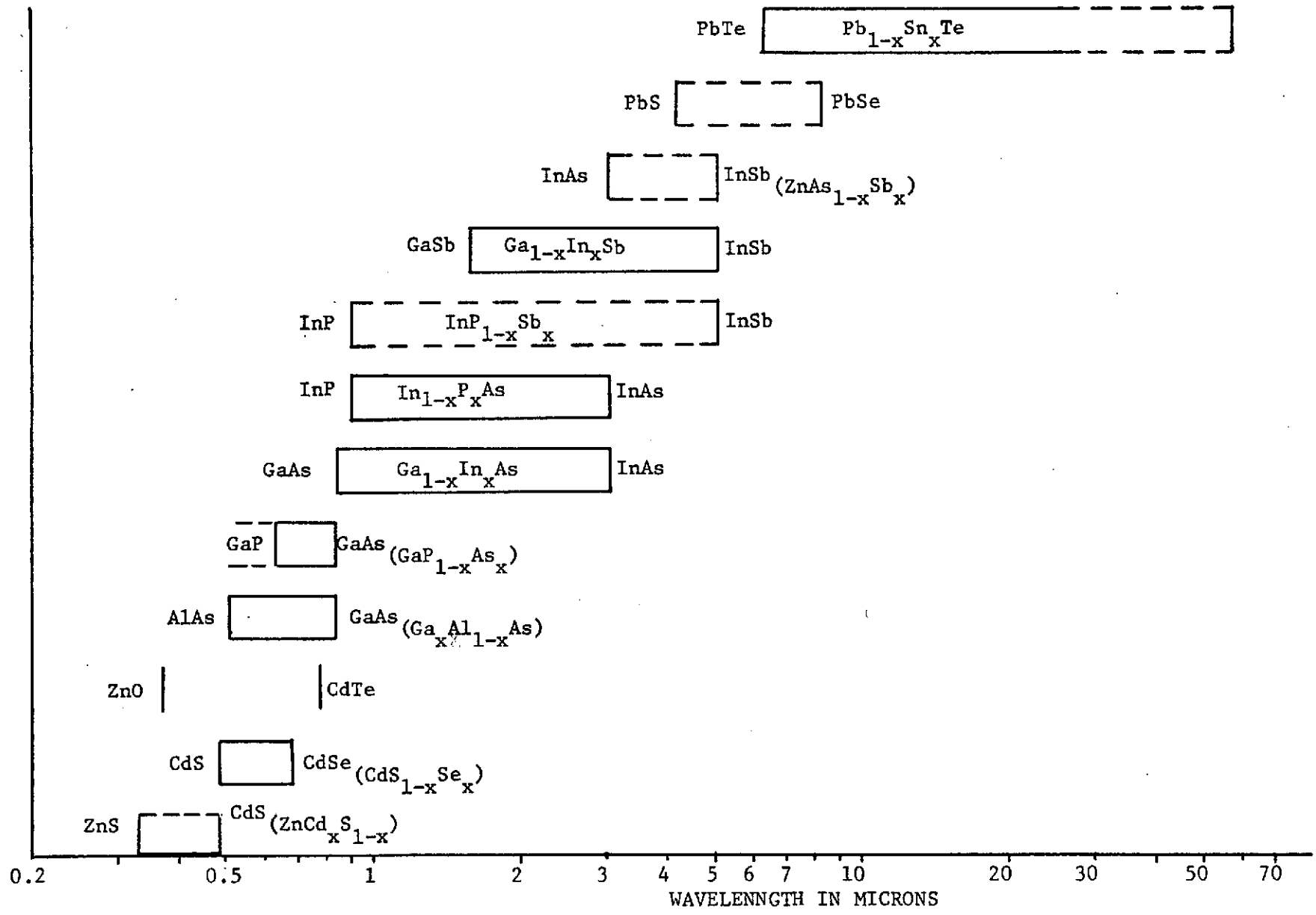

FIGURE 1. SPECTRAL RANGE COVERED BY PSEUDOBINARY COMPOUNDS FOR INJECTION LASERS. SOLID LINES INDICATE THAT ALL THE INTERMEDIATE WAVELENGTHS HAVE BEEN OBSERVED. DASHED LINES INDICATE INCOMPLETE STUDIES THOUGH LASER ACTION IS HIGHLY PROBABLE.

it in 1962[17,18] considerable progress has been made in the field of semiconductor lasers. A variety of semiconductor binary compounds[19] of the type $A^{II}B^{VI}$ (CdTe, CdS, CdSe, ZnSe, ZnS, ZnO, ZnTe)[20,21,22,23,24], $A^{III}B^{V}$ (GaAs, GaP, AlP, InP, GaSb, InAs, AlAs, InSb)[17,18,25,26,27,28], $A^{IV}B^{IV}$ (PbSe, PbTe, Pbs)[29,30,31] which provide discrete laser outputs in the ultraviolet, visible and infrared regions of the spectrum, have been discovered. Moreover, semiconductor lasers have been fabricated from pseudobinary compounds prepared by alloying two binary compounds containing a common element. Lasers fabricated out of these mixed crystals provide coherent light covering the spectral range from about $3000A^{o}$ to 60 μ (Figure 1) with a good chance of further extension at both ends of the spectrum. This range can be continuously covered by varying the composition of the alloying elements. For example, $GaAs_{1-x}P_x$ or $Ga_xAl_{1-x}As$ ($0 \leq x \leq 0.45$)[32] diode laser emits coherent output in the range 0.6 to 0.9 μ. This can serve an ideal source to optically pump Rb and Cs-alkali metals.

As_xP_{1-x} ($0 \leq x \leq 1$) diode lasers cover[33] the range 0.91 to 3.1 μ. An important spectral range of 8 to 14 μ, the atmospheric window, can be covered by lasers[34] prepared from $Pb_xSn_{1-x}Te$ or $Pb_xSn_{1-x}Se$.

Laser action in $Pb_xSn_{1-x}Te$ from 6.5 μ to 28 μ has been reported[35] by varying x from 0 to .27. Longer wave lengths up to 60 μ are anticipated for X = 0.4. Further extension of the laser wave lengths is possible because the conduction and valence bands in $Pb_xSn_{1-x}Te$ cross when going from lead compound to tin compound[36]. In brief, the semiconductor lasers can be 'tailor-made' to provide output wave lengths to fit the desired application.

Despite significant advances in Semiconductor Laser Technology, it is not yet possible to fabricate pn-junction lasers to cover the entire range of 0.3 to 60 μ. It has been possible to completely cover the spectral range from 0.6 μ to 30 μ by diode lasers made out of mixed crystals. Out of these, GaAs lasers are the most studied and widely manufactured lasers. They emit radiation close to the 8521 A^{o} line of Cs^{133} when operated at about 77°K. We also have studied some of its characteristics and performed optical pumping in Cs^{133}.

C. Gallium Arsenide Junction Lasers.

The GaAs diode lasers are p-n-junction devices. They are operated at forward bias and at high current densities. GaAs lasers emit radiation at a wave length of approximately 8500A^{o}, when operated at 77°K. They are most frequently operated in the pulsed mode. Their operation in the continuous mode is made difficult by the spiraling increase in the threshold current due to the increase in the temperature of the junction caused by the injection current. It is only by a careful design of the junction that one can operate it in the continuous mode. Three different types of junctions have so far been invented. Because of their importance in relation to the CW operation of the diode lasers, they are very briefly described next.

1. Diffused Junctions

Diffused junction lasers operate in the pulsed mode reasonably well even at room temperatures. Their operation in the continuous mode is possible at about 77°K or below. Operation at higher temperatures, which may be desired to tune the output wave length to match the

D_2-transition in Cs-133, becomes difficult. The major disadvantage is that this structure requires a very high threshold current density creating a difficult technological problem of heat sinking. Typical threshold currents of well constructed lasers are approximately 10^3 A/cm^2(77^{o}K) and 3-5x10^4 A/cm^2 (300K^o).

2. Epitaxial Junctions

An epitaxial junction is made by growing a layer of p-type material on a n-type substrate (or vice versa). Epitaxial junction lasers have slightly higher threshold current densities below 77^{o}K and lower thresholds above 77^{o}K than for the diffused junctions. CW operation at temperatures as high as 200^{o}K has been demonstrated in carefully prepared lasers[37].

3. Heterostructure Junction Lasers

A complex junction structure [1,38] called 'Double Hetro'structure has recently been perfected. These lasers operate continuously at heat-sink temperatures as high as 311K^o. Threshold currents as low as 1000A/cm^2 at room temperature have been observed in some selected diodes [1].

Hetero-structure for GaAs injection lasers was first proposed[39] in 1963 predicting higher efficiency and low threshold. It was only recently when single-hetero structure (SH) type of junction lasers were made [40-42]. The SH-structure is a three layer junction consisting of a thin layer (1 μ) of P^+-GaAs sandwiched between N^+-GaAs and P^+-$Ga_xAl_{1-x}As$ where X $\simeq$ 0.5. This provides considerable improvement over the other two types of junction structures. The band gap in $Ga_xAl_{1-x}As$ is larger

than the band gap of GaAs and this structure results in a potential step at the P^+-GaAs and $Ga_xAl_{1-x}As$ boundary. This potential step prevents the injected electrons from diffusing into the P- region thus increasing the average electron density in the active region for a given current. This mechanism of confinement of electrons decreases the current required for a given gain at the operating temperature. Consequently, the threshold current density [42] required at room temperature, can be as low as 6000A/cm^2. Where as the conventional laser, with diffused or epitaxial junction, requires threshold current density (in the pulsed mode) of about 40,000A/cm^2 (at 300°K). Further improvement in the threshold has been achieved by the use of a double-heterostructure-(DH) $Al_xGa_{1-x}As$-GaAs-$Al_xGa_{1-x}As$-with a very thin active region. This structure confines both electrons and holes injected into the thin active region. DH also provides a better optical guiding. This results in a considerable reduction in the threshold. Values as low as 1000A/cm^2 (for CW operation at 297°K) have been observed [1].

D. Degradation In GaAs Junction Lasers and Its Physical Basis.

It has been demonstrated [43,44] that at moderate power levels the degradation process is caused by fundamental changes in the material in the vicinity of the junction. These changes are attributed to the formation of lattice defects. It has been estimated [44] from the work of Weiser [45] and Longini [46] that the net energy required to excite a Zn atom from its gallium substitutional to an interstitial site, where the Zn atoms act as a donor [46], is 1.0ev. This is substantially less

than the energy available from a recombining electron-hole pair. Zinc atoms can thus be displaced to where they act as 'impurity' centers and introduce interband states. The interband states are very effective in the tunneling of the injected carriers. This is manifested as a loss of carriers and hence an increase in the lasing threshold. The increase in threshold current results in an excessive heat generation at the junction thus increasing the laser threshold in a two fold way. It has also been demonstrated [44] that interstitial Zn ions diffuse more rapidly than substitutional Zn atoms. Diffusion of interstitial Zn ions across the junction is further enhanced by the forward bias, causing a significant change in the doping levels. It is thus concluded that stabler lasers would be possible if impurities with higher binding energies are used. It is the task of material oriented research to discover suitable doping materials with higher binding energies and acceptable to the host GaAs lattice.

Another cause of degradation of GaAs lasers has been attributed to surface damage [47]. This is particularly important in the case of high output GaAs lasers. Damage to the surface is predominently on the p-side and results from the heating of the junction area of the surface caused by the absorption of laser radiation at inhomogeneities. Heat drives off arsenic atoms resulting in the destruction of the Fabry-perot cavity. Moreover, with the increase in the photon density the phonon density also increases. It might mechanically damage the laser crystal.

CHAPTER II

PROPERTIES OF THE GaAs LASER

A. Laser Modes.

1. Mode Structure of the Laser Output

The spectral output of a GaAs laser, just above or close to the threshold, may consist of a single mode peaking out near the maximum of the spontaneous emission. Some selected diodes may oscillate in a single mode at currents above their thresholds. In most cases a number of modes may get excited at higher currents. In some cases of multimode operation the modes may come from different families of Fabry-Perot cavity modes. This phenomenon has been attributed to cleavage steps on the reflecting faces of the laser cavity. It may also occur as a result of crystal defects leading to regions of differing refractive indices[48]. The above statements are supported by the spectra of the diode laser (#3) when operated at 77°K and at different currents (Figures 2 a-c). We also experienced that in a multimode laser the modes were unstable and the spectra could hardly be reproduced. Figures 2 b and 2 c illustrate this behavior. The two spectra were recorded one after the other without making any change.

2. Mode Separation of the Laser Output

Different modes will arise whenever an integral number of half wave lengths are contained between the ends of the Fabry-Perot cavity:

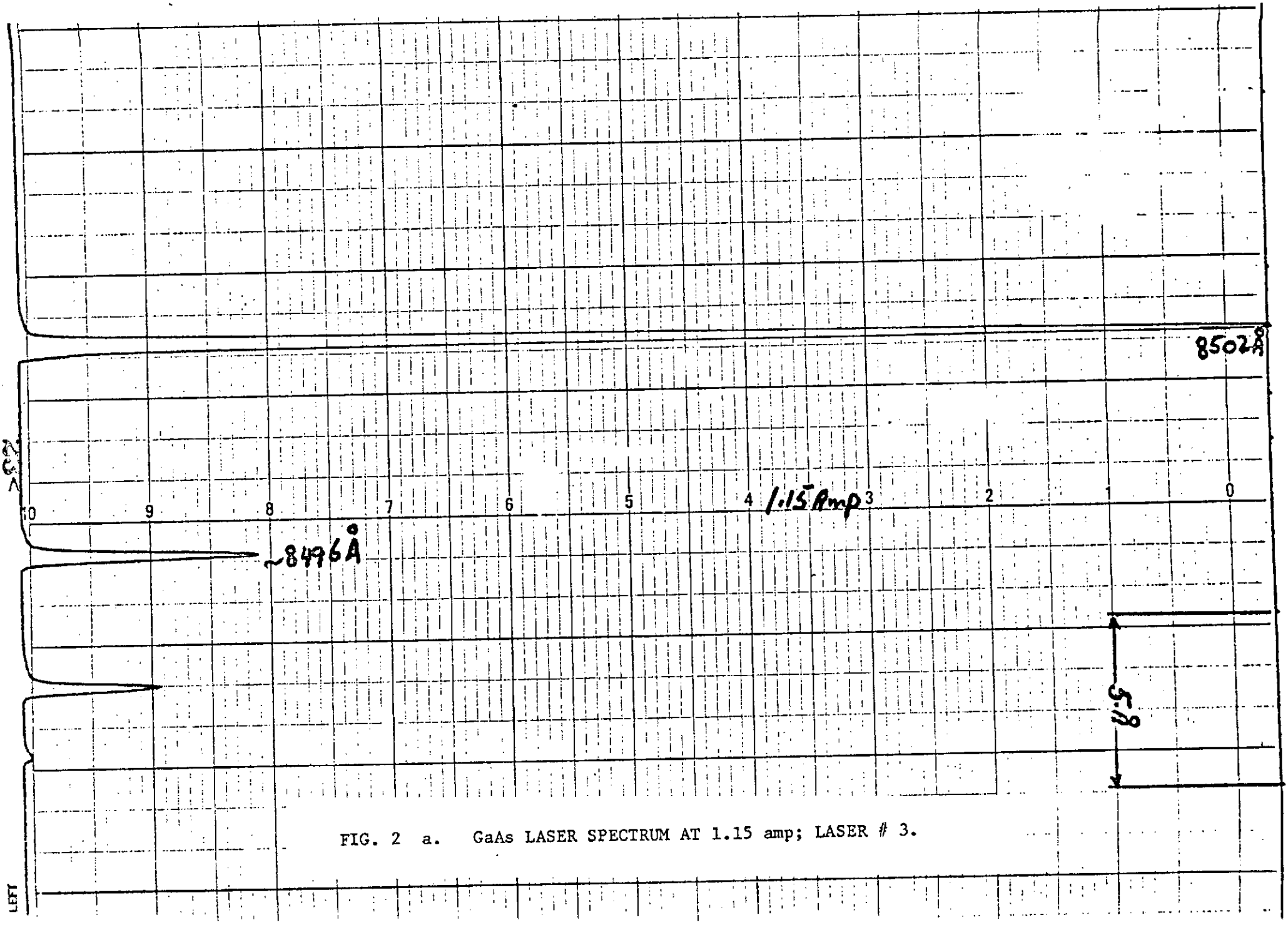

FIG. 2 a. GaAs LASER SPECTRUM AT 1.15 amp; LASER # 3.

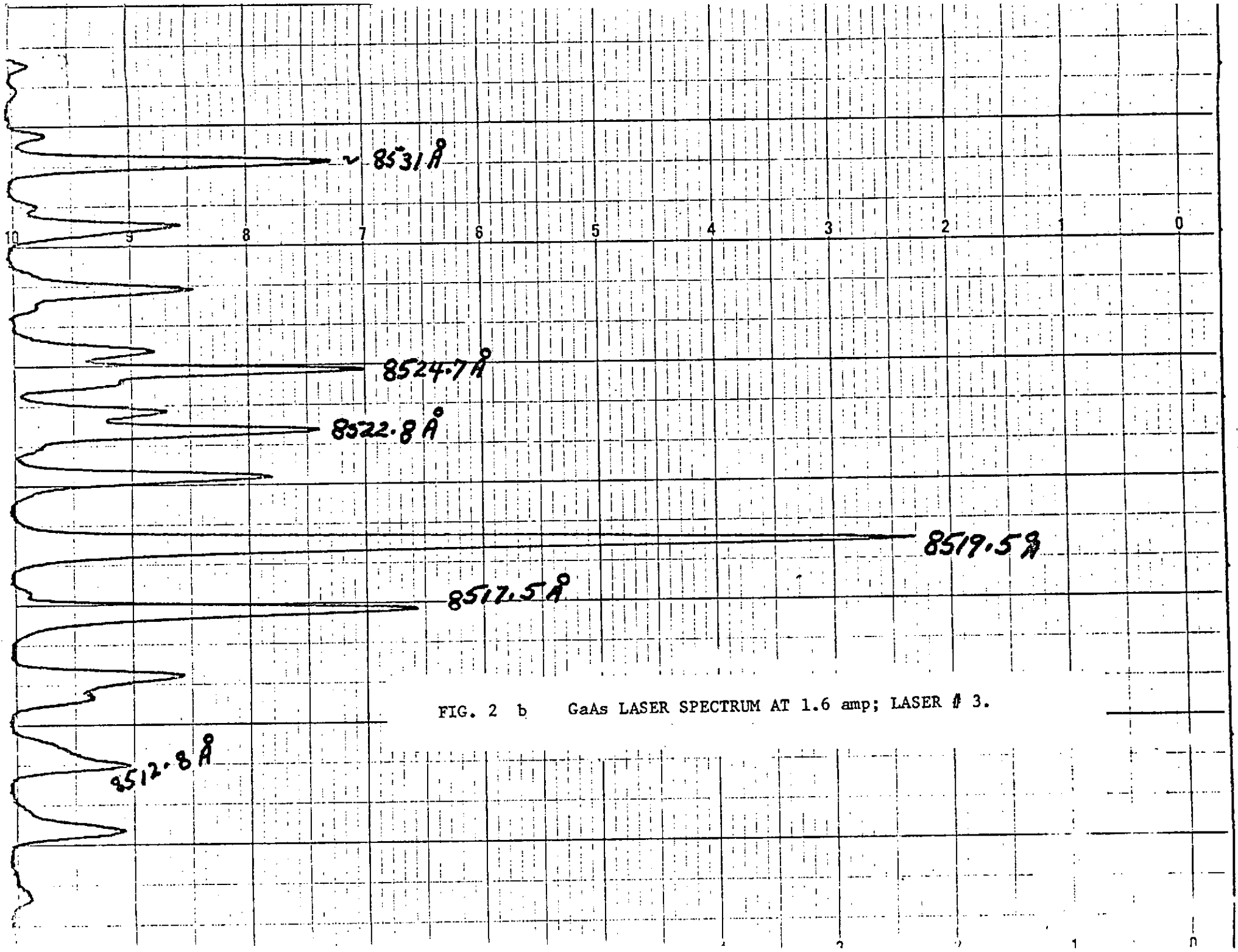

FIG. 2 b GaAs LASER SPECTRUM AT 1.6 amp; LASER # 3.

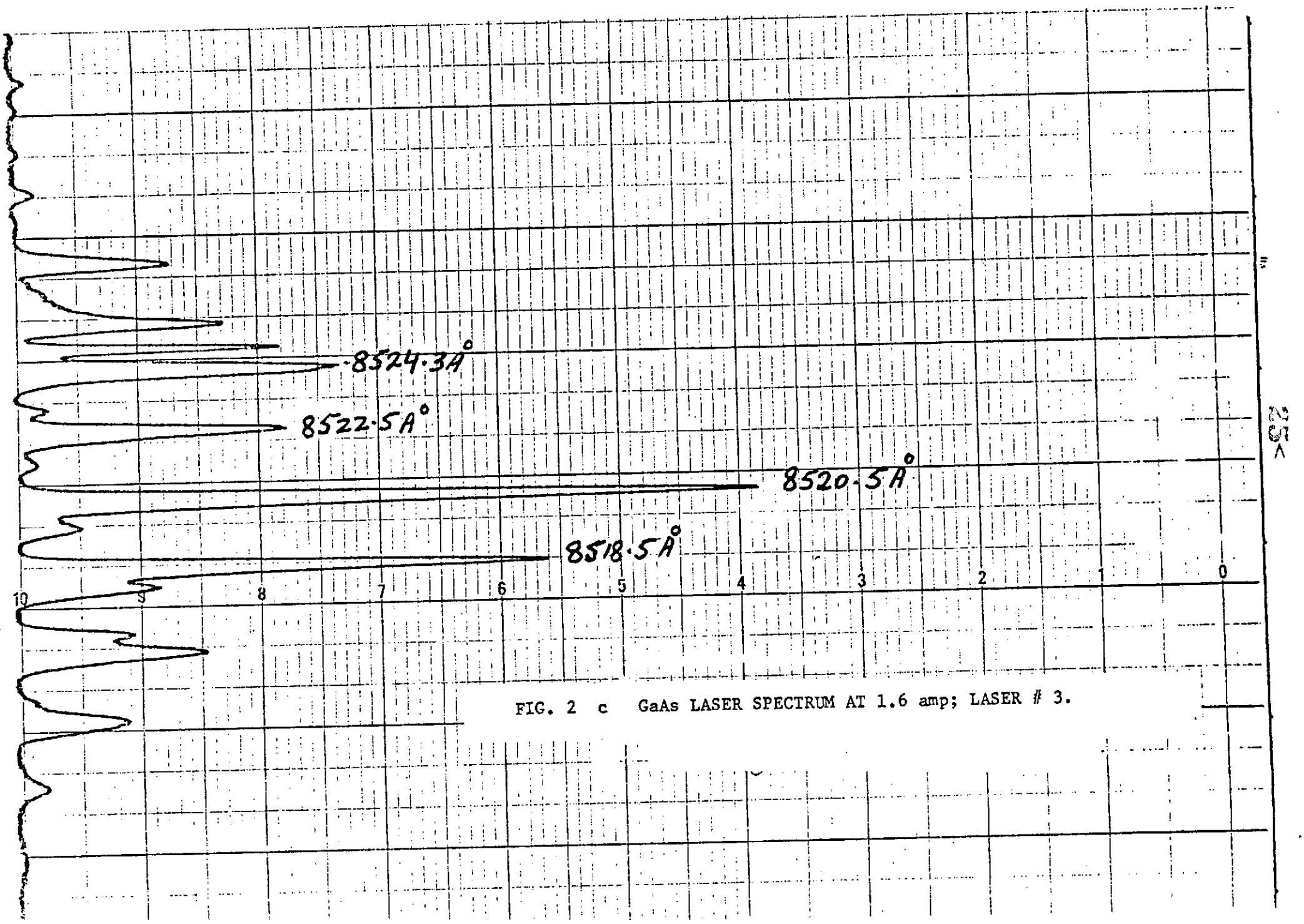

FIG. 2 c GaAs LASER SPECTRUM AT 1.6 amp; LASER # 3.

$$L = \frac{m\lambda}{2\eta} \qquad \text{II.1}$$

or

$$\lambda = \frac{2\eta L}{m} \qquad \text{II.2}$$

where m is an integer, η = average value of the index of refraction, λ = wave length, and L is the cavity length.

For a GaAs laser, $\lambda \simeq 8500A^{o}$, L = .4mm, η = 3.6, one finds $m = 4 \times 10^{3}$.

Noting that the index of refraction η is a strong function of λ (because λ is very close to the absorption edge), spacing between the two adjacent modes can be written as

$$\Delta\lambda = \frac{\lambda^{2}}{2L}\left[\eta - \lambda \frac{d\eta}{d\lambda}\right]^{-1} \qquad \text{II.3}$$

Knowing η and $\frac{d\eta}{d\lambda}$, $\Delta\lambda$ can be computed. Calculated values agree very well with the observed value of $\Delta\lambda$ which is about 1.5 - 2.5A^{o} depending on L. Figures 2 a-c show modes separation of about 2 - 2.25A^{o}. The cavity length of this laser was close to 400 μ.

B. Efficiency of the Diode Lasers.

Semiconductor junction lasers are operated to transform the electrical energy directly into coherent radiation thus yielding a theoretical internal efficiency approaching 100%. Moreover, they are capable of yielding a gain almost equal in absolute value to the absorption coefficient because of the high density of the absorbing electrons. Also, the magnitude of the gain in semiconductors is much larger than the corresponding gain in other laser materials. Thus a semiconductor

laser with extremely small dimensions can give rise to a relatively large coherent light output. Diode lasers have experimentally been found to have the highest external efficiency of all the lasers. It is about 30% at room temperature [19] and more than 60% at low temperatures[19] (~ 4^{o}K). They can emit coherent outputs higher than 10W continuously (at helium temperature). The highest power level observed by us was close to 0.2 watts at 77^{o}K and at an efficiency of 8%.

C. Dependence of the Junction Temperature on the Injection Current in CW Operated Diode Lasers.

The increase in the junction temperature results in less efficient performance of the laser. There always exists a considerable temperature difference between the junction and the ambient (which may be the 'cold finger' holding the diode or the diode may be dipped in the low temperature bath). This results from the finite conductivity of the laser material and that of the 'heat sinks' attached to the diode. It is thus important to review briefly the problem of flow of heat away from the junction where a constant supply of heat is being provided by the injection current. Detailed analysis of this problem and its experimental verification has been discussed by a number of investigators[49,50,51].

The rate at which heat is generated at the junction plane is JV per unit area, where J is the current density and V is the voltage applied across the junction. The value of V is very close to the energy gap. The order of magnitude of this heat for a typical GaAs laser is about 3×10^{3} watts/cm^{2}. The rate at which one can transfer heat[49] to

liquid nitrogen by a boiling nucleus is less than 10 watt/cm^2. However, the heat transfer capability is greatly enhanced[49] (by a factor greater than 10^3) by sandwiching the 'laser grain' between 'heat sinks'. These heat sinks are made out of oxygen-free copper coated with indium to improve the thermal contact between the crystal diode and the sink. Laser so sandwiched can be either held between cold fingers or dipped in the cold bath (liquid N_2 or He) while in operation. Even with this much heat sinking, the temperature of the junction can be about 10 to 60°K higher than its ambient temperature depending on the current through it.

D. Effect of Junction Temperature on the Threshold Current.

An experimental study[52] reveals that the reciprocal of the gain through the medium and hence the threshold current are almost constant in the temperature range $0<T<20^{\circ}K$. At temperatures higher than 100°K, it varies as T^m (where $m = 2.6 \rightarrow 3$) and as $T^{3/2}$ in the vicinity of liquid nitrogen temperature[53].

In physical terms, the main cause of the increase of the threshold current with the rise in temperature is due to the decrease in the degeneracy of the electron and hole populations in the participating levels. In other words, the carriers get distributed over states in a wider energy belt at higher temperatures. It thus requires an increase in the injection current to produce the required degree of population inversion. At low temperatures, the conditions are ideal in the sense that a very high degree of degeneracy exists in the population of the carriers near the conduction and valence band edges. Since the states

near the band edges are close to full and any further decrease in the temperature does not increase the population density and hence the gain. Consequently, a constant threshold is expected at very low temperatures. Other factors contributing to the temperature dependence of the threshold are losses due to the absorption of light, by the free carriers and the scattering effects within the active region. Free carrier absorption alone is known to be greater by an order of magnitude at $300^{o}K$ than it is at $77^{o}K$[54].

E. Shift of Laser Modes With the Rise in the Junction Temperature.

Spontaneous emission from gallium arsenide shifts to longer wave lengths as the temperature is raised by about $1.2A^{o}/K^{o}$ at $77^{o}K$. This essentially indicates the shrinking of the forbidden energy gap. The energy of the gap at any temperature is given by the relation

$$E_g(T) = E_g(0) - \beta T^2 \qquad \text{II.4}$$

where $E_g(0) = 1.52$ ev. and $\beta = 1.2 \times 10^{-6} ev/K^{o2}$ (For GaAs lasers).

The shift in the lasing mode position has been found[55,56] to be $0.4/K^{o}$ (at $77^{o}K$ and $8400A^{o}$).

Since the temperature coefficient of an individual mode is smaller than that for the spontaneous emission, the modes at shorter wave lengths get out of step with the shifting spontaneous emission and hence decrease in intensity and finally die; while new modes on the longer wave length side begin to lase and increase in intensity.

Therefore, when doing the resonance scattering from Cs-133 vapors, one has to be careful in distinguishing between the scattering from the

two hyperfine levels by the sweep of a single mode and the scattering due to the onset of new modes. The latter is more likely to happen if the junction temperature is raised very rapidly by injecting a square current pulse.

F. Line Width of the Mode of a Diode Laser.

A theoretical expression for the line width $\Delta\nu_{coh}$ (full spectral width at half intensity) of a GaAs is given by the following expression:[57]

$$\Delta\nu_{coh} = \frac{2\Pi h\nu_o(\Delta\nu_{cav})^2}{P} \qquad \text{II.5}$$

where $\Delta\nu_{cav}$ is the band width of the cavity, P is the coherent power in the mode, other symbols have the conventional meaning. The expression for the cavity width as obtained by Armstrong and Smith[58] is

$$\Delta\nu_{cav} = \frac{2\ C}{4\Pi\eta^1 L}(1 - R\ e^{-\alpha L})(R\ e^{-\alpha L})^{-1/2} \qquad \text{II.6}$$

where C/η^1 is the group velocity (C/5.3) and R stands for the reflectivity of the ends of the cavity. For a typical laser with its faces cleaved, the reflectivity $R = (\frac{\eta-1}{\eta+1})^2 = .32$ (since $\eta = 3.6$), absorption coefficient $\alpha \simeq 35cm^{-1}$. For a laser with cavity length = .04 cm,

$$\Delta\nu_{cav} = 7.4 \times 10^{10} \text{ cps.}$$

At 8500A°, the line width of the laser mode having 1mw of power output, is close to 9.5MHz. For a laser giving out 250 mw in a single mode, its mode width should be 38kc. The narrowest observed line has been reported[39]

by Ahearn and Crowe. The line width was measured to be 150 KHz and was limited by the system resolution. The measurement was made by using a Michelson interferometer with a path difference of 3000 ft and heterodyne detection. Their laser had the dimensions close to the one for which the calculations are given above, ($L = 400\mu$). It was selected from many and emitted 250mw of coherent light (cw) in a single mode.

The lasers operated by us were selected from those available to us. They were selected not for maximum output but for their having a mode at 8521^{o}A with a reasonable output power to give detectable pump signals from Cs-133. The laser used in the pumping of Cs-133 had power in excess of 10 milliwatts in a single mode and hence it is expected to have a mode width less than 1 MHz.

CHAPTER III

OPERATION OF THE GaAs LASERS

A. Problems Associated with the Matching of a GaAs-Laser Mode with the D_2-Transition of Cs-133.

As shown in Figure 3 , the D_2-transition $S_{1/2}P_{3/2}$ in Cs-133 corresponds to 8521.1A^{o} and of photon energy 1.454ev. Consequently, the photons from the laser must have the same energy to excite these atoms.

In GaAs, the band gap energy is close to 1.51ev, where as the laser emission is generally below 8500A^{o} (at 77^{o}K) i.e. slightly greater than 1.454ev. This difference of 0.056ev is caused by the creation of impurity bands near the conduction and valence band edges. Because of the high concentration of the dopants, the impurity bands form a continuum and effectively extend the conduction and valence bands into the forbidden gap. The extended bands are called tails and the laser emission occurs between states which form these tails.

It is clear that the extension of the bands and hence the photon energy of the laser emission depends on how heavily the laser has been doped and what dopants have been used. So one has to make a selection of the laser by investigating quite a few to select the one whose output might match the D_2-transition in Cs-133.

Another way would be to operate the laser at a slightly higher temperature than 77^{o}K. The band gap decreases with the increase in the

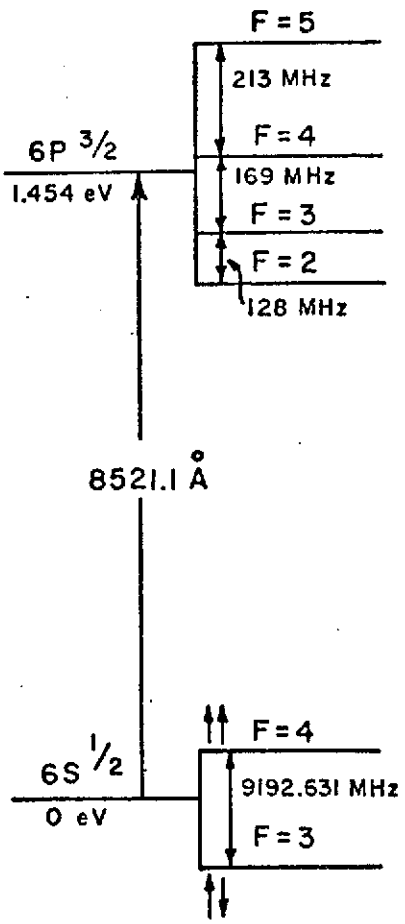

FIGURE 3 THE RELEVANT ENERGY LEVELS OF Cs - 133 .

temperature of junction. One would expect to be able to match the laser output with the desired transition. This method of tuning has its own problems. As the temperature is raised, the gain in the laser drops and the laser may not operate CW at ambient temperatures higher than $77^{o}K$. During our experimentation we came across a few of the lasers which would operate CW when dipped in liquid nitrogen but would not lase when put in contact with a copper sink partially dipped in liquid nitrogen.

B. CW Operation of the GaAs Lasers.

1. General Discussion.

In the present application, the GaAs laser needs to be operated CW and at slightly higher temperatures than the liquid nitrogen temperature so that the output mode could be matched to the $8521A^{o}$ optical transition in Cs-133. It should be pointed out that, at present, it would be impossible to obtain a diode laser which would operate continuously (CW) at room temperatures and would also match with the $6P_{3/2} \rightarrow 6S_{1/2}$ optical transition in Cs-133.

Operation of the laser by simply dipping it in liquid nitrogen does not suffice. While the laser is being fed with continuous current, the heat dissipated to the surrounding cryogen boils it violently causing large temperature fluctuations and hence making the frequency of the output radiation fluctuate. Bubbling will also cause the outcoming beam suffer unpredictable scattering. This type of fluctuations in frequency and intensity are not only undesirable but detrimental to

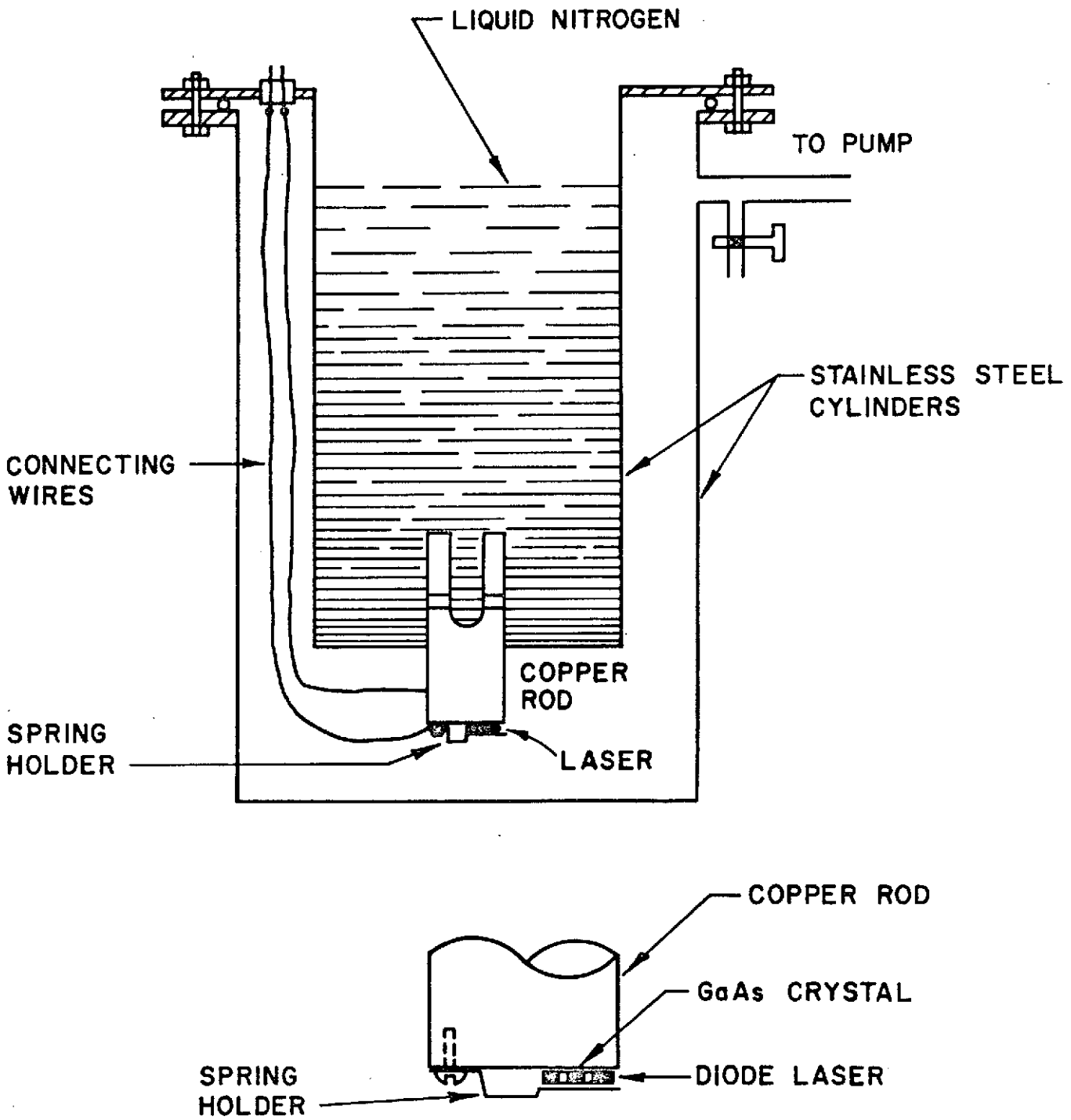

Fig. 4 ARRANGEMENT FOR OPERATING THE DIODE LASERS

to the success of the present experiment. Moreover, it was desired to have the ambient temperature (as mentioned above) slightly higher that $77^{o}K$. Consequently, the laser had to be cooled differently. It was done by placing the laser in good thermal contact with copper blocks cooled by dipping them partly into liquid nitrogen.

2. Construction of the Cryostat

A few different designs for the cryostat to house the diode laser were tried with varying degree of success. In our early investigations, the cryostat was designed to cool the laser from both sides. This was necessary because of the high threshold currents of the available diode lasers at that time. Relatively recently, the quality of the lasers has very much improved. Our recent investigations with diodes obtained from IBM have shown lower threshold current densities. The improvement is almost by a factor of 2 to 3 in the threshold currents of lasers of about the same size as used previously.

In view of these improvements it was decided to cool the laser only on its p-side. This very much simplified the construction of the cryostat.

Figure 4 shows the later version of the cryostat. It was made by modifying the earlier cryostat. The p-side of the laser is pressed against the copper rod by the spring action of a metal strip. An indium sheet ($\sim$.002" thick) is placed between the laser and the copper rod for better thermal contact. The copper rod and the strip served as the two electrodes. The copper rod is partially dipped in liquid nitrogen contained in a thin wall stainless steel cylinder. The cavity ends of the

POWER vs INJECTION CURRENT
The laser was operated by dipping it into liquid nitrogen. Fluctuations in power are due to the bubbling of nitrogen.

FIG. 5 POWER vs CURRENT CHARACTERISTICS FOR GaAs LASER # 1.

37

laser face the glass windows in the outer stainless steel cylinder. Vacuum is maintained in between the two cylinders with the help of a vacuum pump. The cryostat when once filled with liquid nitrogen could last for about an hour.

3. Output Power Versus Injection Current Characteristics

The laser was operated CW by DC current derived from a commercially available low voltage power supply.

Figure 5 represents the power output versus injection current of laser #1. (This # is for future reference.) This was one of the early diodes and this characteristic was taken with the help of a chart recorder. The laser was operated by dipping it in liquid nitrogen. Wiggles on the power characteristic curve are due to fluctuations in the power output caused by the bubbling of liquid nitrogen. Bubbling also causes random scattering of the radiation resulting in fluctuations of the energy reaching the detector. It will also cause local temperature fluctuations causing fluctuations in the output of the laser.

Lasers obtained more recently showed a very similar power-vs-current characteristic but had lower thresholds. These lasers were of about the same size (400μ x 100 μ) and had thresholds at 0.5 - 0.7 Amp.

4. Study of the Laser Modes and Selection of the Laser

A large number of GaAs diode lasers (~ 60) were investigated. Spectral characteristics of these lasers varied from laser to laser. Each diode behaved differently. Many had multiple mode structure and some did not come close to the desired output length. These lasers

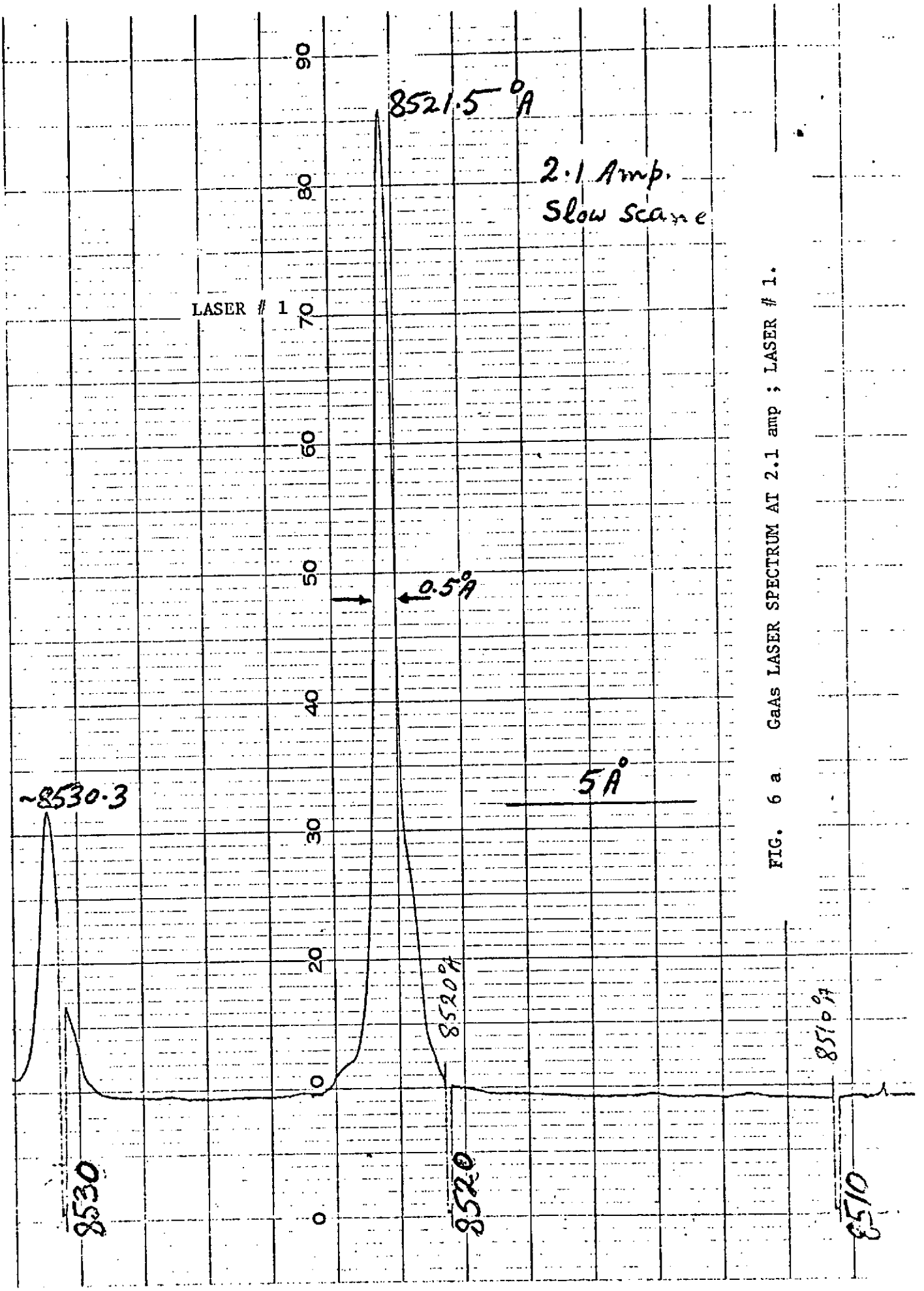

FIG. 6 a GaAs LASER SPECTRUM AT 2.1 amp ; LASER # 1.

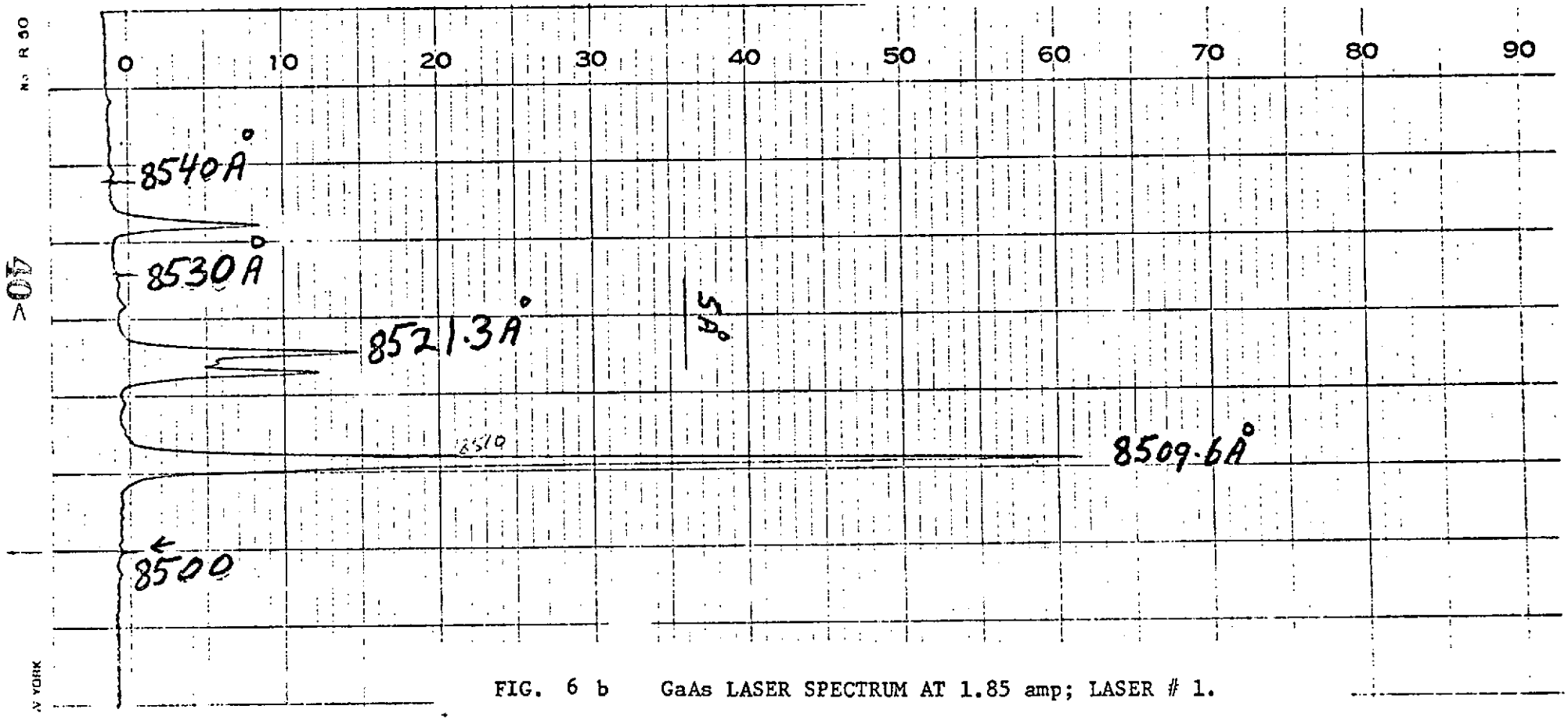

FIG. 6 b GaAs LASER SPECTRUM AT 1.85 amp; LASER # 1.

were first examined by dipping them in liquid nitrogen. It gave information about their threshold currents, approximate location of their modes, etc. This mode of operation provides a quick check and is much less time consuming. After the first check the selected lasers were operated by putting them in contact with a copper rod partially dipped in liquid nitrogen. The power output of the laser in this mode of operation was very stable when operated at a constant DC current. Only those lasers which showed strong modes close to 8521^{o}A are reported here. The position of the mode could be shifted (10-20^{o}A) to match the D_2 - transitions of Cs-133 by varying the injection current.

Figures 6a and 6b show the spectra of laser #1 at different injection currents. The laser showed a strong mode close to 8521.5A^{o}. Moreover, the two spectra demonstrate that the laser mode could be shifted by more than 10A^{o}. This laser was operated in the earlier version of the cryostat which provided cooling on its both sides.

Figures 7a through d show the spectral distribution of laser #2 operated at different currents. They also show, as above, the shifting of the mode toward higher wave lengths as the injection current is increased. This laser also showed a very strong mode close to 8521A^{o} and this mode could be tuned over a wide range of wave lengths by simply changing the injection current. It is important to note that the output consisted of very strong single mode at 8521A^{o} and the mode could be shifted either way by more than 5A^{o} without exciting any additional mode.

Figure 7a showing the mode at 8521^{o}A was observed at a slightly higher sensitivity than the other three to find out the relative strength

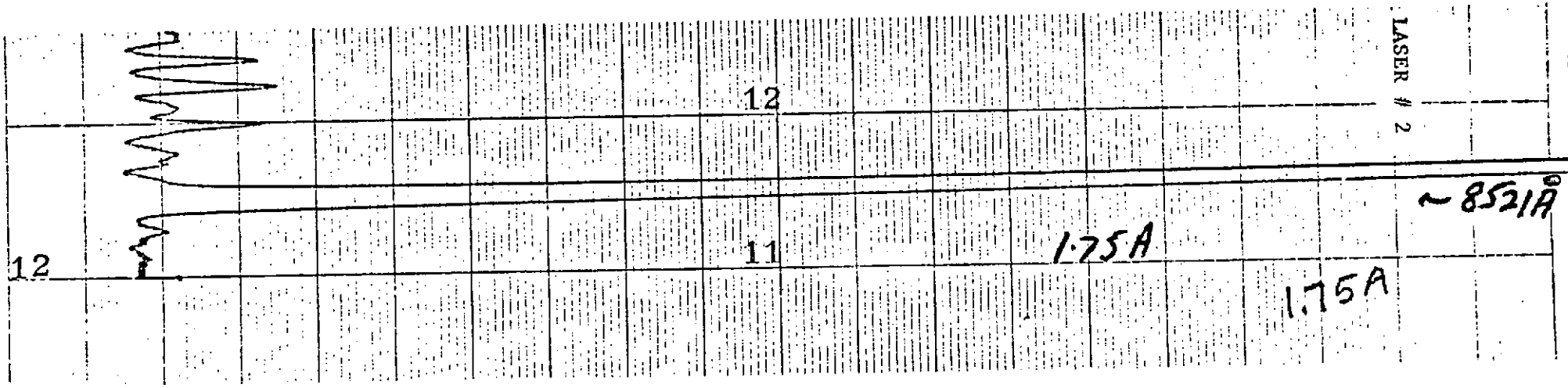

FIG. 7a GaAs LASER SPECTRUM AT 1.75 amp; 1" = 10°A.

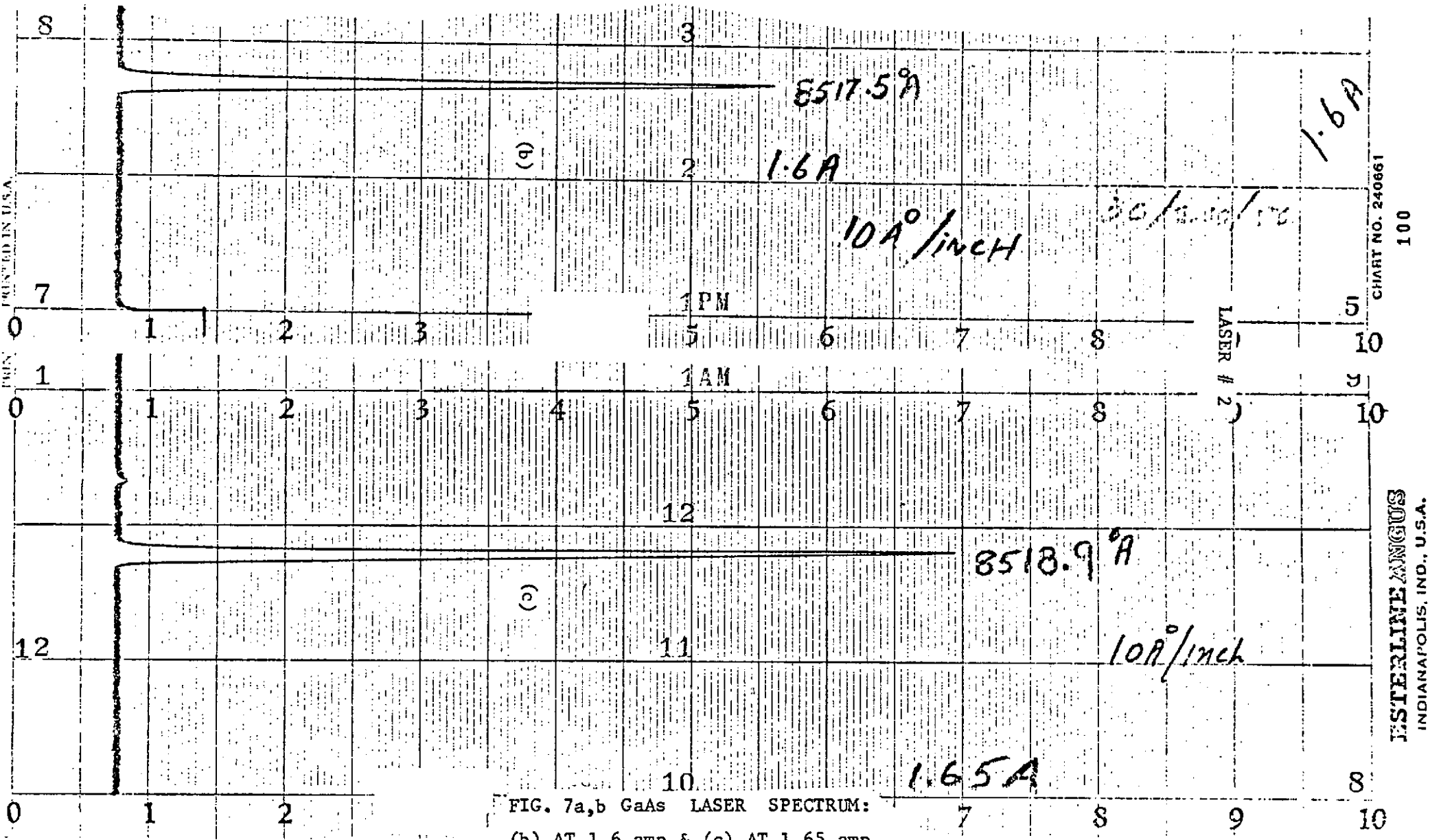

FIG. 7a,b GaAs LASER SPECTRUM:
(b) AT 1.6 amp & (c) AT 1.65 amp.

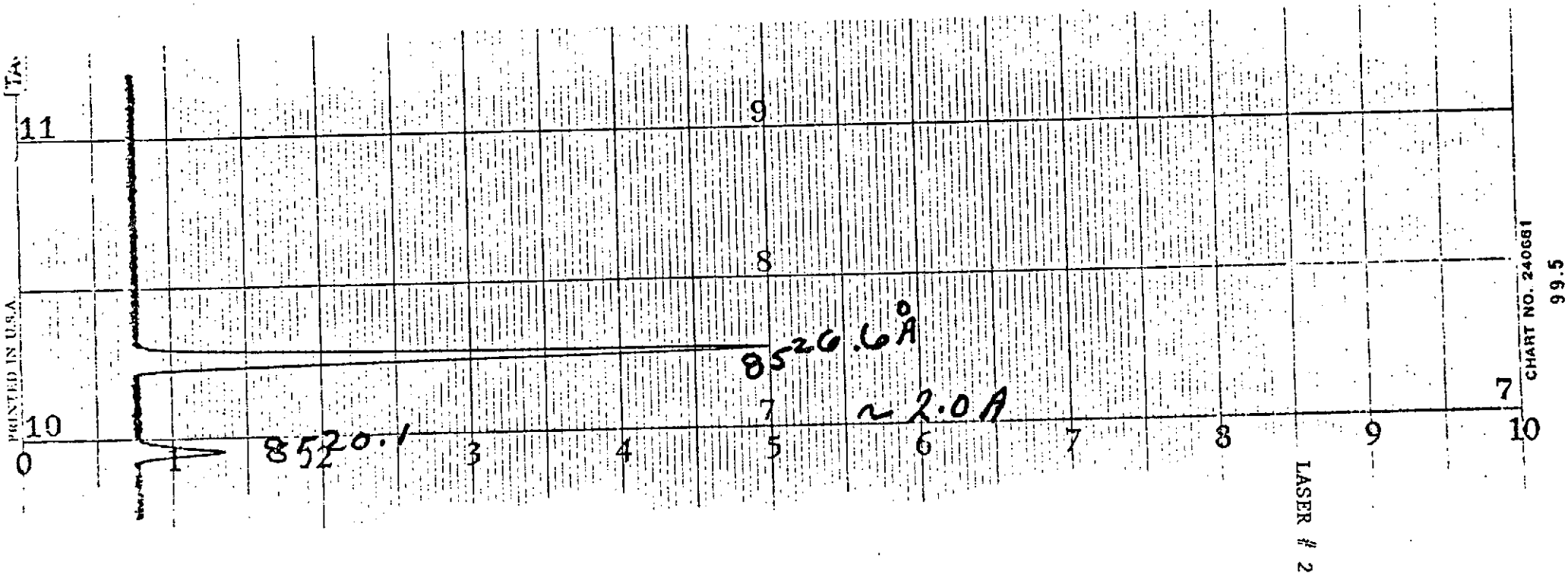

FIG. 7 d GaAs LASER SPECTRUM AT 2amp.; 1" = 10°A.

of any other mode in its neighborhood. There was none on either side.

Observed width of the modes is no indication of the actual width of the mode. It is very much limited by the resolution of the detecting system. Moreover, the noise in the DC supply voltage can also give some jitter to the position of the mode.

Observations with laser #3 have already been given in Figures 2 a-c. This laser showed a strong mode at 8502A^{o} at an injection current of 1.15 Amperes. The laser developed a multi-mode structure when the current was increased. This laser showed an unstable mode close to 8521A^{o} along with many extra modes.

CHAPTER IV

OBSERVATIONS ON THE GaAs LASER INDUCED POPULATION INVERSION IN THE GROUND STATE HYPERFINE LEVELS OF Cs^{133}

A. Experimental Set Up.

A very simple experimental arrangement, as shown in Figure 8 was used to observe the resonance scattering from Cesium vapor cells. The cells were held at room temperature, so no arrangement was provided for maintaining the cells at higher temperatures, except in one situation where one cell was dipped in hot water and placed back in position. This was done in connection with various tests performed to make sure that the scattered radiation was from the Cs vapors. Radiation from one side of the GaAs laser diode was focused by a lens on the Cesium vapor cell. The laser mode was swept through the resonance lines of Cs-133 (at 8521^{o}A) by modulating the injection current. Resonance scattering was observed at angles normal to the incidence radiation with a RCA 7102 photomultiplier tube. Arrangement was also provided to observe resonance absorption. The laser output from the other side of the laser was used to monitor its power output.

B. Modulation of the Injection Current.

In order to sweep the laser mode across the resonance transitions, the current through the laser was slowly modulated. This modulation was on top of the DC current. The value of the DC current could be

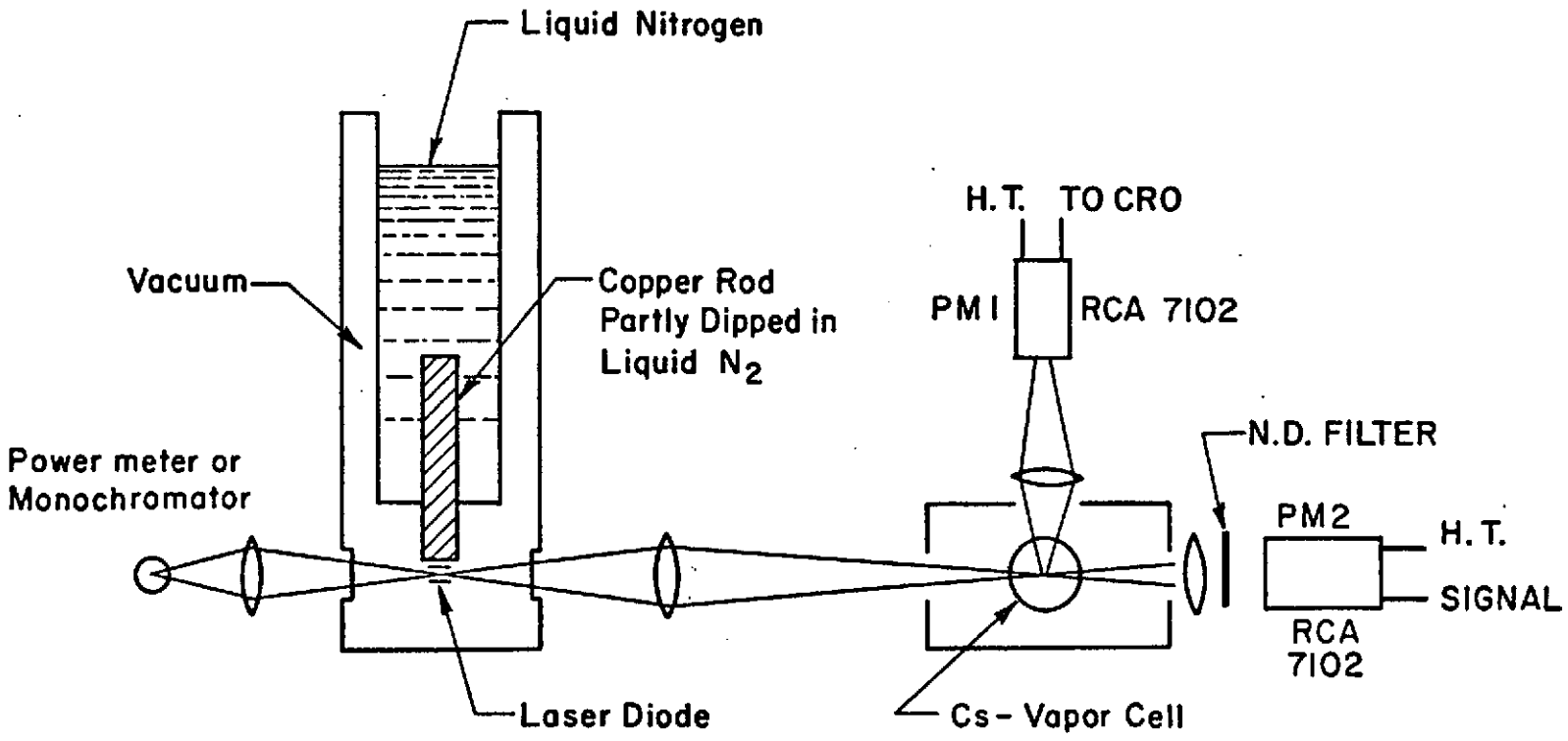

FIGURE 8

Block diagram of the experimental arrangement to observe resonace scattering from Cs^{133} vapor cells.

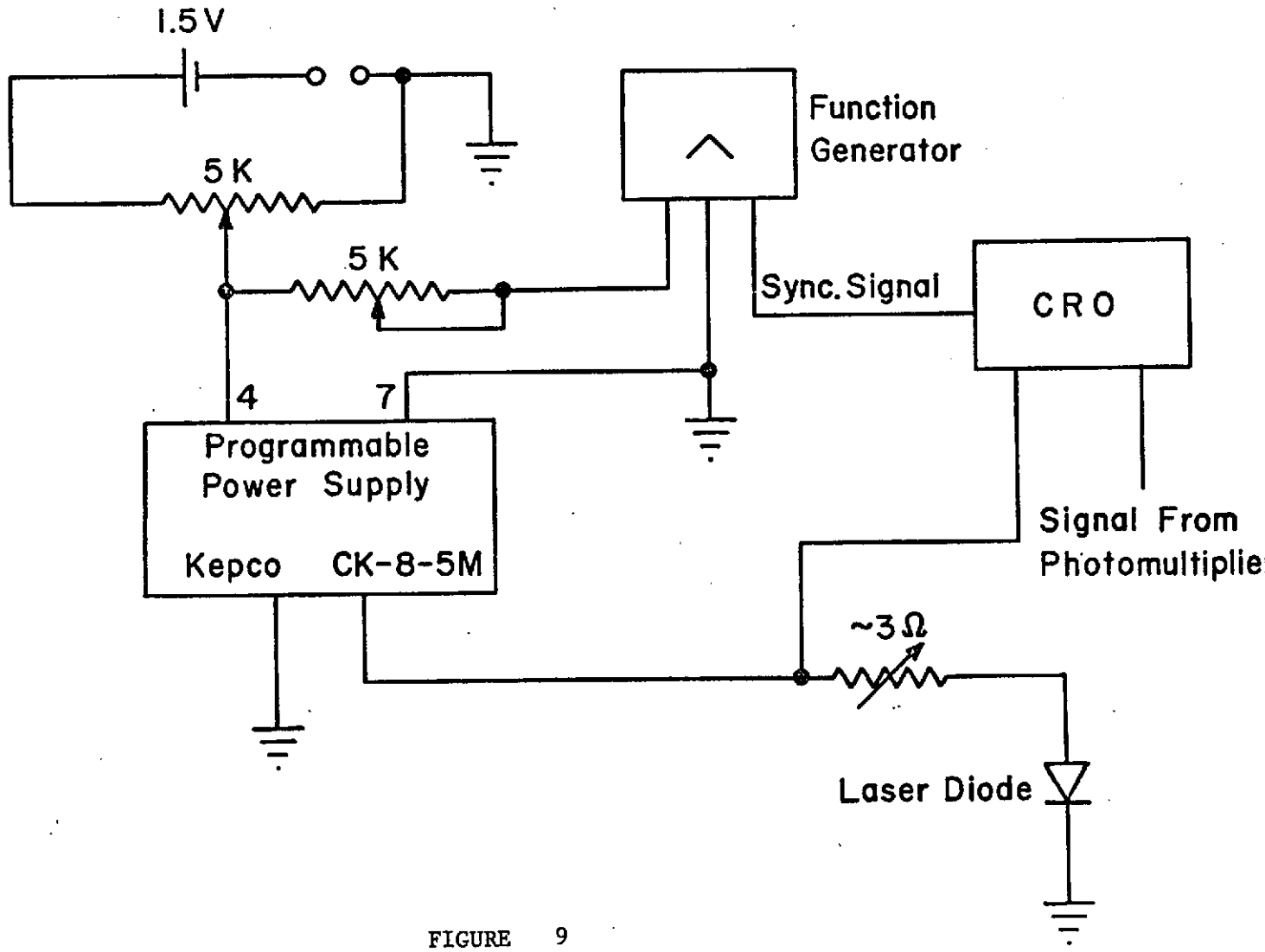

FIGURE 9

Circuit for modulating the current through the laser diode

adjusted independent of the modulation. This was done by using a programmable low voltage power supply (Kepco-CK-5M). Complete circuit diagram is shown in Figure 9.

The current modulation was triangular in shape. This was essentially dependent on the shape of the control voltage from the function generator. Voltage across a small resistance in series with the diode laser, was used to monitor the change in the current. A sync-signal from the function generator provided the trigger for the scope. Amplitude and frequency of modulation could be controlled by adjusting the amplitude and frequency of the control signal-voltage.

C. Population Inversion in the Ground State Hyperfine Levels of Cs-133.[59,60]

The laser mode was used to monitor the populations in the two ground state hyperfine levels as well as to perform the hyperfine pumping. The laser mode was swept through the resonance line of Cs-133 at 8521A^{o}. The intensity of the radiation scattered from cesium vapor served as an indicator of the populations of the hyperfine levels under observation. Observations made with two lasers are discussed below.

1. Observations with Laser #1

This was our first successful attempt to observe the resonance scattering, though incomplete. We visually observed the two resonance scattering peaks, corresponding to the transitions ending on the two ground state hyperfine levels, on the screen of CRO. Before we could get ready to take the picture, the laser died. The laser was examined under microscope and a dark filament was observed as seen in Figure[10]

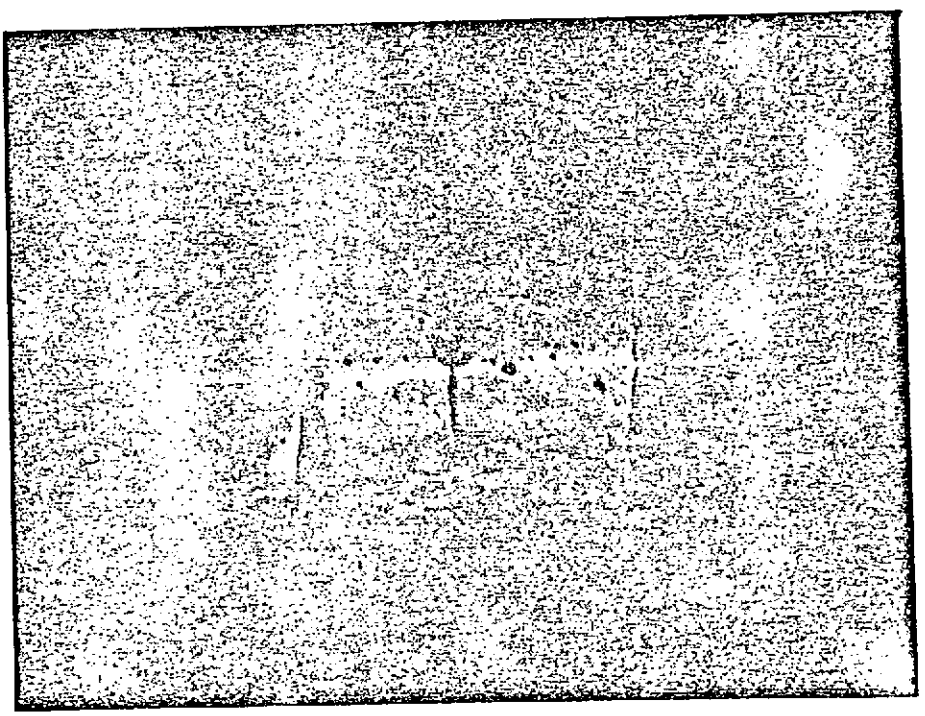

FIG. 10 PHOTOGRAPH OF THE BROKEN/BURNT DIODE LASER. THE WHITE HORIZENTAL LINE INDICATES THE POSITION OF THE JUNCTION.

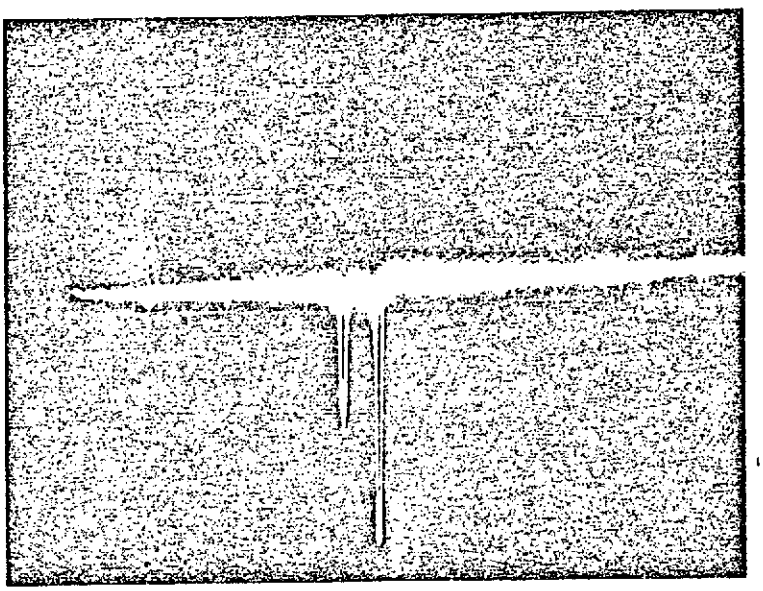

FIG. 11. THE RESONANCE RADIATION SCATTERED BY A Cs-133 CELL FILLED WITH 100 TORR OF NEON. (TIME SCALE: 50 ms/cm, VERTICAL SCALE: ARBITRARY)

One possible explanation can be that the laser crystal broke under excessive pressure from the holder. Another broken piece is seen on the left side in the picture. Another possible explanation can be that the current was excessively confined in a filament and it locally burned the diode.

2. Observations with Laser #2

Observations with this laser provided the maximum useful data and information concerning optical pumping effects in Cs-133. Figure 11 shows the resonance radiation scattered at an angle of 90^{o} to the incoming radiation as the laser mode was swept in frequency decreasing from left to right. In this case the Cs-133 vapor cell contained 10cm of Neon as a buffer gas. The transitions involved were $6P_{3/2}$ to $6S_{1/2}$ (F = 3 and F = 4) resulting in the two recorded lines. These lines were observed as the injection current was increasing. This means that the temperature of the junction was also increasing, and that the band gap of the semiconductor material was decreasing. In other words, the picture was taken during a time of increasing wave length of the laser radiation. Therefore, the first peak on the left corresponds to the transition which ends in the F = 3 state, and the second one to the transition ending in the F = 4 state. Since the separation of these two transitions is 9192 MHz, and the oscilloscope time base is 50 msec/cm, the laser radiation was sweeping at about 18GHz/cm in this trial.

The excited state hyperfine levels are unresolved because the Doppler- and pressure-broadened line widths are greater than the hyperfine separations. Using the known separation of the two observed peaks,

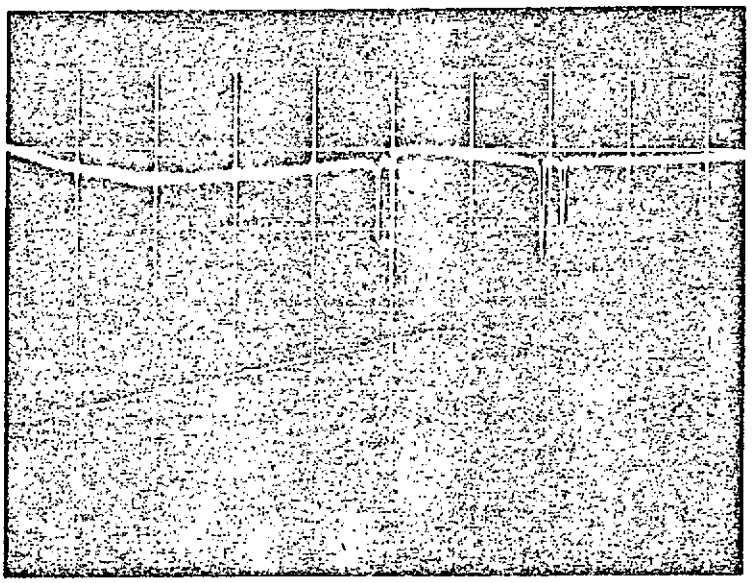

FIG. 12 THE RESONANCE RADIATION SCATTERED BY THE SAME CELL AS IN FIGURE 11 BUT AT A SLOWER LASER SWEAP RATE. THE LOWER TRACE SHOWS THE INJECTION CURRENT. (TIME SCALE: 200 ms/cm, VERTICAL SCALE IS ARBITRARY.)

and assuming a linear sweep of the laser mode, the measured line width of each of the two lines is approximately 1300 MHz.

The unequal amplitudes of the two peaks would be expected to result from two effects: first, and mainly, the degeneracy of the F = 3 level is 7 and that of the F = 4 level is 9, so that the strengths of the two lines are in the ratio 7:9. Secondly, the power output of the laser may vary slightly with increasing current. However, an examination of Figure 11 shows that the ratio of amplitudes is not 7:9 but closer to 1:2. The clue to the reason for this is shown in Figure 12 in which the left two resonances correspond to increasing current (and hence increasing wave length) from left to right, and the right two to decreasing current (because of triangular sweep).

In this case, the ratio of the peak heights for each pair has fallen closer to 7:9. The only difference in these two cases is that, in Figure 11 the sweep rate is such that the time required to pass from one resonance line to the next is about 25 msec, and in Figure 12 it is about 40 msec. This indicates that substantial number of atoms are being pumped into the F = 4 level and that the hyperfine relaxation time is long enough so that there is still greater than an equilibrium population in the F = 4 state when the laser radiation sweeps through that line 25 msec later but near to equilibrium population 40 msec later. In the cesium cell being examined, the spin relaxation time was measured to be about 18 msec. In the case of atoms for which the hyperfine relaxation time [61,62] can be measured, for example Rb^{87}, the spin relaxation time and the hyperfine relaxation time are roughly the same at

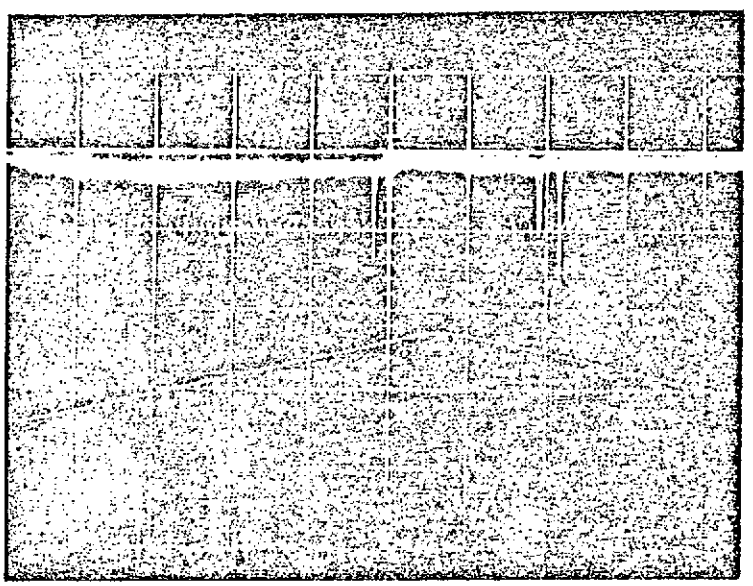

FIG. 13 THE RESONANCE RADIATION SCATTERED BY THE WALL-COATED CELL (AND WITHOUT ANY BUFFER GAS). (VERTICAL SCALE: ARBITRARY; TIME SCALE: 200 ms/cm)

room temperature, so one might reasonably expect the hyperfine relaxation time for cesium in this cell to be close to 18 msec.

Additional evidence in support of the hypothesis of hyperfine pumping is provided by the experiment displayed in Figure 13. Here the sample cell has been replaced by one with "Paraflint" coated walls, in which the cesium atoms have a spin relaxation time of over 200 msec. It can be seen in this case that the ratio of the amplitudes of the peaks of the pair on the ascending sweep is different from the ratio on the descending sweep: on the ascending sweep there is pumping of the atoms from the lower hyperfine level into the upper hyperfine level where they can exist for times longer than the sweep time for the pair. On the descending sweep the process is reversed, so that the relative amplitudes are greatly changed. The above-mentioned observations with the buffered and coated cells were consistently repeatable (except for minor variations corresponding to the variations of the laser output) from sweep to sweep and on interchanging the cells back and forth.

It was also encouraging to note that the laser mode could be held for a few seconds on either of the absorption lines by manually controlling the injection current, indicating that automatic locking should be easily possible.

D. Conclusions.

It should now be relatively easy to make a cesium maser. The power available in a single mode from a GaAs laser is considerably in excess of what is required to operate an alkali maser. Since small aperatures will suffice to let the resonance radiation from diode lasers

into the cavity, it should be easily possible to make a cavity with a high Q-value. CW operation of a maser may then be achieved by locking the laser mode to the center of the shorter wave length hyperfine absorption line.

Onealso could make a miniaturized, cell-type frequency standard by utilizing the selective hyperfine pumping of cesium vapor. With the foreseeable development of appropriate semiconductor lasers, it also should be possible to make a rubidium maser and frequency standard in a similar way.

It will be most interesting to experimentally examine the results of using coherent radiation from lasers in optical pumping experiments. For one thing, it should now be possible to measure the hyperfine relaxation time of cesium atoms. Perhaps even more interesting will be an examination of the effects of using a coherent light source; if coherent radiation is used to perform optical pumping the behavior of the atomic electric dipoles should be similar to that of magnetic dipoles subjected to a radio frequency field. A restudy of the light shifts of the ground state levels of alkali vapors will be worthwhile. One could, for example, study the behavior of the light shifts as the laser line is swept through the Doppler-broadened absorption lines. Non-linear interactions between microwave and optical transitions exhibited in the light shifts may be useful in relating these regions of the electomagnetic spectrum. It should also soon be possible to eliminate errors due to the light shifts of atomic frequency standards by locking the laser line to the center of the hyperfine absorption line.

REFERENCES

1. I. Hayashi, M. B. Panish , P. W. Foy and S. Sumski, Appl. Phys. letters, 17, 109 (1 Aug. 1970).
2. P. P. Sorokin and J. R. Lankard, IBM J. of RES. and DEV., 10, 162,1966.
3. P. P. Sorokin, J. R. Lankard, H. C. Hammond, V. L. Moruzzi, IBM J. of Res. and Dev., 11, 130, 1967.
4. O. G. Peterson and B. B. Snavely, Appl. Phys. Letters, 12, 238, 1968.
5. O. G. Peterson, S. A. Tuccio and B. B. Snavely, Appl. Phys. Letters 17, 245 (Sept. 1970).
6. Yalushi Miyazoe and Maeda, Appl. Phys. Letters, 12, 206, (1968).
7. P. P. Sorokin, J. R. Lankard, V. L. Moruzzi, and A. Lurio, Appl. Phys. Letters, 15, 179 (1969).
8. P. A. Franken, A. E. Hill, C. W. Peters and G. Weinreich, Phys. Rev. Letters, 7, 118 (1961).
9. N. M. Kroll, Phys. Rev. 127, 1207, 1962.
10. J. A. Armstrong, N. Bloemberger, J. Ducuing and P. S. Pershan, Phys. Rev. 127, 1918, 1962.
11. R. H. Kingston, Proc. IRE 50, 472, 1962.
12. J. A. Giordmaine and Robert C. Miller, Phys. Rev. Letters, 14, 973, 1965.
13. R. G. Smith, J. E. Geusic, H. J. Levinstein, J. J. Rubin, S. Singh, and L. G. Van Uitert, Appl. Phys. Letters, 12, 308, 1968.
14. S. E. Harris, Proc. IEEE, 57, 2096 (1969).
15. S. E. Harris, Appl. Phys. Letters 14, 355 (1969).
16. R. Braunstein, Phys. Rev. 99, 1892, 1955.

17. R. N. Hall, G. E. Fenner, J. D. Kingsley, T. J. Soltys and R. O. Carlson, Coherent light emission from GaAs junctions: Phys. Rev. Letters Vol. 9. pp 366-378, Nov. 1962.

18. T. M. Quist, R. H. Rediker, R. J. Keyes, W. E. Krag, B. Lax, A. L. McWhorter and H. J. Zeiger, Semiconductor maser of GaAs. Appl.

19. N. G. Basov and Y. U. M. Popov: Semi-Conductor Lasers; Sovt Physics-Semiconductors Vol. 1 #11, p. 1325, May 1968.

20. V. S. Vavilov and E. L. Nolle; CdTe Laser with Electron Excitation, Sovt. Phys. Doklady; Vol. 10 #9, p. 827, March 1966.

21. C. Benoit a La Guillaume and J. M. Deberier: Effect Laser Dans Le Sulfure de Cadmium par Bombardment Electronique; Comptes Rendus, Vol. 261, #25, p. 5428, 1965.

22. C. E. Hurwitz: Efficient Untraviolet Laser Emission in Electron-Beam excited InSb:Appl. Phys. Lett. Vol. 9, #3, p. 116, 1966.

23. C. D. Hurwitz: Electron Beam pumped lasers of CdSe and CdS; Appl. Phys. Lett. Vol. 8 #5 p. 121, 1966.

24. F. H. Nicoll: Ultra violet ZnO Laser pumped by an electron beam; Appl. Phys. Lett. Vol. 9, #1, p. 13, 1966.

25. C. Chipauk, G. Duraffourg, J. Loudette, J. P. Novlanc, and M. Bernard: Emission stimulee dans l'Antimoniure de Gallium; Proc. Conf. on Radiative Recombination in Semiconductors; p. 217, Dunod, Paris 1965.

26. R. H. Phelan, A. R. Calawa, R. H. Rediker, R. J. Keyes and B. Lax: Infrared InSb laser diode in high magnetic fields; Appl. Phys. Lett. Vol. 3, #9, p. 143 1963.

27. K. Weiser and R. S. Levitt: Stimulated emission from InP; Appl. Phys. Lett. Vol. 2, #9, p. 178, 1966.

28. I. Melgailis: Maser action in InAs diodes; Appl. Phys. Lett. Vol. 2, #9, p. 176, 1963.

29. J. F. Butler, A. R. Calawa, R. J. Phelan, T. C. Harman, A. J. Strauss and R. H. Rediker: PbSe diode laser, Appl. Phys. Lett. Vol. 5, #4, p. 75, 1964.

30. J. F. Butler, A. R. Calawa, R. J. Phelan, Jr., A. J. Strauss, and R. H. Rediker "PbSe diode laser". Solid State Commun. Vol. 2, #10, p. 303, 1964.

31. J. F. Butler and A. R. Calawa: PbSe diode Laser; J. Electrochemical Soc. Vol. 112, #10, p. 1056, 1965.

32. J. J. Tietjen, J. I. Pankove, I. J. Hegyi and H. Nelson, Trans. Metallurgical Soc. of AIME, 239, 385 (1967).

33. F. J. Reid: Semiconductor light emitters; Battelle Technical Rev. p. 3, 1967. Laser Focus, March,69, p. 40.

34. J. O. Dimmock, I. Melgailis, and A. J. Strauss: Band structure and laser action in$Pb_xSn_{1-x}Te$; Phys. Rev. Lett. Vol. 16, #26, p. 1193, 1966.

35. J. F. Butler, T. C. Harman, J. Quant. Electronics QE 5, 50, (1969).

36. A. J. Strauss, Phys. Rev. 157, 608, 1967.

37. P. G. Eliseev, I. Ismailov, A. I. Krasil'nikov, M. A. Manko, and V. P. Strakhov, Soviet Physics-Semiconductors, Vol. 1, #8, 1094 (1967).

38. M. B. Panish, I. Hayaski and S. Sumski, Appl. Phys. Letters 16, 326, (1970).

39. W. E. Ahearn and J. W. Crowe: IEEE J. Quantum Electronics, QE-2, p. 597, 1966.

40. M. B. Panish, I. Hayashi and S. Sumski, IEEE J. Quantum Electron. 5, 210, (1969).

41. I. Hayashi, M. B. Panish and P. Foy, IEEE J. Quantum Electron. 5, 211 (1969).

42. I. Hayashi and M. B. Panish, J. Appl. Physics 41, 150, 1970.

43. Henry Kressel and N. E. Byer, Proc. IEEE, 57, 25 (1969).

44. S. A. Steiner and R. L. Anderson, Solid State Electron. 11, 65, (1968).

45. K. Weiser, J. Appl. Phys. 34, 3387 (1963).

46. R. L. Longini, Solid State Electron., 5, 127 (1962).

47. C. D. Doleson and F. S. Keeble, Symp. on GaAs pp. 68 (1966).

48. M. I. Nathan: Proc. IEEE, Vol. 54, p. 1276, 1966.

49. Wataru Susaki, Japanese J. of Appl. Phys., Vol. 6, p. 977, 1967.

50. R. W. Keyes: IBM Journal of Research & Development, Vol. 9, p. 303, 1965.

51. S. Mayburg: J. Appl. Phys., Vol. 34, p. 3417, 1963.

52. M. Pilkuhn, H. Rupprecht, and S. Blum: Solid State Electronics, Vol. 7, p. 905, 1964.

53. S. Mayburg: J. Appl. Phys., Vol. 34, p. 1791, 1963.

54. W. J. Turner and W. E. Reese: J. Appl. Phys., Vol. 35, p. 350, 1964.

55. W. E. Engler and M. Garfinkel: J. Appl. Phys., Vol. 34, p. 2746, 1963.

56. G. Burns and M. I. Nathan: Proc. IEEE, Vol. 52, p. 770, 1964.

57. A. Yariv: Quantum Electronics (John Wiley), p. 409, 1967.

58. J. A. Armstrong and A. W. Smith: J. Appl. Phys., Vol. 4, No. 11, p. 196, 1964.

59. Gurbax Singh, P. Dilavore, and C.O. Alley: J. Quantum Electronics, QE-7, #5,p.196,(1971).

60. Note- Sweeping of the 8521 Å line of Cs-133 by a laser pulse obtained by the superposition of a dc and a 5-10 μsec current pulse[60a] and a by a nanosecond current pulse[60b] has been reported previously. But to our knowledge no evidence of population inversion has ever been reported before this work[59] .

60a. S. Siahatgar and U. E. Hochuli : J. Quantum Electronics, QE-5,295, (1969)

60b. B. Bolger and J. C. Diehls, Phys. Lett. 28A, 401 (1968).

61. M. Arditi and T. R. Carver, Phys. Rev. 136, A643 (1964).

62. M. A. Bouchiat, Thesis, Paris 1964; Publications Scientifiques et Techniques du Ministere de Paris N.T. 146, 1965.

****

PART TWO

TABLE OF CONTENTS

Chapter		Page
OPTICAL PUMPING OF ALKALI VAPORS AND PHASE DESTRUCTION DETECTION OF GROUND STATE HYPERFINE TRANSITIONS IN CESIUM -133.		
I.	GENERAL DISCUSSION	1
	A. Introduction	1
	B. A Brief Review of the Concept of Optical Pumping	2
	C. The Triple Resonance Coherent Pulse Technique for the Study of 0-0 Transitions	5
	D. Energy Spectrum of Alkali Atoms in a D.C. Magnetic Field	9
II.	THEORY OF OPTICAL ORIENTATION AND DETECTION . . .	12
	A. Theory of Optical Orientation	12
	B. Optical Detection of the Angular State of the Atomic System in the Ground State . . .	14
	C. Optical Detection of Magnetic Resonances . .	18
III.	PHASE DESTRUCTION METHOD AND LIGHT SHIFTS . . .	20
	A. Theory of the Phase Destruction Method Using Coherent Pulse Technique	20
	B. Light Shifts in Alkali Atoms	25
IV.	ENHANCEMENT OF OPTICAL SIGNALS	28
	A. General discussion	28

Chapter | Page

B. Relation Between the Longitudinal Relaxation and the Hyperfine Frequency Shifts in Coated Cells . 29

V. INSTRUMENTATION 35

A. General Description 35

B. Effects of the Instability and Inhomogeneity of the D.C. Magnetic Field 40

1. Effect of Magnetic Field Instability . . 40

2. Effect of Magnetic Field Inhomogeneity . . 42

C. Production of the D.C. Magnetic Field . . . 42

D. Generation of the Rotating Magnetic Field Pulses 44

1. Need for Circularly Polarized Resonance Radio-frequency Fields 44

2. Generation of the ±90°-Rotating Field Pulses 47

3. Effect of the Instability of the 100 KHz Oscillator 47

E. Transmission Gates 49

F. Performance of the Gates and the 90 - Phase Shifters 51

G. Stabilized Microwave Sources 51

1. Automatic Phase Control System (APCS) . . 51

2. Phase Locked Points 54

3. Coupling of Microwave Fields to the Vapor-cells 54

Chapter		Page
	4. Pulsing of Microwaves	54
VI.	CONSTRUCTION OF THE PULSED CESIUM RESONANCE LAMP . .	58
	A. Difficulties in Pulsing the Resonance Lamp . .	58
	B. Considerations for the Design of the Pulsed Cesium Resonance Lamp	60
	C. Construction and Excitation of the Lamps . .	60
VII.	PREPARATION OF WALL-COATED CESIUM VAPOR CELLS . .	65
	A. Coating with Paraflint	65
	B. Properties of Paraflint	65
	C. Fractional Distillation of Paraflint . . .	66
	D. Experimental Procedure for Wall Coating . .	68
	E. Distilling of Cs Into the Cells	69
	F. Cells With Wall-coating and a Buffer Gas . .	69
	G. Performance of the Vapor Cells	69
VIII.	DETECTION OF HYPERFINE RESONANCES OF Cs-133 BY THE METHOD OF PHASE DESTRUCTION	73
	A. Preliminary results	73
	1. Effect of 180° -Pulses	73
	2. Effect of one 90° - Pulse	73
	3. Effect of $+90^{\circ}$ - Pulse Followed by a -90°- Pulse	80
	4. Pumping Light Off in Between the $\pm 90^{\circ}$ - Pulses	80
	B. Observations on the Hyperfine Resonances . .	86
APPENDIX	EFFECT OF A ROTATING MAGNETIC FIELD PULSE ON A PURE QUANTUM STATE $\|F,\mu\rangle$	91
REFERENCES	. . . . .	96

LIST OF TABLES

Table		Page
I.	$D^{4}_{\mu\mu}$,(0,Π/2,0)	22
II.	$D^{2}_{\mu\mu}$,(0,Π/2,0)	23
III.	Resonance Frequency Corresponding to the (4,0) ↔ (3,0) Transition	88

LIST OF FIGURES

Figure		Page
1.	Schematic Representation of the Triple Resonance Coherent Pulse Technique	6
2.	Energy Level Diagram of Cs^{133} ($I = \frac{7}{2}$)	10
3.	Schematic Represention of Optical Transitions in the Optical Pumping Cycle in Cs^{133}	15
4.	View of the Experimental Arrangement	36
5.	Schematic Representation of the Experiment	38
6.	Feedback System Used to Eliminate Noise in the Magnetic Field.	43
7.	Illustration of the Performance of the Feedback System	43
8.	90°-Phase Shifters and Mixers for the $\pm 90^{\circ}$ RF Pulses	46
9.	Binary Driven Transmission Gates	48
10.	100KHz Pulses From Gate 1 and Gate 2	50
11.	90°-Phase Shifted Components of an 100KHz Pulse	50
12.	Klystron Phase Lock Stabilizer	52
13.	Control Circuit for the Microwave Switch	55
14.	Demonstration of the Performance of the Microwave Switch	56
15.	Schematic of the Two Identical Exciter Oscillators	59
16.	Performance of the Dumbbell Shape Resonance Lamp	61
17.	Illustration of the Stability of the Cesium Resonance Lamp.	63
18.	Arrangement for Making Paraflint Coated Cesium Vapor Cells	67

Figure		Page
19.	Plot of 'Inverse Relaxation Time' vs Light Intensity for 2.5" and 2" diameter wall coated cells . . .	70
20. a, b	Absorption of the Pumping Light Versus Time . . .	74
21.	Modulation of the Transverse Beam of Resonance Light by the Freely Precessing Cs-133 Atoms . . .	75
22. a-f	Absorption of the Pumping Light Intensity for Different Time Intervals	77 78
23. a, b	Absorption of the Pumping Light When the Incident Light Intensity was Reduced to $I_o/2$.	79
24. a-j	Absorption of the Pumping Light for Different Time Intervals Between the +90° and -90° RF Pulses. . .	81-85
25. a, b	Detection of the 0-0 Transition in the Ground State of Cs-133	87

CHAPTER I

GENERAL DISCUSSION

A. Introduction

In principle the operation of gas cell atomic frequency standards depends on the creation of an excess population in one of the two $M_F = 0$ hyperfine states which are otherwise almost equally populated at room temperature. In order to create optically the desired population difference, it is necessary to irradiate the atoms in the states to be depleted. However, the hyperfine lines of the optical doublet emitted by a resonance lamp excite nearly equally the atoms in both of the $M_F = 0$ states. It is thus essential to filter out one hyperfine component in order to achieve differential pumping of the $M_F = 0$ states. In general, it is virtually impossible. Fortunately, rubidium atomic standards are practical because of a unique energy level structure. One of the hyperfine optical transitions of Rubidium-87 happens to be nearly coincident with one of Rubidium-85. Thus, the atoms of the one isotope may serve as a hyperfine filter for the radiation from the atoms of the other and it is possible to selectively pump the hyperfine levels of the desired isotope. In the case of cesium, no such happy coincidence exists in a convenient source, and a cesium maser or a practical cell type cesium atomic clock is yet to be produced. However, since cesium atomic frequency standards which operate upon a beam of atoms are capable of a high degree of stability and reproducibility, and constitute the present international

frequency standard, it seems highly desirable to operate a cesium maser or a cell type cesium frequency standard.

One of the most important aspects of this investigation was to develop a technique to solve the problem associated with the hyperfine pumping of Cs-133. The new technique makes it possible to optically detect the 0-0 transition in the ground state of the alkali vapors (Cs-133, Rb-87, etc.) without using a hyperfine filter. A compendium to this technique is given in this chapter after giving a brief review of the concept of optical pumping. The details form the subject matter of the rest of part I of this report.

B. A Brief Review of the Concept of Optical Pumping

The term optical pumping (Pompage Optique) means the creation by optical means of non-statistical populations of atoms among a set of quantum states at the temperature of the experiment. It is done by the transfer of angular momentum or energy (or both) from polarized or unpolarized photons to the atoms. It is one of the most important techniques for obtaining non-statistical distribution of atoms among their energy levels. The states in question might be electronic vibrational or rotational energy levels, or they might be zeeman, hyperfine or stark sublevels.

Brossel & Kastler[1] were the first to draw attention to the possibility of optical orientation of atoms, in 1949. In 1950, Kastler[2] expounded a detailed scheme to optically polarize atoms. His paper was followed by a great deal of both experimental and theoretical work[3-20]. Presently, the methods of optical pumping and of optical detection of magnetic or hyperfine resonances form a field of research that has

expanded rapidly in several directions during the last two decades. They form a powerful method of investigating the atomic level structure in the excited or ground state, including the precise determination of nuclear hyperfine interactions and their light shifts and pressure shifts, the determination of disorientation cross-sections and spin exchange cross-sections for atomic collisions. On the practical side, these concepts have led to the development of the maser, laser, various kinds of atomic frequency standards, and very sensitive magnetometers.

In the course of time, experimental techniques were refined, and new concepts and techniques introduced. A novel method for the optical detection of 0-0 magnetic hyperfine transition in the ground state of Rb-87 was first conceived and demonstrated by C. O. Alley.[16-18] This method relies on the destruction of the phase relationship between the 0-states and their partner Zeeman states which are in a coherent superposition state describing free precession. It provides a very sensitive scheme for the detection of 0-0 hyperfine resonances, and yields relatively large optical detection signals. Moreover, it makes possible artificial line narrowing by exciting the hyperfine resonances with two phase coherent microwave pulses separated in time to select the long lived atoms.

In a typical optical pumping experiment, a beam of circularly polarized photons is passed through a resonance cell containing the atoms to be pumped. The light beam is in the direction of a uniform D.C. magnetic field. The selection rules governing the process of absorption and re-emission dictate that $\Delta M_F = +1$ (absorption) and $\Delta M_F = \pm 1$ or 0 (re-emission); consequently the atoms are gradually pumped from the sublevels of low M_F to levels of high M_F values in the ground state.

In the absence of ground state relaxation, all the atoms can ultimately be forced into the state of highest angular momentum, resulting in a non-zero magnetic moment.

Inert gas is generally added to the cell containing the atoms to be pumped in order to inhibit the atoms from reaching the walls of the container; because on collision with untreated walls, the atoms are most unlikely to retain the state to which they were originally pumped. Though the presence of buffer gases can prolong the life of the pumped atoms in the ground state, it has an adverse effect on the attainment of the degree of polarization when alkali vapors are pumped with D_2 light. This is because when the atoms are excited to the $P_{3/2}$ state with circularly polarized D_2 light, collisional interactions between the alkali atoms and the buffer gas atoms mix the atoms among excited state sublevels prior to de-excitation. An atom in the $|F,F>$ ground state may be excited to the $P_{3/2}$ state where this collisional mixing process makes its return equally probable to each of the ground state sublevels. Thus it is lost to the pumped ground state to which it originally belonged, and that state is depopulated. In the case of pumping with $D_1(S_{1/2}{\rightarrow}P_{1/2})$ photons, the atoms, once pumped into $|F,F>$ state, have zero probability for σ^+- D_1 absorption. Thus they accumulate in the $|F,F>$ state except for relaxation.

Consequently, if pumping with - D_2 is desired, the atoms must be contained in a cell with its walls coated with nonrelaxing materials and buffer gas must not be used. Coated wall cells are also as good when Pumped with D_1 radiation .

Any change in the distribution of populations between the hyperfine or Zeeman sublevels, produced by microwave or radio frequency

fields, causes a change in the overall absorption or scattering of light by the sample, and can therefore be detected by means of optical photons. The superiority of this method of detection over others lies in the fact that resonances involving RF photons of 3×10^{-5}ev energy are detected by optical photons of 1-2ev energy. This obvious gain in energy considerably improves the signal-to-noise ratio of the detected signals. Since the Doppler breadth of the photons does not enter in this type of experiments, because information on the intensity or polarization of the absorbed or scatterd light rather than its frequency distribution is sought, it provides a very sensitive method of detecting narrow magnetic transitions (hyperfine or Zeeman).

C. The Triple Resonance Coherent Pulse Technique for the Study of 0-0 Transitions

In what follows, we shall specialize this technique to the case of cesium atoms contained in a wall-treated gas cells. In our experiment, Cs atoms were polarized with σ^+ D_1 light along the direction of the pumping light. (A weak magnetic field was also applied in the same direction). The cesium atoms are thus pumped into the highest angular ground state $|4,4\rangle$. The polarized atoms are then subjected to a 90° rf pulse at Zeeman splitting frequency to induce free precession in the plane perpendicular to the magnetic field. The initial $|4,4\rangle$ state becomes a coherent superposition of the partner magnetic states and can be written as

$$\Psi\left(\frac{\pi}{2}\right) = \frac{1}{16}|4,4\rangle + \frac{1}{4\sqrt{2}}|4,3\rangle + \frac{\sqrt{7}}{8}|4,2\rangle + \frac{\sqrt{14}}{8}|4,1\rangle + \frac{\sqrt{70}}{16}|4,0\rangle + \frac{\sqrt{14}}{8}|4,-1\rangle + \frac{\sqrt{7}}{8}|4,-2\rangle + \frac{1}{4\sqrt{2}}|4,-3\rangle + \frac{1}{16}|4,-4\rangle \qquad \text{I.1}$$

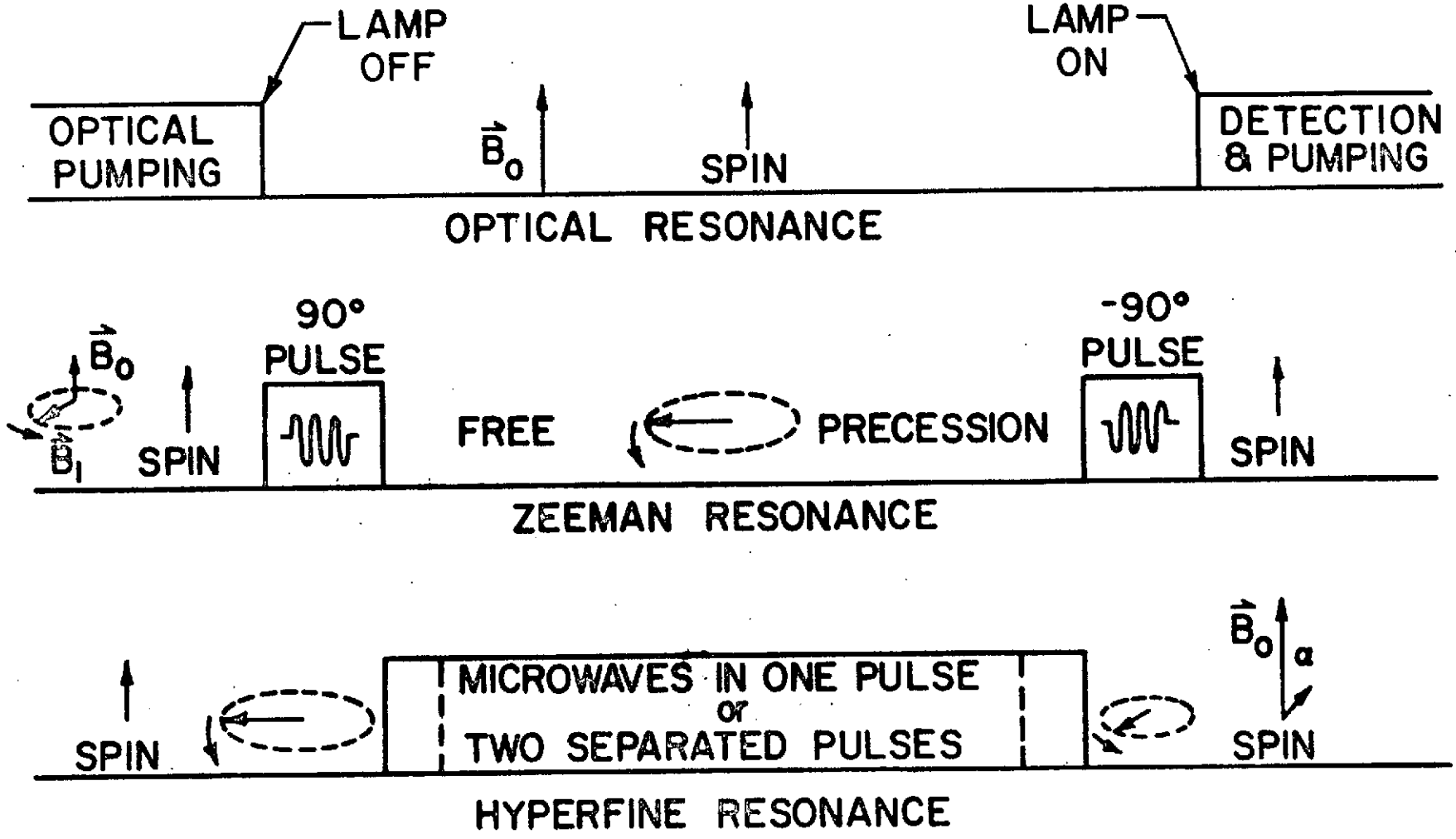

Fig. 1

SCHEMATIC REPRESENTATION OF THE TRIPLE RESONANCE COHERENT PULSE TECHNIQUE

The original $|4,4\rangle$ state can be reproduced by a -90°rf pulse (i.e. coherent with the first pulse but phase inverted) provided relaxation or other disturbing effects were neglegible. This sequence of pulses would bring back the original state of polarization with the same optical absorption (Fig. 1).

One notices in the coherent superposition state $\Psi(\pi/2)$ that the amplitude of the $|4,0\rangle$ state is quite large as compared to the rest of the states. If it were coupled to the $|3,0\rangle$ state by microwaves at resonance with the hyperfine splitting, the wave function would be altered considerably. In our experiment, the sample atoms are subjected to a microwave pulse by getting the output from a klystron which is phase locked to a highly stable crystal oscillator. If the microwave pulse is followed by a -90° pulse, it does not produce the original $|4,4\rangle$ as it doesin the absence of the microwave pulse. The net result of this set of operations is to change the optical absorption of the sample from what it would have been if the microwave pulse was absent or off resonance. By monitoring the light passing through the sample and varying the frequency of the microwaves, the hyperfine separation in the ground state may be determined. Some of the advantages of this technique are listed below.

1. One can study the hyperfine transitions by optical means in atoms where hyperfine filtering is impossible. A practical application of this method can be the making of a cell type cesium atomic clock.

2. The optical pumping radiation can be switched off when the microwave fields are on. This eliminates any perturbation of the hyperfine levels due to the optical fields (light shifts) at the time, when these levels are being examined with the help of the microwaves.

3. The study of the interaction of the atoms with the walls of the container (wall shifts) can be made in the absence of light shifts.

4. The signal-to-noise ratio is much higher, so the line width can be artificially narrowed by selecting the long lived atoms. This is done by increasing the time interval between $\pm 90°$ rf pulses and by applying the microwaves for a longer interval or in two coherently phased pulses at the beginning and at the end of this interval. One expects the line width to be of the order of the reciprocal of the time interval between the microwave pulses. However, this interval cannot be arbitrarily extended due to the finite relaxation time and dephasing caused by the very small but not insignificant instability in magnetic field.

This technique was first conceived and demonstrated by C. O. Alley (for the case of Rb-87). In his experiments performed at the Princeton University, the time interval between the 90°- pulses was limited to about 6msec or less due to the instability and inhomogeneity of the magnetic field. In the present investigation, an interval of over 50 msec. between the 90°- pulses has been used. However, a small signal could be seen up to an interval of 80 msec.

D. Energy Spectrum of Alkali Atoms In a D.C. Magnetic Field

For a quantitative understanding of optical pumping, coherent pulse technique and other related topics, a brief discussion of the energy spectrum of alkali atoms in a weak magnetic field will be useful. The Hamiltonian of the atom in a D.C. magnetic field B_o can be written in the standard notation as:

$$H = E_{LJ} + A\vec{I}.\vec{J} + \frac{B}{2I(2I-1)J(2J-1)}\{3(\vec{I}.\vec{J})^2 - \frac{3}{2}(\vec{I}.\vec{J}) - I(I+1)J(J+1)\} - g_J\mu_e\vec{J}.\vec{B}_o - g_I\mu_n\vec{I}.\vec{B}_o \qquad \text{I.2}$$

where E_{LJ} is the multiplet and spin-orbit energy. For the ground state of the alkali atom, J=1/2 and the electric quadrupole interaction constant B vanishes. In a weak magnetic field, as in this investigation, $\vec{I}$ and $\vec{J}$ remain coupled due to the $\vec{I}.\vec{J}$ interaction and there is a precession of each about the total angular momentum, $\vec{F}=\vec{I}+\vec{J}$.

Therefore, the energy operator that describes the magnetic interaction of the nucleus with the valence electron $(\vec{I}.\vec{J})$ and their interactions with the external magnetic field can be written as:

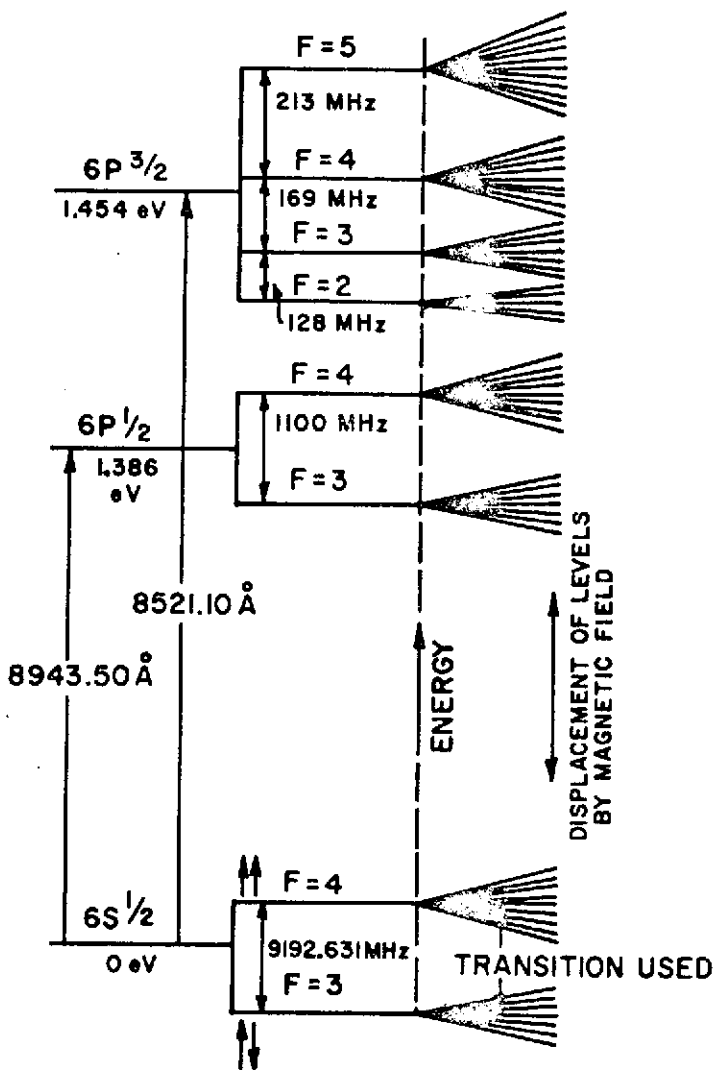

FIG. 2. ENERGY LEVEL DIAGRAM OF Cs^{133} ($I = \frac{7}{2}$)

$$H_m = H - E_{LJ} = \frac{AC}{2} - M_F B_o \{ g_J \mu_e \frac{F(F+1)+J(J+1)-I(I+1)}{2F(F+1)} + g_I \mu_n \frac{F(F+1)+I(I+1)-J(J+1)}{2F(F+1)} \} \quad \text{I.3}$$

where $C=F(F+1)-I(I+1)-J(J+1)$

The second term in the brackets is about 2000 times smaller than the first and can be neglected. Thus

$$H_m = \frac{AC}{2} - g_F \mu_e M_F B_o$$

$$\text{where } g_F = g_J \frac{F(F+1)+J(J+1)-I(I+1)}{2F(F+1)} \quad \text{I.4}$$

Energy levels of Cs-133 for which I=7/2 is depicted in figure 2. The magnetic dipole transition $|4,0\rangle \rightarrow |3,0\rangle$ is vital to the construction of Cesium atomic clocks. Its frequency is close to 9192.632 MHz.

The frequency of the other magnetic transitions between the Zeeman levels $|4,M_F\rangle$ was adjusted to 100KHz because of the availability of a very stable source at this frequency.

CHAPTER II

THEORY OF OPTICAL ORIENTATION AND DETECTION

A. Theory of Optical Orientation

Attainment of optical orientation in the ground state of alkali atoms essentially depends on the selective absorption of circularly polarized resonance radiation and its re-emission. The degree of polarization thus obtained depends very much on whether pumping is done by D_1 or D_2 radiation. It also depends on the amount of disorientation that may occur when the alkali atoms are in the excited state during the optical pumping cycle.

Consider an aggregate of alkali atoms placed in a weak magnetic field and subjected to right circularly polarized resonance radiation. Let $|F,\mu\rangle$ and $|F',m\rangle$ characterize the ground and the excited state respectively. The transition probability from the state $|F,\mu\rangle$ to the state $|F',m\rangle$ is given by

$$T = \frac{8\pi^3\nu}{hc}\left|\langle F,\mu|\hat{e}\cdot\vec{P}|F',m\rangle\right|^2 \rho_\nu \qquad \text{II.1}$$

where $\hat{e}$ is the polarization vector for the incident radiation and $\vec{P}$ is the electric dipole moment ($e\vec{r}$) of the atom, ρ_ν is the photon flux density at the frequency ν. Equation II.1 can be conveniently simplified by expressing $\hat{e}$ & $\vec{P}$ in terms of their spherical components and applying the Wigner-Eckert theorem. The interaction matrix elements can then be written as:

$$\langle F,\mu|P_\lambda|F',m\rangle = \langle F,\mu|F'm\lambda\rangle\langle F||P||F'\rangle \qquad \text{II.2}$$

P_λ refers to the spherical components of $\vec{P}$. The second factor on the right hand side is the reduced matrix element of $\vec{P}$ and is independent of the orientation numbers μ, m, and λ. The first factor (called the Clebsh-Gordon coefficients) contains the conservation of angular momentum. The Clebsh-Gordon coefficients vanish unless

$$m = \mu - \lambda$$
$$\text{and } F' - F = 0, \pm 1 \qquad \text{II.3}$$
$$F' = F = 0 \text{ being forbidden}$$

In simple words, if the incident light is pure circularly polarized σ^+, the absorption probability vanishes except for $m = \mu + 1$ and it is proportional to the square of the C.G. coefficients ($|\langle F,\mu | \vec{F} | m\lambda \rangle|^2$). During the process of emission, the photon can carry an angular momentum ± 1 or 0, and the change in angular momentum of the emitting atom must be ± 1 or 0.

Thus atoms in the ground state $|F,\mu\rangle$ absorb the σ^+ photon with an axial angular momentum +1 and go into the excited state $|F,\mu + 1\rangle$. This excited state will decay releasing a photon σ or π with angular momentum ± 1 or 0. On the average, the atoms which originally started from the ground state with an angular momentum μ will return to it with an increase in their angular momentum by unity. Thus if the atoms continuously go through the cycle of absorption and re-emission, principally all the atoms can be pumped to the highest angular momentum state. However, relaxation processes in the ground and excited states severely limit the applicability of the above argument. Relaxation of the polarized atoms in the ground state leads to an equilibrium value between the

pumping and the relaxation processes. One obtains fewer atoms pumped to the highest angular momentum state.

On the other hand, in the presence of high buffer gas pressures, excited atoms may have relaxation times for disorientation within the magnetic sublevels of the excited states shorter than their mean life time; loss of memory in the excited state may even result in a negative polarization in the ground state depending on the pressure of the buffer gas[21].

Figure 3 illustrates the optical pumping cycle for the case of Cs-133 being pumped by $\sigma^+ D_1$ radiation. It is important to note that in the case of pumping with D_1 radiation, the atoms which once get into the $|4,4\rangle$ ground state cannot absorb the $\sigma^+ D_1$-photons because there is no level in the $P_{1/2}$ state with a higher angular momentum. Thus the atoms cannot leave this state except on relaxation. However, this is not true when pumping with $\sigma^+ D_2$-radiation is desired because there is a level with higher angular momentum in the excited $P_{3/2}$ state. Atoms once pumped into the highest angular momentum ground state can still absorb a circularly polarized D_2-photon and may not return to the original state. So pumping with D_2 radiation is not as efficient as with D_1-radiation.

B. Optical Detection of the Angular State of the Atomic System in the Ground State.

The angular state of an atomic system in the ground state can be determined purely by optical means. The method is based on the fact that the absorption coefficients of oriented atoms for resonance light

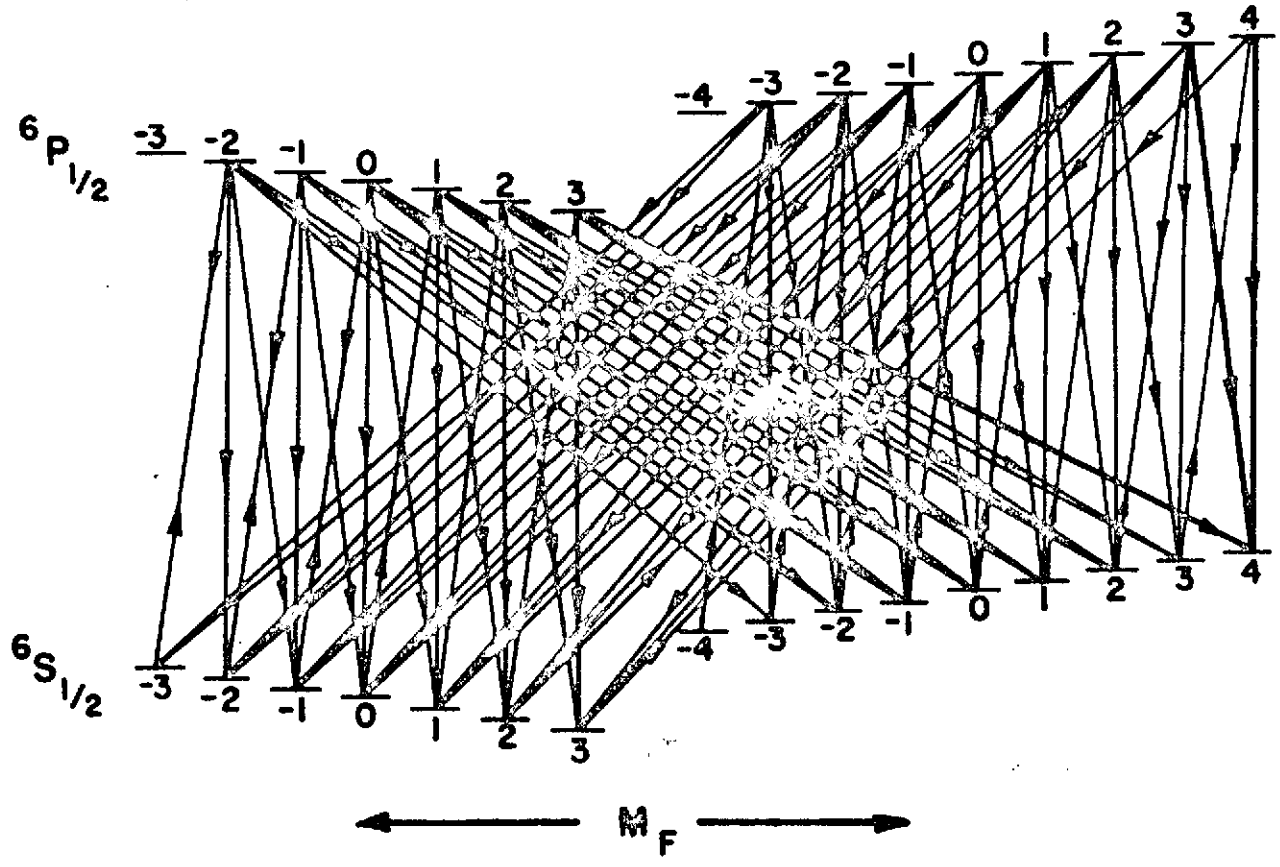

FIG. 3. SCHEMATIC REPRESENTION OF OPTICAL TRANSITIONS IN THE OPTICAL PUMPING CYCLE IN Cs-133

is different from the absorption coefficient for atoms in the disoriented state. Any change in the orientation can be observed by the corresponding change in the transmitted beam of resonance light. The absorption cell containing the atomic vapors will be fully transparent on complete orientation except for the small amount of light absorbed to cover up the relaxation loss. To make the discussion quantitative let us consider an atomic system whose ground and excited state are designated by μ and m. Let the density matrix elements in the laboratory representation be denoted by σ_{ij}. Here $\sigma_{\mu\mu}$ and σmm will represent the populations of the states μ and m respectively. Obviously, the number of photons absorbed in a unit time by the system is equal to the number of atoms that leave the ground state or arrive in the excited state in the same time. Hence, we can define a monitoring or an absorption operator M_A as

$$M_A = -\sum_{\mu} \frac{d}{dt} \sigma_{\mu\mu} = \sum_{m} \frac{d}{dt} \sigma_{mm} \qquad \text{II.4}$$

Neglecting the spontaneous emmission and the causes of population changes other than the interaction between the monitoring light and the atoms, one can write in the notation of Cohen-Tannoudji[19]

$$-\frac{d\sigma_{\mu\mu'}}{dt} = \left(\frac{1}{2T_p} + i\Delta E'\right)\sum_{\mu''} A_{\mu\mu''}\sigma_{\mu''\mu'} + \left(\frac{1}{2T_p} - i\Delta E'\right)\sum_{\mu''}\sigma_{\mu\mu''}A_{\mu''\mu'} \qquad \text{II.5}$$

$$\frac{d}{dt}\sigma_{mm'} = \frac{1}{T_p}\sum_{\mu\mu'} \langle m|\vec{e}.\vec{P}|\mu\rangle\langle\mu'|\vec{e}.\vec{P}|m'\rangle\sigma_{\mu\mu'} \qquad \text{II.6}$$

where

$$\frac{I}{2T_p} = \int_o^{+\infty} u(k)\,|A_k|^2 dk \frac{\Gamma/2}{[k - (\tilde{k}_o + \vec{k}.\vec{v})]^2 + \Gamma^2/4}$$

$$\Delta E' = \int_o^{+\infty} u(k)\,|A_k|^2 dk \frac{k - (\tilde{k}_o + \vec{k}.\vec{v})}{[k - (\tilde{k}_o + \vec{k}.\vec{v})]^2 + \Gamma^2/4} \qquad \text{II.7}$$

$$A_{\mu\mu'} = \sum_m \langle\mu|\vec{e}.\vec{p}|m\rangle\langle m|\vec{e}.\vec{p}|\mu'\rangle$$

$\tilde{k}_o = k_o + \Delta E$

k_o = Optical resonance frequency wave vector

$\vec{p}$ = Electric dipole moment of the atom

Γ = The natural width & ΔE = self-energy (of the excited state)

$u(k)dk$ = Number of photons having energies in the range k to k + dk

$|A_k|^2$ = Probability of absorption for the photons of wave vector $\vec{k}$

$\vec{v}$ = Velocity of the absorbing atom

So one can easily write

$$M_A = \frac{1}{T_p} \Sigma_{\mu\mu'} A_{\mu\mu'} \sigma_{\mu'\mu} \qquad \text{II.8}$$

This equation dictates that if one switches on photons of polarization $\vec{e}$ at an instant t, their absorption is determined by the angular state of the system at that instant. Consequently any time variation in the angular state of the system will give rise to a corresponding variation in M_A, the absorbed light. If the incident light is purely polarized i.e. σ^+, σ^-, orΠ, matrix A is diagonal[22] and one can write

$$M_A = \frac{1}{T_p} \Sigma_\mu A_{\mu\mu} \sigma_{\mu\mu} \qquad \text{II.9}$$

Equation II.9 has been further simplified for the case of a circularly polarized light by Alley[17] and by Bouchiat[22]. It has been shown that

$$M_A = \frac{2}{3T_p}\left(\frac{1}{2} - \langle S_z \rangle\right) \quad \text{For } \sigma^+ D_1\text{-radiation} \qquad \text{II.10}$$

where $\langle S_z \rangle$ is electron longitudinal polarization.
Equation II.10 is the restatement of what has been said earlier, that the absorption M_A approaches zero for a fully oriented system.

C. Optical Detection of Magnetic Resonances.

It has been shown above that by observing the changes of intensity of the light coming through the absorption cell, one can determine the state of orientation of the atoms. This forms the basis of a family of optical methods of detecting the magnetic resonances in the ground state. The system is first allowed to attain non-statistical distribution among the various magnetic states under a certain set of conditions; then one of the conditions is suddenly altered. It could be an rf pulse or a change of frequency in the existing rf field at resonance. The monitoring operator M_A will vary with $(\omega - \omega_s)$, where ω_s is the resonance frequency of the system and ω is the frequency of the applied rf field. This enables one to determine the resonance curve and hence the resonance frequency.

The most important advantage of the method of optical detection lies in the fact that the emission or absorption of small energy radio frequency photons are monitored by the high energy optical photons. Since the high energy optical photons can be more easily detected than the rf photons, this makes the sensitivity of the optical method of detection far greater than the sensivity of the conventional methods of the radio frequency resonance detection. In this way, the atomic system itself acts as a quantum amplifier with an amplication of over 100 decibels

It is important to point out that the doppler width of light is not of much significance because it is the polarization rather than the frequency distribution of light which is of significance. The width of resonance curve is predominantly determined by the relaxation or the life times of the states involved.

CHAPTER III

PHASE DESTRUCTION METHOD & LIGHT SHIFTS

A. Theory of the Phase Destruction Method Using Coherent Pulse Technique.

A non-mathematical discussion of this technique was given in Chapter I. In this chapter a quantum mechanical treatment is given. In this treatment reference is made to cesium atoms only though the theory is applicable to other alkali atoms as well.

Consider the cesium atoms contained in a cell and placed in a weak homogeneous and stable magnetic field B_o. Let the cell be illuminated by $\sigma^+ D_1$ resonance radiation from a discharge lamp to pump the atoms into the $|4,4\rangle$ quantum state. A pulse of rf-rotating magnetic field of amplitude B_1 and frequency coincident with the Zeeman splitting frequency, is applied with its plane of rotation at right angles to B_o and sense of rotation corresponding to $-\gamma$. (The direction of B_o is in the z-axis which is also the direction of propagation of the pumping light. The amplitude and the time duration for which the rf field is applied is so adjusted that a coherent supperposition state describing free precession in the plane normal to B_o is formed. (This rf-field pulse will be referred to as 90^o -pulse).

It is shown in appendix I that the resulting wave function after an atom originally in state $|F,\mu\rangle$ is subjected to a rotating magnetic field pulse beginning at t_1 and ending at t_2, can be written as

$$\Psi(t_2) = \sum_{\mu'} e^{i\omega_z(\mu' t_2 - \mu t_1)} D^F_{\mu\mu'}(0, \omega_1(t_2 - t_1), 0) |F,\mu\rangle \qquad \text{III.1}$$

where ω_z = the frequency of the rf field

$\omega_1 = -\gamma B_1$

B_1 = the amplitude of the rf magnetic field. The direction of B_1 has been taken to be along the Y-axis in the rotating coordinate system.

μ, μ' = the ground state magnetic quantum numbers.

$D^F_{\mu\mu'}$ = the well-known D- rotation matrices .

When applied to the present experiment, $\omega_1(t_2 - t_1) = \Pi/2$ or Π. A general expression for the $D^F_{\mu\mu'}$ can be written as

$$D^F_{\mu\mu'}(0, \tfrac{\Pi}{2}, 0) = \sum_0^\infty (-)^s \left(\tfrac{1}{2}\right)^F \frac{\{(F+\mu)!\,(F-\mu)!\,(F+\mu')!\,(F-\mu')!\}^{1/2}}{(F-\mu-s)!\,(F+\mu'-s)!\,s!\,(\mu-\mu'+s)!} \qquad \text{III.2}$$

$$D^F_{\mu\mu'}(0, \Pi, 0) = (-1)^{F-\mu} \delta_{\mu,-\mu'} \qquad \text{III.3}$$

The values of matrices $D^F_{\mu\mu'}(0, \Pi/2, 0)$

for F = 4 (applicable to Cesium atom)

and F = 2 (applicable to Rubidium atom)

have been calculated by using the above formula and given in Tables I and II. $D^F_{\mu\mu'}(0, \Pi, 0)$ are skew diagonal matrices beginning with 1 in the right top corner.

The initial state ($|4,4\rangle$ for the case of Cesium and $|2,2\rangle$ for the case of Rubidium) when subjected to a 90° rf pulse, becomes a coherent supposition state and can be written as (after absorbing the phase factors in the wave functions):

μ \ μ'	4	3	2	1	0	-1	-2	-3	-4
4	1/16	$\frac{\sqrt{2}}{8}$	$\frac{\sqrt{7}}{8}$	$\frac{\sqrt{14}}{8}$	$\frac{\sqrt{70}}{16}$	$\frac{\sqrt{14}}{8}$	$\frac{\sqrt{7}}{8}$	$\frac{\sqrt{2}}{8}$	1/16
3	$\frac{-\sqrt{2}}{8}$	- 3/8	$-\frac{\sqrt{14}}{8}$	$\frac{-\sqrt{7}}{8}$	0	$\frac{\sqrt{7}}{8}$	$\frac{\sqrt{14}}{8}$	3/8	$\frac{\sqrt{2}}{8}$
2	$\frac{\sqrt{7}}{8}$	$\frac{\sqrt{14}}{8}$	$\frac{1}{4}$	$\frac{-1}{4\sqrt{2}}$	$\frac{-5}{4\sqrt{2}}$	$\frac{-1}{4\sqrt{2}}$	$\frac{1}{4}$	$\frac{\sqrt{14}}{8}$	$\frac{\sqrt{7}}{8}$
1	$\frac{-\sqrt{14}}{8}$	$\frac{-\sqrt{7}}{8}$	$\frac{1}{4\sqrt{2}}$	$\frac{3}{8}$	0	$\frac{-3}{8}$	$\frac{-1}{4\sqrt{2}}$	$\frac{\sqrt{7}}{8}$	$\frac{\sqrt{14}}{8}$
0	$\frac{\sqrt{70}}{16}$	0	$\frac{-5}{4\sqrt{2}}$	0	$\frac{3}{8}$	0	$\frac{-5}{4\sqrt{2}}$	0	$\frac{\sqrt{70}}{16}$
-1	$\frac{-\sqrt{14}}{8}$	$\frac{\sqrt{7}}{8}$	$\frac{1}{4\sqrt{2}}$	$\frac{-3}{8}$	0	$\frac{3}{8}$	$\frac{-1}{4\sqrt{2}}$	$\frac{-\sqrt{7}}{8}$	$\frac{\sqrt{14}}{8}$
-2	$\frac{\sqrt{7}}{8}$	$\frac{-\sqrt{14}}{8}$	$\frac{1}{4}$	$\frac{1}{4\sqrt{2}}$	$\frac{-5}{4\sqrt{2}}$	$\frac{1}{4\sqrt{2}}$	$\frac{1}{4}$	$\frac{-\sqrt{14}}{8}$	$\frac{\sqrt{7}}{8}$
-3	$\frac{-\sqrt{2}}{8}$	$\frac{3}{8}$	$\frac{-\sqrt{14}}{8}$	$\frac{\sqrt{7}}{8}$	0	$\frac{-\sqrt{7}}{8}$	$\frac{\sqrt{14}}{8}$	$-\frac{3}{8}$	$\frac{\sqrt{2}}{8}$
-4	$\frac{1}{16}$	$\frac{-\sqrt{2}}{8}$	$\frac{\sqrt{7}}{8}$	$\frac{-\sqrt{14}}{8}$	$\frac{\sqrt{70}}{16}$	$\frac{-\sqrt{14}}{8}$	$\frac{\sqrt{7}}{8}$	$\frac{-\sqrt{2}}{8}$	$\frac{1}{16}$

TABLE I.

$D^4_{\mu\mu'}(0,\pi/2,0)$

μ \ μ'	+2	+1	0	-1	-2
+2	1/4	1/2	$\frac{\sqrt{3}}{2\sqrt{2}}$	1/2	1/4
+1	-1/2	-1/2	0	1/2	1/2
0	$\frac{\sqrt{3}}{2\sqrt{2}}$	0	-1/2	0	$\frac{\sqrt{3}}{2\sqrt{2}}$
-1	-1/2	1/2	0	-1/2	1/2
-2	1/4	-1/2	$\frac{\sqrt{3}}{2\sqrt{2}}$	-1/2	1/4

TABLE II

$D^2_{\mu\mu'}(0,\Pi/2,0)$

$$\Psi_{\text{Cesium}}(\Pi/2) = \frac{1}{16}|4,-4\rangle + \frac{1}{4\sqrt{2}}|4,-3\rangle + \frac{\sqrt{7}}{8}|4,-2\rangle + \frac{\sqrt{14}}{8}|4,-1\rangle$$

$$+ \frac{\sqrt{70}}{16}|4,0\rangle + \frac{\sqrt{14}}{8}|4,1\rangle + \frac{\sqrt{7}}{8}|4,2\rangle + \frac{1}{4\sqrt{2}}|4,3\rangle + \frac{1}{16}|4,4\rangle \qquad \text{III.4}$$

$$\Psi_{\text{Cesium}}(\Pi) = |4,-4\rangle \qquad \text{III.5}$$

$$\Psi_{\text{Rubidium}}(\Pi/2) = \frac{1}{4}|2,-2\rangle + \frac{1}{2}|2,-1\rangle + \frac{\sqrt{3}}{2\sqrt{2}}|2,0\rangle + \frac{1}{2}|2,1\rangle + \frac{1}{4}|2,2\rangle \qquad \text{III.6}$$

$$\Psi_{\text{Rubidium}}(\Pi) = |2,-2\rangle \qquad \text{III.7}$$

The time development of $\Psi(\Pi/2)$ or $\Psi(\Pi)$ after t_2 will be obtained by multiplying it by $e^{i\omega_z(t_3-t_2)}$ where $t_3>t_2$. Thus each of the partner state is multiplied by the same time dependent phase factor maintaining coherence among them. Let us now see the effect of -90° pulse following the $+90^\circ$ pulse. It can easily be described by the composite operator

$$D_{NM} = \sum_K D_{KN}(-\theta) D_{MK}(\theta) \qquad \text{III.8}$$

where:

$$\theta = (0,\Pi/2,0)$$

$$-\theta = (0,-\Pi/2,0)$$

We know from the properties of the D- functions

$$D_{KN}(-\theta) = D_{NK}^*(\theta)$$

and

$$\sum_K D_{NK}^*(\theta) D_{MK}(\theta) = \delta_{NM} \qquad \text{III.9}$$

one gets

$$D_{NM} = \sum_{K} D_{NK}^{*}(\theta) D_{MK}(\theta) = \delta_{NM} \qquad \text{III.10}$$

This shows that one can recover the original pure state by applying a -90^{o} pulse following a $+90^{o}$ pulse provided nothing happened to the relative phases of the wave functions and their amplitudes. In practice, there will be some loss in their amplitudes and phases due to longitudinal and transverse relaxation processes. If somehow these relaxation times are made very large compared to the time interval between the 90^{o} - pulses, one can recover a large fraction of the original state.

However, if a pulse of microwaves at resonance with the hyperfine splitting frequency is applied, the state $|4,0\rangle$ is coupled to the $|3,0\rangle$ state and its phase changes with respect to the partner states. The state formed by -90^{o} pulse will no longer be the original $|4,4\rangle$ state but a different state of supperposition for which the optical absorption is greatly different. It has been shown by C.O. Alley[17] the magnitude of the change in absorption is of the same order as that obtained by inverting the oriented population by means of a 180^{o} pulse.

B. Light Shifts in the Alkali Atoms.

The excited state of an atom acquires a finite life time or a line width and self energy or an energy shift due to its interaction with the vacuum fluctuations of an electromagnetic field. The ground state may also acquire a finite life and displacement when the atoms are irradiated with the real optical fields. The shifts may be different for different sublevels and hence relative shifts among the levels may result. These shifts are called light shifts or 'lamp shifts'.

Barrat and Cohen Tannoudji[20] were the first to develop a formal theory of the process of optical pumping and predict this shift. They verified their result by observing it in mercury. Since then this shift has been observed in other atoms including rubidium-87 and Cesium-133.[23,24] A more detailed theory of the light shifts has also been worked out by Happer & Mathur[25] and verified in the case of Rb-87.[26] The shifts are proportional to the convolution of the spectral profile of the pumping light with an appropriate spectral response function. The relative shift increases with the assymmetry in the spectral distribution of the light intensity until a maximum is reached after which it drops sharply. It is also proportional to the pumping light intensity. It is of the order of a few parts in 1×10^9 in Rb-87. Thus the frequency stability of the optically pumped atomic frequency standards (like a rubidium maser or a gas cell frequency standard) depends on the spectral output of the resonance lamp and the temperature of the hyperfine filter cell. The spectral output of the lamp is known to change with the age of the lamp and its temperature. The performance of the hyperfine filter cell also changes with age and temperature. Consequently one would like to eliminate such effects in the atomic standards. One way to achieve this is to construct the frequency standards based on the principle of phase destruction method of detecting the 0-0 transition as developed in this report.

Experimental study of the light shifts by Barrat et al and Happer et al has been done by using incoherent broad light sourceslike discharge resonance lamps. It is only the integrated effect, arising from

the assymmetry in the pumping radiation with respect to the absorption line of the atoms, which is observed. It will be interesting to measure the light shifts with tunable narrow band coherent sources of optical radiation of known frequency and intensity. Such sources are not yet easily available to match the lines of the alkali atoms. However, we have been successful in matching a GaAs laser mode with the 8521.1A^{o} line of Cs-133 to observe population inversion among the hyperfine levels of the ground state.[27] Details of this experiment on hyperfine pumping are discussed in Part II of this report.

CHAPTER IV

ENHANCEMENT OF OPTICAL SIGNALS

A. General Discussion.

In most of the double radio-optical resonance experiments, it is highly desirable to have the longest possible relaxation time of the atoms optically pumped into a desired state. This is achieved in two different ways. In the first, the walls of the container (cell) are coated with long straight-chain saturated hydrocarbons like paraflint or with different kinds of silicone compounds (e.g. SC-2 or SC-77 which are mixtures of dimethyl-dichlorosilane and methyltrichorosilane.[28]) In the second, noble gases like Ar, Ne, He, etc. are used at pressures ranging from a few torr to several centimeters of Hg.

In the wall coated cells, the atoms tend to retain their characteristic state on collision with the walls. In the case of cells containing a buffer gas, the atoms are slowed down from reaching the walls of the container because of collisions with the molecules of the buffer gas. The disorientation cross-section for the atoms on collisions with the buffer gas atoms is quite small and hence long relaxation times result (it takes on the average $10^6 \rightarrow 10^9$ collisions between a Cs (or a Rb) atom and the buffer gas atoms to produce electron depolarization[29]). Relaxation of optically pumped Rb-atoms on coated walls has been studied by Franzen[30], Alley[28], Bouchiat[31], and others[32,33]. Bouchiat's[31] experiments on spin relaxation of optically aligned rubidium atoms contained in cells coated with saturated straight hydrocarbons

have shown that relaxation times are practically independent of the length of the chain and it takes about 1.3×10^3 Rb atom-wall collisions to destroy the orientation of a Rb atoms. However, we preferred the longer chain parafins for coating our cells because of their higher melting and boiling points and hence low vapor pressures at the working temperatures.

We have used paraflint RG for wall coating and have developed a technique which can give excellent coatings. Details of the method are discussed in detail in Chapter VII. We have observed relaxation times of 250 ms for Cs-133 atoms in the coated cells of 2.5 inch in diameter. This amounts to about 10^3 Cs atom-wall collisions to destroy the orientation and is in good agreement with the results of Bouchiat[31].

B. Relation Between the Longitudinal Relaxation and the Hyperfine Frequency Shift in Coated Cells.

Collisions can effect the radiative process in two different ways:

They may quench the upper state of the radiating atom by releasing the energy of excitation prematurely - They are called Non-adiabatic collisions and result in an additional line width and reduction in line intensity.

Secondly, they may weakly perturb the colliding atom resulting merely in a small change in the spacing of the energy levels. They are referred to as adiabatic collisions.

Nonadiabatic collisions are insignificant when the target wall is coated with saturated hydrocarbons. This is shown as follows:

Probability for transition during an atom-wall collision is

$$P = \left(\frac{H_I t_a}{\hbar}\right)^2 \qquad \text{IV.1}$$

where H_I is the interaction hamiltonian and t_a is the mean physical absorption time for the colliding atom on the wall. Since the walls are supposedly coated with saturated parafins, the surface is free from unpaired electrons. Consequently H_I may be regarded as the hamiltonian of interaction between the electron (belonging to the alkali atom) and the nuclear dipole moment of hydrogen atom on the surface. This argument is supported by the observations of Bouchiat[31]. It has been found that the relaxation times are several times larger on deuterated hydrocarbons than on ordinary hydrocarbons.

In order that such collisions are insignificant, the following inequality must be satisfied.

$$P = \left(\frac{(\vec{\omega}_e \cdot \vec{\mu}_p) \cdot t_a}{(\vec{X}_e - \vec{X}_p)^3 \hbar}\right)^2 \ll 1 \qquad \text{IV.2}$$

where $\hbar = \frac{h}{2\Pi}$

or

$$t_a < \frac{(2\text{x}10^{-8})^3 \hbar}{2\text{x}10^{-23}\ \text{x}10^{-20}} \simeq 4\text{x}10^{-8}\ \text{sec.} \qquad \text{IV.3}$$

The observed[31] value for t_a is of the order of 10^{-11} sec. Hence the above inequality is satisfied concluding that the non-adiabatic collisions are negligible.

The adiabatic collisions, as mentioned before, will cause a small perturbation in the internal state of the colliding atom resulting in a shift in its energy levels. We shall be interested in the (0-0) transition in the ground state and shall compute the corresponding shift in the observed frequency of the transition. The observed frequency ν_{obs} is the time average of the frequencies ν_a and ν_o corresponding to when the atom is absorbed on the surface and when it is 'free'. Denoting by t_a and t_o the mean absorbed and 'free' times, one can write for ν_{obs}:

$$\nu_{obs} = \frac{\nu_o t_o + \nu_a t_a}{t_o + t_a} \qquad \text{IV.4}$$

t_a and t_o are of the order of 10^{-12} sec. and 10^{-4} sec. respectively, one can approximate the equation IV.4 in a more useful form as

$$\nu_{obs} - \nu_o = (\nu_a - \nu_o)\frac{t_a}{t_o} \qquad \text{IV.5}$$

$$\Delta\nu_{shift} = (E_a - E_o)\frac{t_a}{2\pi\hbar t_o} \qquad \text{IV.6}$$

It has been shown by Adrian[34], Goldenberg et al[35], and Margenau et al[36,37] that the change in the hyperfine energy when the atom is absorbed on the surface can be written as:

$$E_a - E_o = E_w h\nu_o \left(\frac{1}{\Delta E + V_1} + \frac{2}{V_2}\right) \qquad \text{IV.7}$$

where V_1 is the mean ionization potential of the coating material, V_2 is the ionization potential of the alkali atom, and ΔE is the

difference in energy between the S and P levels in the alkali atom. E_w is the absorption energy for the alkali atom when absorbed on the surface. Combining IV.7 and IV.6, one gets:

$$\frac{t_a}{t_o} = \frac{\Delta\nu_{shift}}{E_w \nu_o \{\frac{1}{\Delta E + V_1} + \frac{2}{V_2}\}} \qquad \text{IV.8}$$

Let us now investigate disorienting effect of atom-wall collisions resulting in the longitudinal relaxation of the optically oriented atoms. The probability of disorientation Γ resulting from a collision of the alkali atom with a rare gas atom has been worked out by Bernheim[38] and is reproduced below:

$$\Gamma \simeq \frac{\mu^2 \tau_c^2 H^2}{\hbar^2} \qquad \text{IV.9}$$

where μ magnetic moment of the alkali atom, τ_c collision time and H is the magnetic field acting on the alkali atom and is supposed to have the time dependence as:

$$H(t) = H \exp(-t^2/\tau_c^2) \qquad \text{IV.10}$$

and is of the order of the field present in hyperfine interactions.

The expression IV.9 for the transition probability can be modified to the situation where the atom collides with a coated-wall: It is experimentally known that the disorientation transition probability is much higher in the case of collisions with wall than with the rare gas atoms[32]. It has been argued by Brewer[32] that it is mainly because of the large difference in the time of interaction whereas differences

in matrix elements contribute negligibly and one can define Γ^* for a wall collision:

$$\Gamma^* = \Gamma \left| \frac{\chi \, t_a}{\tau_c} \right|^2 \qquad \text{IV.11}$$

χ is a numerical constant.

Conbining IV.11, 9 and 8:

$$\Gamma^* = t_o^2 \, \P \left(\frac{\chi \mu \Delta\nu_{shift} H}{\hbar \nu_o E_w \left\{ \frac{1}{\Delta E + V_1} + \frac{2}{V_2} \right\}} \right)^2 \qquad \text{IV.12}$$

But the longitudinal relaxation time T_1 is related to Γ^* as $1/T_1 = \Gamma^*/t_o$, therefore

$$1/T_1 = \frac{t_o \Delta\nu_{shift}^2}{\nu_o^2} \left(\frac{\sqrt{\P} \, \chi \mu H}{\hbar E_w \left\{ \frac{1}{\Delta E + V_1} + \frac{2}{V_2} \right\}} \right)^2 \qquad \text{IV.13}$$

This expression is in agreement, at least qualitatively, with the observations of Alley[28], Brewer[32], and Bouchiat[31]. Large shift in the Rb^{87} hyperfine transition and small longitudinal relaxation time observed by Alley and the small hyperfine shift and long relaxation time recorded by Brewer in cells coated with paraflint are explained by equation IV.13. The findings of Bouchiat that the longitudinal relaxation time for Rb^{87} in evacuated and coated cells is proportional to the diameter of the cell, is explained exactly by the presence of proportionality factor t_o in IV.13. It is also known that the relaxation times are about five times longer when deuterium is substituted for Hydrogen in the paraffin used for coating. This is partly accounted for by the factor H^2, the

effective magnetic field which is proportional to the magnetic moment of Hydrogen or Deuteron. The square of the ratio of their moments is close to 10. The theoretical analysis assumes ideal conditions and d.d. type of interaction, whereas the practical value is 5 and is on deutrated polyethylene with an impurity of 1.7% of Hydrogen[31].

Equation IV.13 is also in agreement with our observations (discussed later in this report). We have observed longer relaxation times and smaller shifts than the results of reference 28.

CHAPTER V

INSTRUMENTATION

A. General Description.

The apparatus consisted of the following main parts.

1. Resonance lamp
2. Wall-coated Cesium vapor cell
3. Stable and homogeneous-magnetic field producing set up
4. Pulse programming system
5. Electronics to produce rotating field pulses
6. Microwave source including stabilizing and pulsing arrangement
7. Optical arrangement.

This chapter discusses the details and performance of all the different parts of the system excluding the resonance lamp and the vapor cells, which are discussed in Chapter VI and VII respectively.

Figure 4 shows the photograph of the complete apparatus. In the foreground is all the necessary electronics and the magnetic field producing shielded solenoid lies in the background. On the right side is the apparatus essential to the generation, monitoring, and stabilization of the microwaves. On the left are the components required to generate the time, the light, the RF, and the microwave pulses, and other associated electronics. The klystron, along with its wave guide circuit, is placed under the shielded solenoid and is partly visible in the picture.

Figure 5 presents a schematic block diagram of the experimental

EXPERIMENTAL ARRANGEMENT

arrangement. The flow of signal is indicated by arrows. The pulse programming system, in a sense, controls most vital functions. It provides pulses separated by desired length of time. These pulses are used to switch-on-off the optical, radio frequency and microwave fields for any desired length of time and in the desired order.

A commercial pulse programming system made by Navigation Computer Corporation (Navcor) was used for timing the various switching or triggering operations. The system consisted of an electronic switch, a binary decimal counter, 3 shift registers, and a decade unit having ten Tri-input coincident circuits giving out amplified outputs of -15 volts. It was driven for its time base by a 100 KHz oscillator.

The light from a resonance lamp, after filtering, was circularly polarized with the help of HNCP-7 polaroid circular polarizer. It was concentrated onto the absorption cell with Fresnel lenses. Monitoring of the signal was done by an RCA-7102 photomultiplier tube. Electrical pulses necessary to switch on-off the multiplicity of functions were preprogrammed into the pulse programming unit. The whole sequence of pulsing and monitoring was repeated every 800 milliseconds. This time interval was adequate to do the experiment with the pumped ground state of highest angular momentum and to repump it back to its original value for the next cycle of the experiment. Moreover, this interval was close to three times the longitudinal relaxation time of the polarized atoms encountered in this investigation; it was long enough for the atoms to forget their history of the past cycle and not carry it into the succeeding cycle.

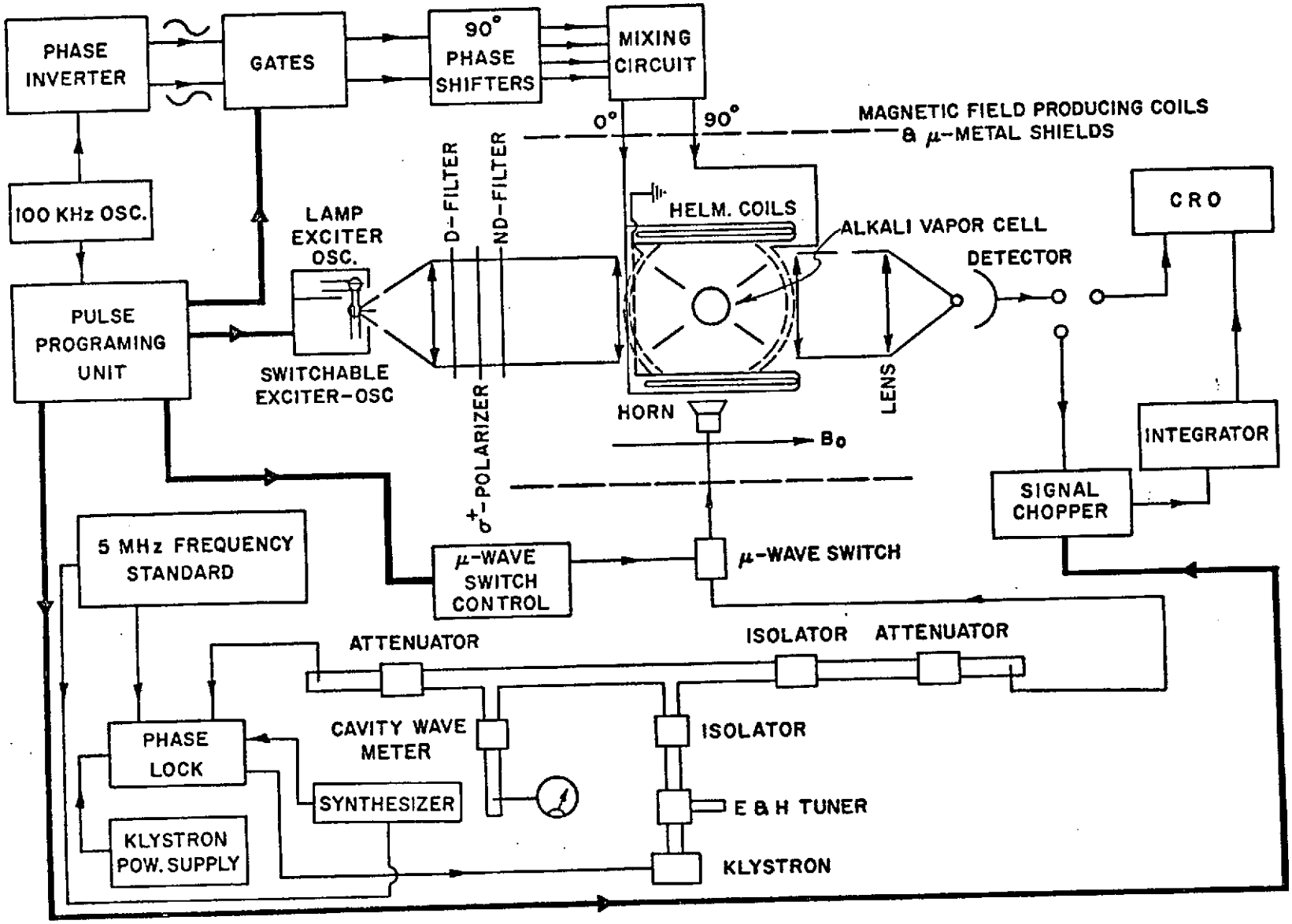

Fig. 5 SCHEMATIC REPRESENTATION OF THE EXPERIMENT

The $\pm 90^{\circ}$-RF pulses were provided through two independent channels, so that they could be phase-shifted by 180° with respect to each other. They were then made to go through a "mixer" so as to provide a common path for the pulses to feed the same set of Helmholtz coils at different times. An X-13 klystron was phase locked to a highly stable frequency standard and served as a source of microwaves. A solid state switch was used to pulse the microwaves. Details are discussed later in this chapter.

In the early part of the experiment, great difficulty was encountered in switching on the resonance lamp in a predictable manner. After the exciter oscillator was turned on, it took several milliseconds before the lamp was on. Moreover, this time delay was not consistent from cycle-to-cycle. The delay also depended on the length of time for which the lamp has been off during the cycle. To get over this difficulty, a new lamp was designed which essentially consisted of two lamps joined together forming a dumbbell. One of them was kept-on continuously while the other was switched on-off. The results of this arrangement were very good. The details of the lamp along with the exciter circuit and the performance of the lamp are discussed in Chapter VI.

Preparation of the Cesium vapor cells was a project in itself. Firstly a few cells were prepared with a buffer gas in them. These cells gave relaxation times of about 18 msec. which were considered small. It was then decided to prepare wall coated cells. Elaborate experimentation was done to perfect the method of coating, in vacuum, a thin layer of wax on the interiors of the glass cells. A few milligrams of

cesium were distilled into the stem of the cell before removing the cell from the vacuum system. Details of the procedure to coat the cells and the performance of the cells are discussed in Chapter VII.

B. Effects of the Instability and Inhomogeneity of the DC Magnetic Field

1. Effect of Magnetic Field Instability

Instability in the magnetic field causes serious problems. If the magnetic field is not constant but has a small time varying component, the Larmor frequency of the atoms will be varying during the interval between the $\pm 90^{\circ}$-pulses. All atoms will not stay in the correct phase relationship with the sequence of rf pulses. The signal may not repeat itself and may thus be meaningless. Instability in the field can be caused by two independent sources:

i. One is due to the slow drift in the power source used to supply constant currents to the field producing coils. Initially, mercury cells were used and it was soon realized that even the slow drop in the voltage of the mercury cells was quite significant; moreover, the effect of the voltage drop is cumulative in time and becomes very significant after a couple of hours of operation. To correct this difficulty, mercury cells were replaced by the best available stabilized power supply (Model QHS -20- 1 Sorenson). This power supply has a drift rate of 200 μv/week, temperature variation of 20 μv/c$^{\circ}$, and voltage regulation of 30 μv for 20 percent change in the line voltage. The power supply was fed from an AC stabilizer and kept on permanently to minimize drifts.

ii. The other source of magnetic field instability was the magnetic fields resulting from the utility lines and the associated apparatus in the vicinity of the solenoid. This noise in the magnetic field was very significant even after its effect has been reduced by a factor of $10^3 \rightarrow 10^4$ by three concentric cylinders of Mu-metal shields. It was detrimental to the success of the experiment and its elimination was essential.

An intuitive approach to the solution of this problem was one of detecting the magnetic field variations with a sensing coil, amplifying the induced voltage, and exciting a solenoid in a manner to produce destructive interference with the unwanted field. This implies the continuous measurement of the field and control through some sort of a feedback system. Design and operation of such a feedback system is discussed later.

An estimate of the tolerable limit of instability due to the slow drifts in the power source can be made as follows. Since the relaxation times were very large, it was desirable to have a large time interval between the $\pm 90^{\circ}$ -pulses. Let it be 50 ms. Let the current through the main solenoid changes from I to I + ΔI. Denoting by $\Delta\phi$ the phase change of the atoms with respect to the phase of rf pulses, and by ϕ the total phase angle, it is easy to see

$$\frac{\Delta B}{B} = \frac{\Delta\phi}{\phi} = \frac{\Delta I}{I} = \frac{\Delta V}{V} + \frac{\Delta R}{R}$$

Taking the worst case of $\Delta\phi$ = 1 radian

$$\frac{\Delta B}{B} = \frac{\Delta V}{V} + \frac{\Delta R}{R} = \frac{1}{\phi} = \frac{1}{2\pi \times 10^5 \times 0.05} \simeq 3 \times 10^{-5}$$

This value is of the order of temperature coefficient of the series resistance or the power supply. The use of mercury cells which were used earlier is out of question because the temperature coefficient of its voltage is poorer by two orders of magnitude than the estimated stability desired. Use of the DC power supply, the one mentioned earlier, was quite satisfactory. A better stability can be obtained by putting the whole thing in a temperature controlled chamber or by an elaborate feedback control system.

2. Effect of Magnetic Field Inhomogeneity

If large field inhomogeneities exist, atoms in different parts of the cell (containing buffer bases) will precess at different Larmor frequencies and will get out of phase with one another in a time less than that one would like to have between the two 90° pulses. In the case of wall-coated cells with no buffer gas, the flying atoms experience an average magnetic field and the inhomogeneity has no serious effect. Details of the effect of field inhomogeneities on experiments involving cells containing buffer gases can be found in reference 17.

C. Production of the DC Magnetic Field

For producing the DC magnetic field, the solenoid coils were designed according to the theory of Garrett[39], Franzen[40], and Hanson, et al[41]. In addition to the main solenoid two correction coils were employed to correct up to 4th order for the variation of the magnetic

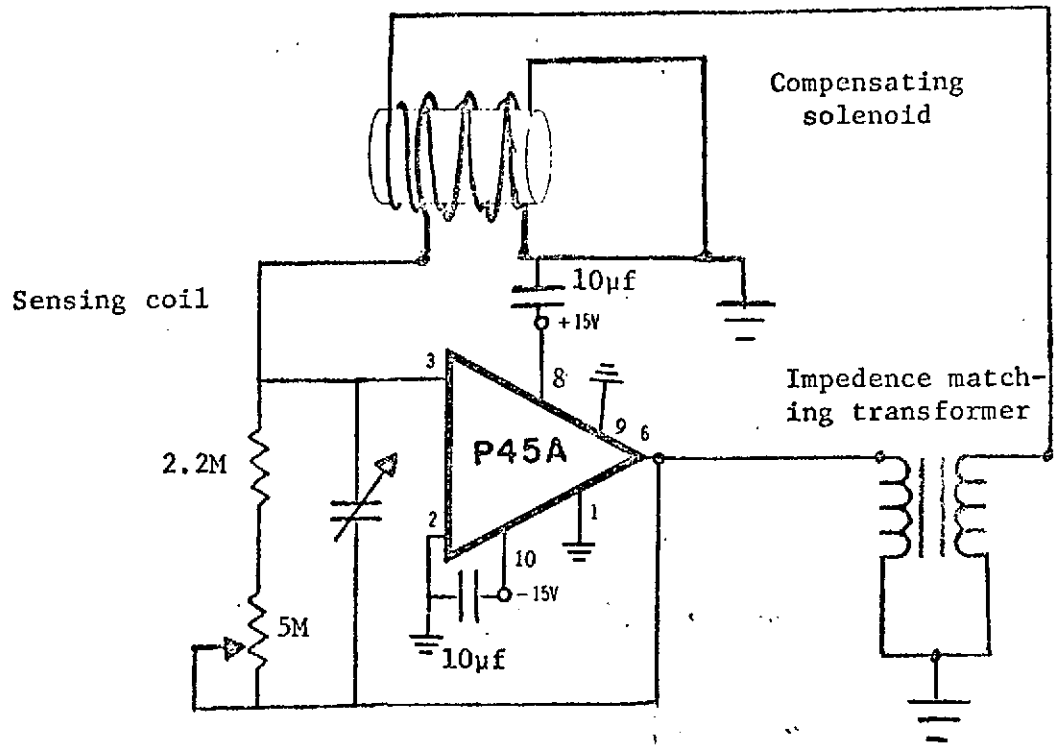

Figure 6 Feedback system used to eliminate noise in the Magnetic Field

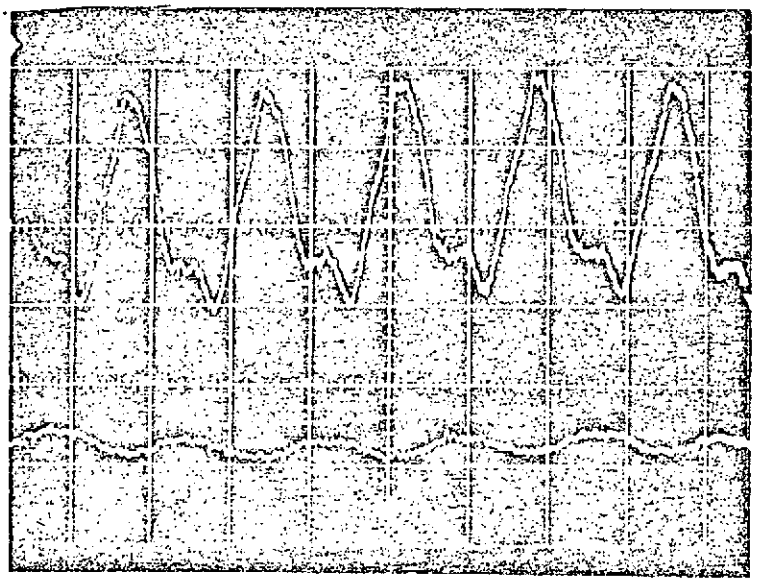

Figure 7 Illustration of the performance of the feedback system

Upper trace: Noise in the magnetic field modulates the signal at resonance

Lower trace: Noise is considerably reduced by switching on the feedback system

field. The coils were wound on a plexiglass cylinder 32" long and 13" in diameter. The solenoid was shielded by three concentric Mu-metal magnetic shields of permeability as high as 10^5.

The 60 cps noise in the magnetic field produced by the utility lines was almost eliminated by using a feedback system. A sensing coil was used to detect the time varying fields in the vicinity of the gas cell. The output of the sensing coil was fed into a Philbrick (Model 45A) solid state operational emplifier. A complete circuit diagram is shown in Figure 6. By changing the RC product of the feedback loop, the gain and time constant could be adjusted. The output from the amplifier was coupled through a line matching transformer to the correcting solenoid in a manner to produce destructive interference with the unwanted fields. The effectiveness of the feedback system is demonstrated in Figure 7.

The construction of the field producing coils was done by Hai-men Lo in connection with his M.S. thesis. More details can be found in his thesis[42]. He made a detailed study of the field homogeneity and found a value of better than 5×10^{-5} averaged over a 2" diameter spherical space at the center of the solenoid.

D. Generation of the Rotating Magnetic Field Pulses

1. Need for 'Circularly Polarized' Resonance Radio Frequency Fields

A magnetic dipole μ when placed in a magnetic field H_o precesses about the direction of the applied field. The rate of its precession (Larmor frequency) is given by the vector equation

$$\vec{\omega}_o = \gamma \vec{H}_o$$

where γ in the gyromagnetic ratio of the dipole which is assumed positive in this discussion. An additional field H_1 (such that $H_1 << H_o$) applied at right angles to the plane containing $\vec{\mu}$ and $\vec{H}_o$, will exert a couple $(\vec{\mu} \times \vec{H}_1)$ tending to increase the angle θ between $\vec{\mu}$ and $\vec{H}_o$. Further, if the small field H_1 is rotated with vector velocity $\vec{\omega}_o$, i.e. in synchronism with the precession of the dipole μ, this couple will steadily increase the angle θ. Moreover, the dipole μ will precess with frequency $\vec{\omega} = \gamma\vec{H}_1$. If, on the contrary, H_1 rotates in the opposite sense or with a different angular frequency from ω_o, the resulting couple $(\vec{\mu} \times \vec{H}_1)$ will vary in direction, as well as, in magnitude according to the relative phases of the two rotations. It is easy to see that this will result in small perturbations causing nutation with no net effect. It is obvious, by now, that resonance effects will occur only when the angular velocity of the rotating field H_1 is equal to that of precession and is in the correct sense.

However, a linearly oscillating field of amplitude $2H_1$ can be effectively decomposed into two circularly polarized fields each of amplitude H_1 but rotating in opposite senses. The component which is in the correct sense gives rise to resonance effect, the other one having negligible effect. Unfortunately the situation is not so simple when dealing with atoms of the type of Cs^{133} or Rb^{87}.

In the case of Cs^{133} or Rb^{87}, gyromagnetic ratios corresponding to the upper and lower hyperfines of the ground state are equal in magnitude but opposite in sign. This results in resonance effects in the magnetic states of both hyperfines, when a linearly oscillating

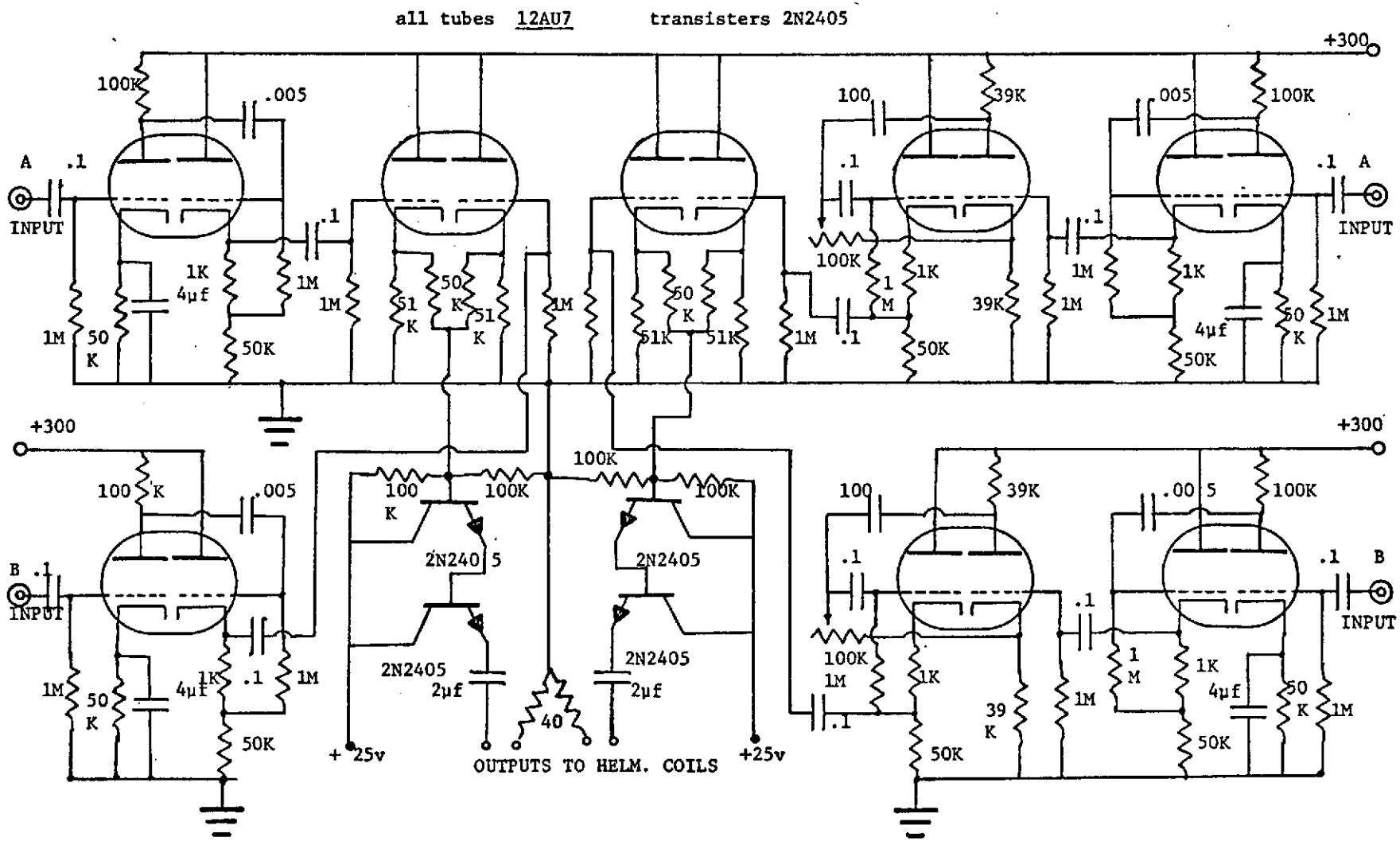

Figure 8. 90°-PHASE SHIFTERS AND MIXERS FOR THE ±90° RF PULSES

field is applied. There are always sufficient atoms in the lower hyperfine state and this makes the interpretation of the results difficult. To avoid this difficulty, it is best to apply a circularly polarized magnetic field rotating with the resonance frequency in the correct sense.

2. Generation of the ±90 - Rotating Field Pulses

The rotating magnetic field was produced by two pairs of Helmholtz Coils. Each coil was 7" in diameter and consisted of 25 turns of #28 copper wire. Each pair had its axis normal to the DC magnetic field and perpendicular to each other. Coils of each pair were connected in series and were fed with 100 KHz signals which were phase shifted by 90°. Pulsed rotating field was produced by gating the 100 KHz signal. To form the $\pm 90^{\circ}$-pulse, the following procedure was adopted. The 100 KHz signal was first amplified and divided into two parts which were phase shifted by 180° relative to each other. The 180°-phase shifted outputs served as the inputs for two independent gates. Output from one gate served as an input for the 90°-phase shifter. The two outputs from the 90°-phase shifter were fed to the two helmholtz pairs. This formed a 90-rf pulse. The output from the other gate after going through another 90°-phase shifter and the mixing circuits formed the -90°pulse. (Circuits used in this connection are shown in Figure 8.)

3. Effect of the Instability of the 100 KHz Oscillator

It is very important that the oscillator from which the rf pulses are derived should be stable. It is easy to see that its stability should be better than 1 in 10^5 so that the precessing atoms remain in phase

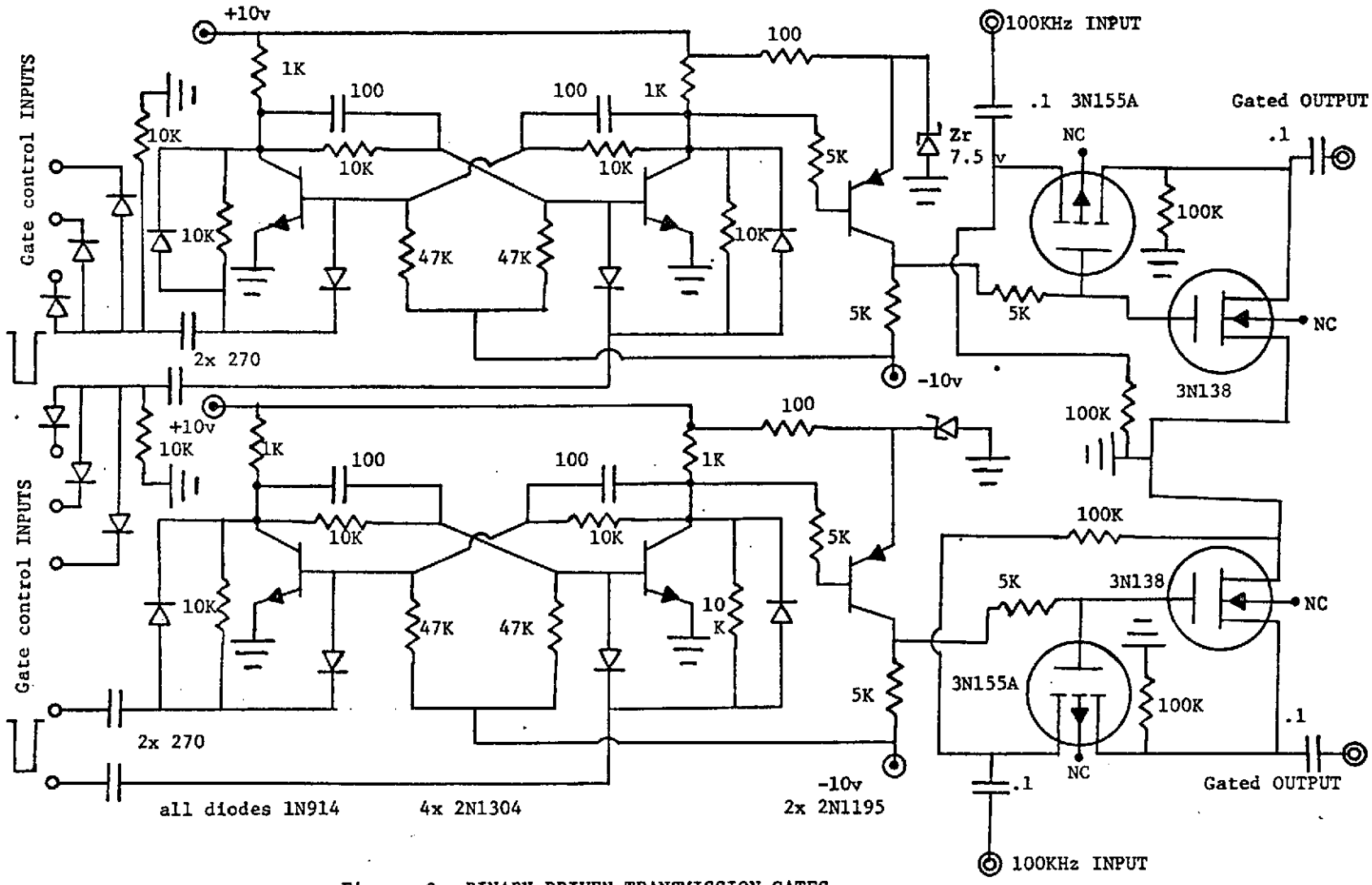

Figure 9. BINARY DRIVEN TRANSMISSION GATES

with the phase of the 90°-pulses. The oscillator used in this experiment was of much higher stability (GR 1115B).

E. Transmission Gates.

Coherently pulsed 100KHz pulses which were needed to rotate the atomic state by $\pm 90^{\circ}$ or 180° were achieved by using two identical gates. Each gate consisted of two MOS insulated-gate-field effect transistors (MOS-IG-FET) placed in a series-shunt arrangement to the incoming 100KHz signal (Figure 9). The FET which was in series with the signal was a p-channel enhancement-type (3N155A), whereas, the shunt FET was an n-channel depletion type (3N138). The operation of the gate was controlled by a flip-flop circuit whose flip-flop action was controlled by programmed pulses from the pulse programming system. The output from the flip-flop was connected to the base of the 2N1195 transistor which acted as a switch to give an output of +7.5v or -10v, appropriate to operate the gates. This output of +7.5v or -10v was connected to the 'control gates' of the FE-transistors. When the control gates are at +7.5v the drain resistance of the series FE-transistor is greater than 10^{11} ohms and that of the shunt FE-transistor is about 250 ohms. Taking into consideration the capacitative effects, an attenuation of about 10^{5} (at 100 KHz) is easily achieved. When the control gates are at -10v, the drain resistances of the MOS-FETS interchange their values and under these conditions attenuation is essentially zero. The most important advantage of using the MOS-IG-FET is that it has no offset voltage as is the case when conventional transistors are used as gates. Moreover, the attenuation achievable when MOS-IG-FET gates are used is

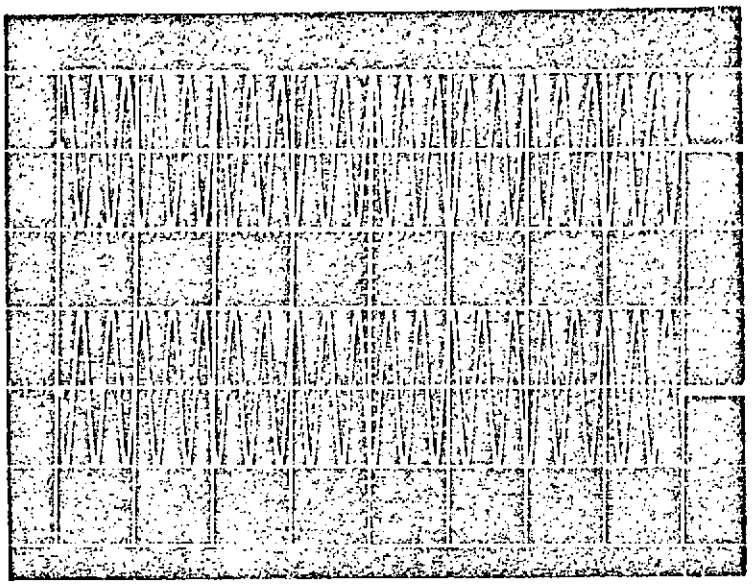

FIG. 10. 100KHz PULSES FROM GATE 1 & GATE 2 DIFFERING IN PHASE BY 180° ILLUSTRATE THE CLEAN OPERATION OF THE GATES

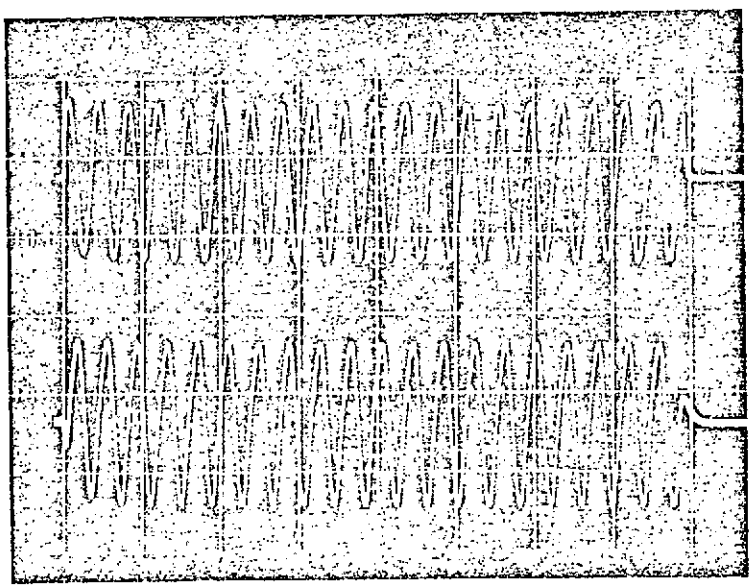

FIG. 11. 90° - PHASE SHIFTED COMPONENTS OF AN 100 KHz PULSE

much higher than that obtainable with transistors or diode-transmission gates.

F. Performance of the Gates and the 90^{o} Phase Shifters.

The gates and the phase shifters worked extremely well. Gated outputs are displayed in Figure 10. Notice the 180^{o}-phase shift in the two outputs. Performance of the 90^{o}-phase shifter is displayed in Figure 11. Output from one of the gates was used as input to the phase shifter to get the outputs which are displayed in this figure.

G. Stabilized Microwave Sources.

The hyperfine lines to be studied are expected to be narrow and should thus require a stable and very narrow microwave source for their investigation. There are two plausible options :

i. One can start with a low frequency, very stable, crystal oscillator and multiply it all the way to the X-band by building a noiseless frequency multiplier chain.

ii. One can phase lock a klystron with reference to a standard frequency. Phase locking of the klystron was preferred over an harmonic chain multiplier, because of its flexibility and adaptability to different desired frequencies for other experiments.

1. Automatic Phase Control System. (APCS)

General Theory of Operation of APC

The system operates in the following manner (refer to Figure 12). A portion of the klystron power output is mixed with a comb of harmonics

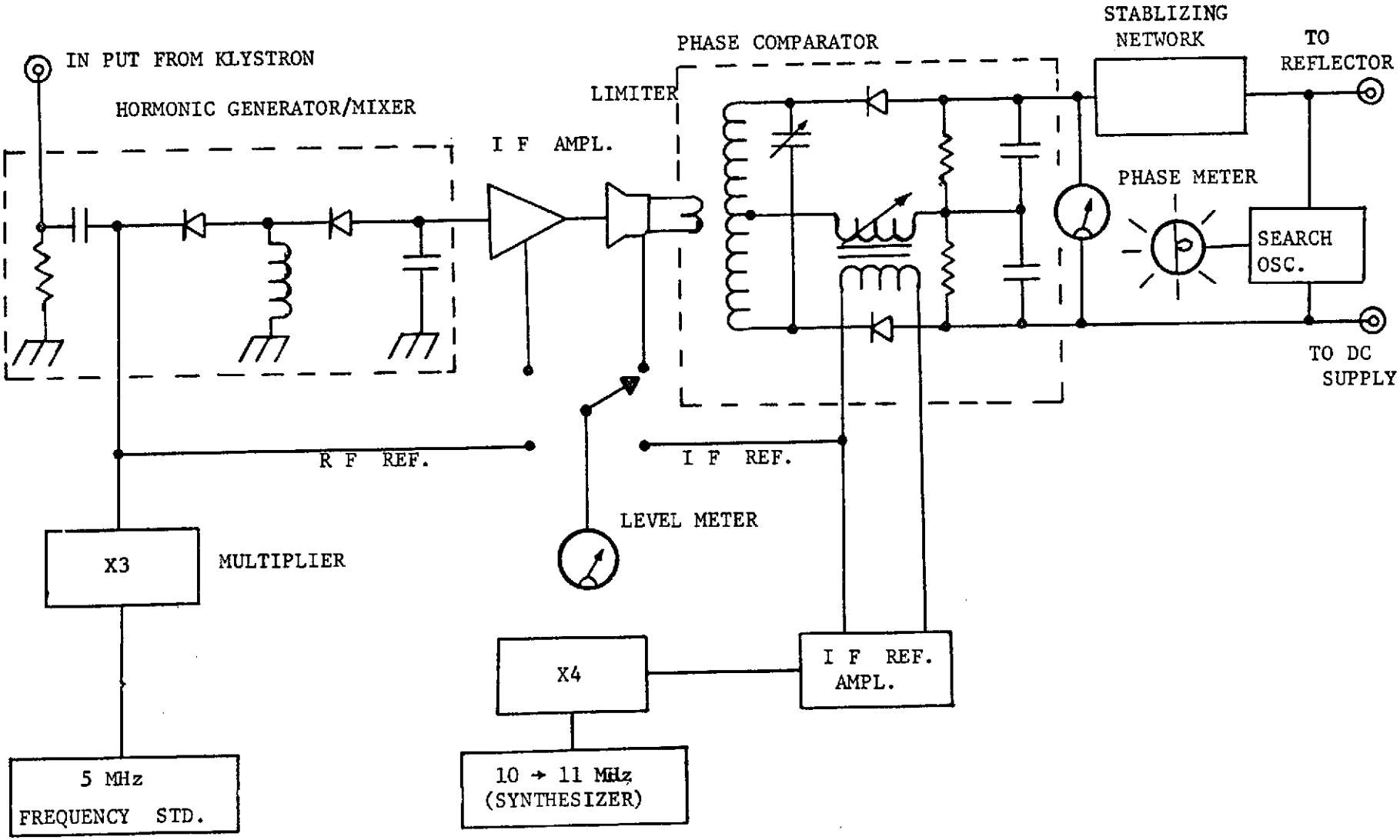

FIGURE 12 KLYSTRON PHASE LOCK STABLIZER

derived from a narrow band frequency multiplication of a reference frequency F_x which is derived by multiplication from a standard reference. The heterodyne output - the IF - Carries the frequency instabilities of the klystron output and the negligible residual instabilities of the reference oscillator. The IF band width and harmonic comb spacing is so selected that only one frequency of the reference comb provides a difference frequency in the IF band-pass at any one tuning position.

The resulting IF is amplified, limited and compared in a phase comparator to another reference frequency called IF-reference (F_I). The phase comparator output voltage is proportional to the cosine of the difference in the phase angles of the two inputs. The error signal after proper amplification is then fed in series with the reflector voltage from the power supply, and it re-adjusts the klystron frequency (hence the phase) to compensate for any mechanical or electrical change that tends to shift its frequency. In an APC system, no steady state frequency error can exist, since the system works on a difference in phase rather than frequency between the klystron and the reference signals. Any change in frequency, and hence in the relative phase, is integrated by the phase comparator which produces an error signal proportional to the phase error rather than frequency difference. Hence a stability of the locked klystron equal to that of the reference oscillator is possible.

An attempt was made to build such a system. There was too much noise in the system built by us and a stable lock could not be achieved.

A commercial unit made by Microwave System Inc. was acquired at a later stage of the experiment.

2. Phase Locked Points

When the klystron is locked, its locked frequency F_o will be given by

$$F_o = Nf_r \pm nf_I$$

f_r was taken from a frequency standard (5MHz), f_I- the intermediate frequency was taken from a general radio synthesizer (1163-7CAD), N and n are integers. In our case the reference frequency f_r was 15 MHz and was obtained from a frequency standard of 5MHz after multiplication by 3. f_I was close to 10MHz which when multiplied by n = 4, served as the IF reference frequency. In fact f_I was adjusted to match F_o with the hyperfine resonance frequency. The klystron was made to lock at N = 3 x 610 th harmonic.

3. Coupling of Microwave Fields to the Vapor-Cells

A horn was used to radiate microwave energy onto the vapor cells. The cell has to be placed in the near fields of the horn because of limited space. As a result, a parallel and normal componentsof the B-field of the microwaves were present to excite the $\Delta M = 0 \pm 1$ transitions, respectively.

4. Pulsing of Microwaves

The need of applying pulsed microwave radiation in the interval between the 90^o Rf pulses was discussed earlier. The microwaves can be very conveniently controlled by a solid state microwave switch. The microwave switch used was a broad band (6GHz-10GHz), coaxial type (Model

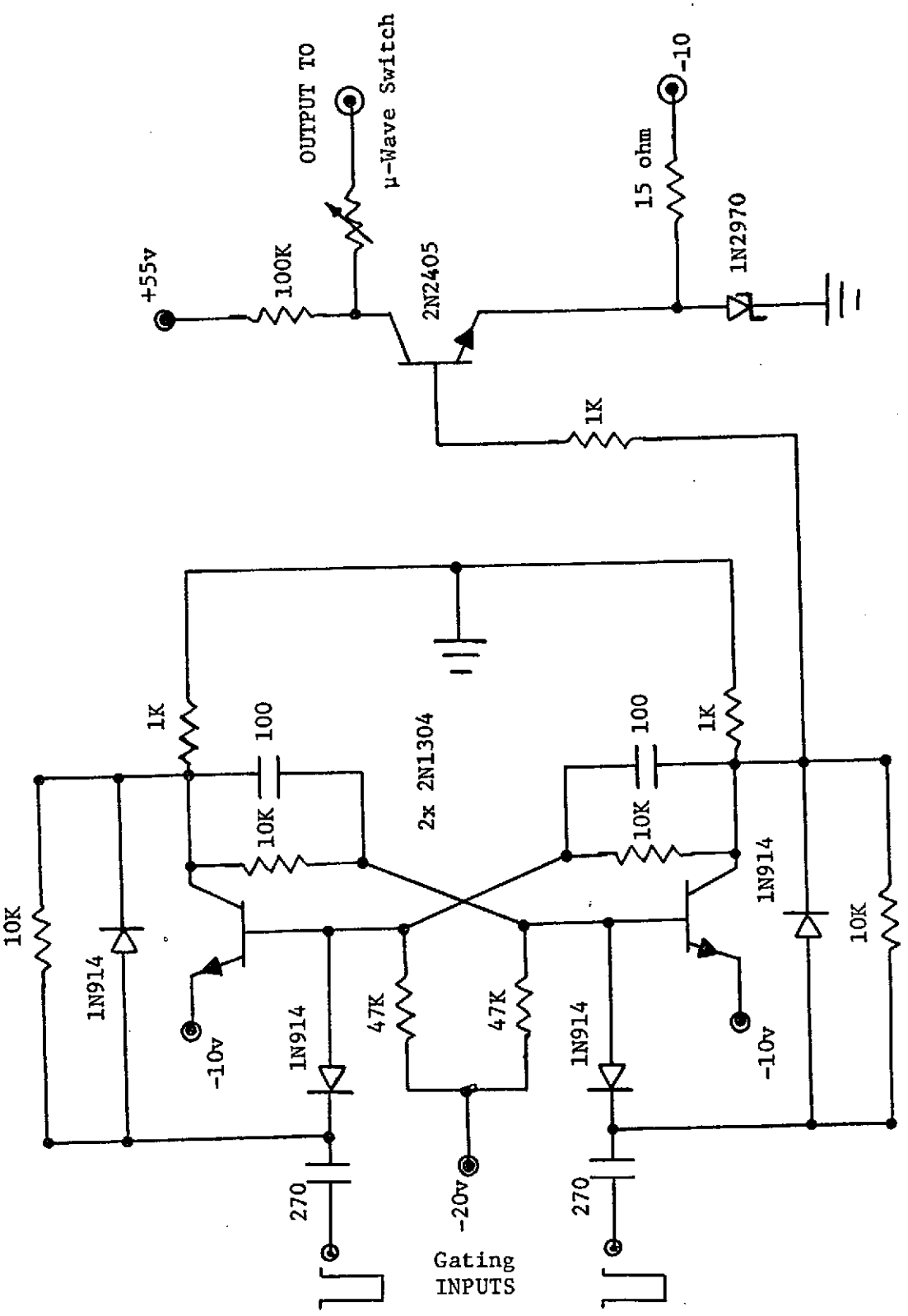

FIG. 13. CONTROL CIRCUIT FOR THE MICROWAVE SWITCH

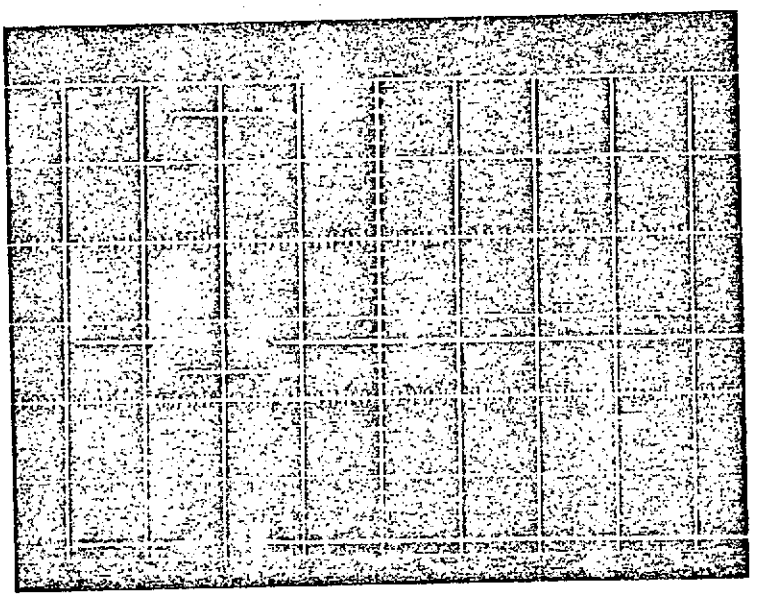

FIG. 14. DEMONSTRATION OF THE PERFORMANCE OF THE MICROWAVE SWITCH

UPPER TRACE SHOWS THE MICROWAVE PULSE SWITCHED ON BY A 50v x 24ms VOLTAGE PULSE (LOWER TRACE)

3604A-Hewlett Packard). It consists of two silicon PIN- diodes which are functionally integrated into 50-ohm miniature coaxial transmission line. It has a minimum isolation of 80db and maximum insertion loss of 1.5db.

The switch required +50v for reverse biasing to keep it closed and about 200mA forward current to keep it open. This was easily achieved by a control circuit as given in Figure 13. Timing the switch into the on-off state was essentially programmed with the help of the pulse programming system. Timed pulses from the programming unit trigger the flip-flop part of the control circuit into '0' or '1' state. This in turn biases the base of the transistor T positive or negative with respect to its emitter. When T is positively biased, A is at about -6.8v and the desired current, as controlled by the resistance R, passes through the microwave switch; when the base of T is negatively biased, +50v is effective in reverse biasing the microwave switch.

Performance of the microwave switch was exceptionally good. Figure 14 shows the pulsing of microwaves at 9192 MHz.

CHAPTER VI

CONSTRUCTION OF THE PULSED CESIUM RESONANCE LAMP

A. Difficulties in "Pulsing" the Resonance Lamp.

In this investigation, it was desirable to turn-off-and-on the pumping light in a predictable way. Moreover, this was to be done by the timed pulses from the pulse-programming unit. The simplest way to do this would be to make a sillicon-controlled-rectifier switch (SCRS) controlled by these pulses. In the early part of the experiment, cesium electrodeless discharge lamps were constructed similar to the description given by Bell, Bloom & Lynch[43](BBL). (In their design a Cs bulb of about 1 cm in diameter is excited by an rf oscillator). To pulse the lamp, the D.C. supply used to energize the excitor oscillator was pulsed by the SCR switch which could be controlled by 1 volt pulses. It was seen that there was considerable delay in the switching-on of the lamp after the D.C. supply was switched-on. This delay depended on the time duration for which the lamp was off in a optical pumping cycle and there was too much jitter in it. This made it unsuitable for this experiment. The delay could be minimized by operating the lamp at an excessively high voltage and hence at the cost of making the lamp self-reversed. Other possibilities like using a mechanical shutter, a rotating wheel, and an electro-optic shutter were also considered. These possibilities were found unacceptable for one reason or another. The best available electronically operated camera shutters have delay times

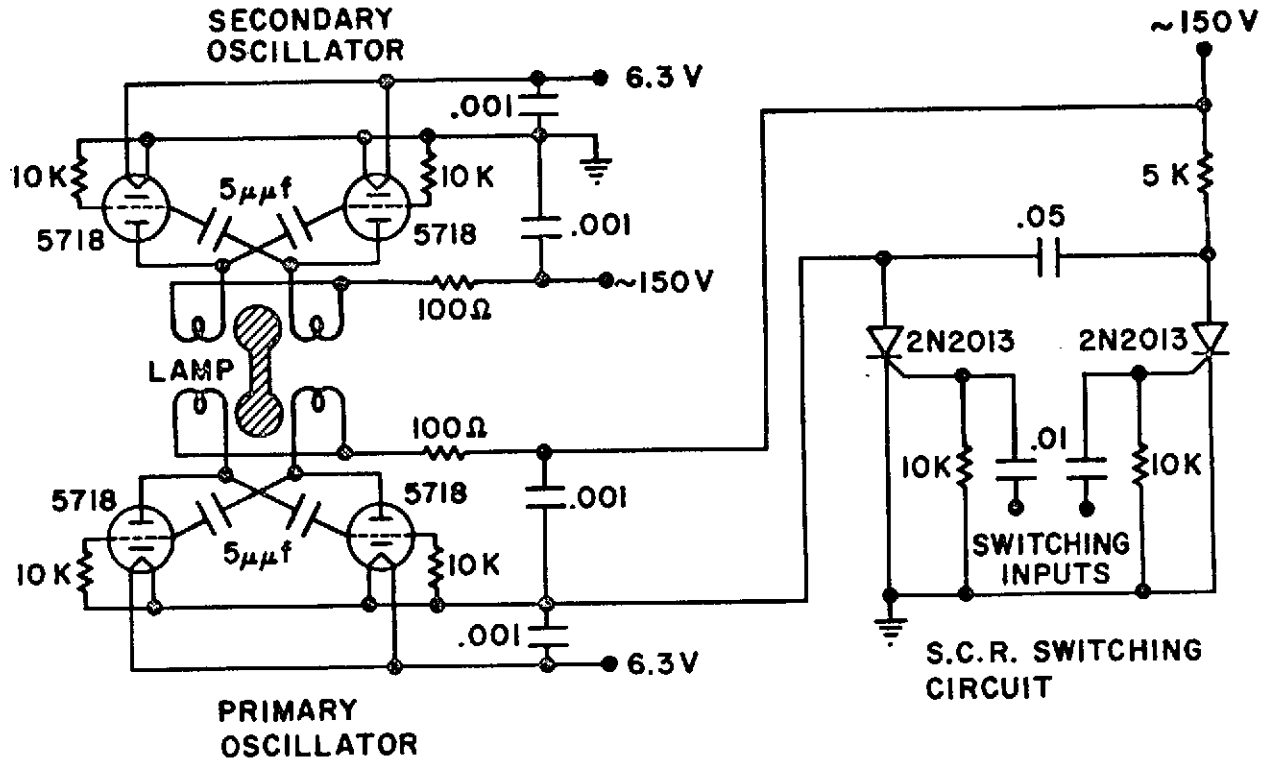

FIG. 15. SCHEMATIC OF THE TWO IDENTICAL EXCITER OSCILLATORS, ONE OF WHICH IS SWITCHED BY THE SCR CIRCUIT

from 10 to 20 ms. The rotating wheel arrangement suffers from the same disadvantages. The third possibility was too expensive. It seemed appropriate to construct the resonance lamp differently. Efforts made in this direction were very successful and resulted in a new design of the lamp[44].

B. Considerations for the Design of the Pulsed-Cesium Resonance Lamp.

The main considerations in the design of the lamp were that the lamp be switchable in a controlled way. Moreover, its switching time must be negligible. Other features like compactness, high resonance yield, etc., were of equal importance. The other essential considerations in making the resonance lamp were its stability against short term fluctuations (short compared to the duration of the repetition time of the pumping and detection cycle - 800ms), and long term drifts so that observations were reproducible.

C. Construction and Excitation of the Lamps.

The lamp was made in a dumbbell shape, as shown in the circuit diagram (Figure 15). Each bulb was about 1.2cm in diameter, blown out of a single pyrex tube of 7mm in diameter. The two bulbs were separated by about 2cm. These dimensions are not very critical. This was filled with a few milligrams of 99.95% pure cesium metal distilled under a vacuum of 10^{-7}mm Hg or better. Following the distillation xenon was filled at a pressure of about 1.5 to 2mm of Hg at room temperature. Xenon was chosen because it has energy levels close enough to the D_1 and D_2 transitions in cesium so that it can excite cesium

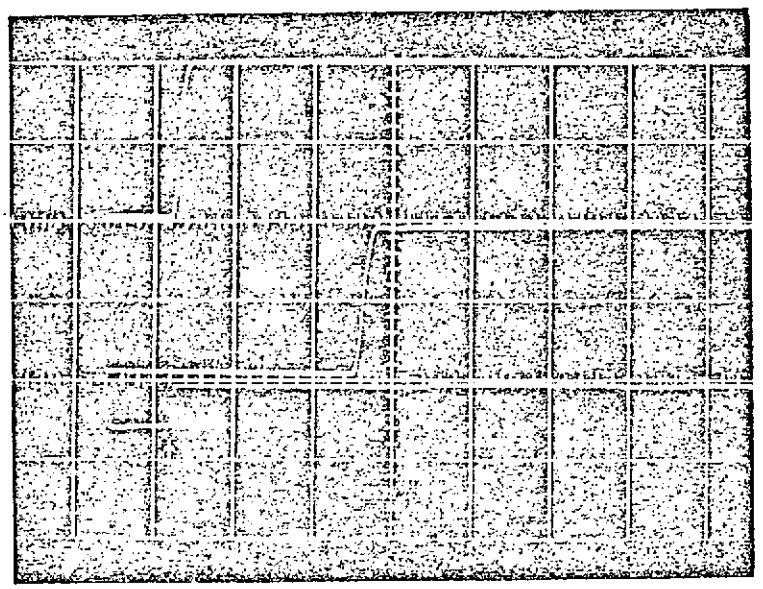

FIG. 16. PERFORMANCE OF THE DUMBBELL SHAPE RESONANCE LAMP. THE BOTTOM TRACE SHOWS THE SWITCHING PULSE WHICH, AT ITS RISING EDGE(ARROW), TURNS ON THE PRIMARY OSCILLATOR. THE OTHER TWO TRACES SHOW THE LIGHT OUTPUT FROM THE SWITCHED PORTION OF THE LAMP. WITH THE SECONDARY DISCHARGE OFF THE MIDDLE TRACE RESULTS, AND WITH IT ON THE UPPER TRACE. (THE TIME SCALE IS 1 ms/cm, VERTICAL SCALE IS ARBITRARY.)

most efficiently yet far enough to be easily filterable from them. Moreover, it is known to give best results in terms of its efficiency and stability of operation[43]. Each bulb was excited by an independent oscillator. The oscillator used was of the same design as used by BBL[43]. It was selected because of its low noise and compactness. Both the oscillators and the dumbbell lamp could be put in a 4" x 2" x 2" aluminum box.

Plate voltage to the tubes of one of the oscillators, the one desired to be pulsed, was supplied through a silicon-controlled rectifier switch. The switch was controlled by 1 volt pulses. The other oscillator was kept on continuously. The discharge plasma in this part of the lamp facilitated the firing of the other part. In this way, firing of the lamp was very uniform and was observed not to depend on the operating voltage of the secondary bulb, within its operating range. Moreover, the switching times were very uniform and stable and did not depend on the off-time of the lamp as it did previously.

Figure 16 represents typical oscillograms of the switching behavior of the lamp (a) when the secondary oscillator is off and (b) when it is on continuously. Note the delay in the switching of the lamp in Figure 16a and the absence of it in Figure 16b. As regards to the light output, it was identical to the lamp of reference 43. The lamp was very stable and its stability is demonstrated in Figure 17.

The usefulness of this kind of a lamp is not limited only to our experiment. There are other experiments in which this capability of accurate switching of the lamp can well be applied. One of the historic

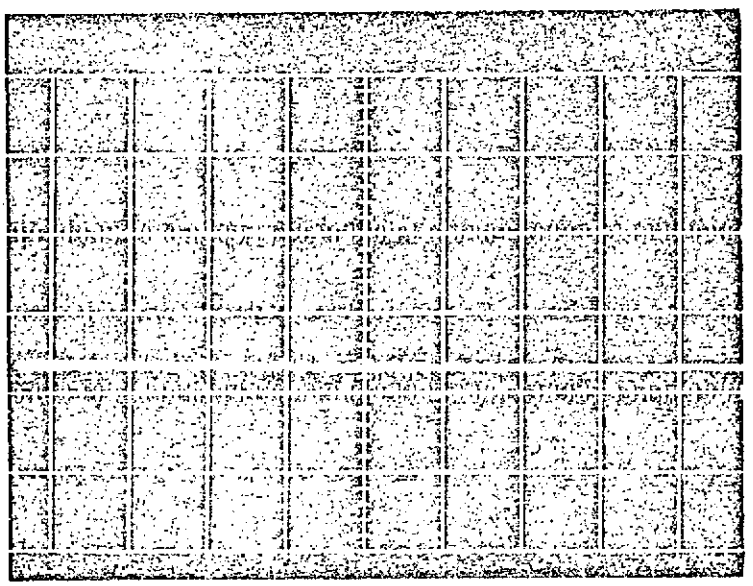

FIG. 17. ILUSTRATION OF THE STABILITY OF THE CESIUM RESONANCE LAMP.

AFTER THE WARM UP, THE OUTPUT OF THE LAMP WAS MONITORED BY AN RCA 7102 PM TUBE. THE SIGNAL WAS FOUND TO BE VERY STABLE. A SAMPLE OVER A PERIOD OF 50 SEC IS SHOWN ABOVE. SCALES: ABOUT 20 v DC SIGNAL WAS SEEN ON A DC COMPENSATED 0.5v/cm SCALE. (A Z-TYPE PLUG IN UNIT WAS USED). TIME SCALE: 5 SEC/cm.

examples is that of the study of relaxation times of optically polarized atoms where the lamp need be switched off for different lengths of time and the polarization studied as a function of time. Another useful area of its application would be where the pulsing rate is matched to the zeeman frequency of the atoms to bring in resonances. There could be other areas of similar nature where the ease and flexibility of switching the lamp may be desirable.

CHAPTER VII

PREPARATION OF WALL-COATED CESIUM VAPOR CELLS

A. Coatings with Paraflint.

Paraflint has been known[28] to preserve spin orientation during collisions between polarized atoms and the paraflint coated walls of the container. Paraflint coated walls have also been found to be very stable[46] though their reproducibility from cell to cell is still an open question. The method of preparing the coatings has varied from one investigator to the other[28,45,46]. The method discussed in reference 46 has been followed by most authors after the publication of this paper. In our early experiments with coatings by a similar procedure as given in reference 46, we felt the method was unnecessarily complicated. However, we did not take great pains in following up this method; rather, we developed a more convenient procedure of wall coating. It is described in every essential detail in the following.

B. Properties of Paraflint[47].

Paraflint is a hard, high melting point hydrocarbon wax. It is essentially a mixture of saturated, straight chain paraffin hydrocarbons, having an average molecular weight of approximately 750, corresponding to approximately 50 to 55 carbon atoms per molecule ($CH_3 - C_nH_{2n} - CH_3$). Its melting point is of the order of 100°c.

Paraflint is synthesized by burning coal in the presence of oxygen, steam, and various catalysts to produce a wide variety of

hydrocarbons depending on conditions. Paraflint wax thus produced is refined but still contains components with low boiling point. To get rid of the volatile contents and to distill a suitable fraction from the commercially available paraflint, the following procedure was adopted.

C. Fractional Distillation of Paraflint.

It has been known[45] before that if the low boiling point components were removed by heating the paraflint at 250°C (under vacuum), the residue has a very low vapor pressure of less than 5×10^{-6} mmHg at 120°C. In view of this observation, we decided to use the highest distillate for coating in order that the vapor pressure due to the paraflint was much smaller than 10^{-6} mmHg. The vacuum and the gas filling system was used for the purpose of fractional distillation. This system was equipped with an excellent baking facility and thermostat control permitting any desired baking temperature up to 500°C. This proved to be ideal for fractional distillation and our method of Wall Coatings.

Paraflint RG was contained at one end of a long glass tube; the other end projected out of the oven and was connected to the vacuum pump and to a side tube for collecting the distillate. The first fraction collected for about 30 hrs. at 275°C was discarded. The next three fractions were collected at 300°C, 350°C, and 375°C. Baking was done for sufficient times to make sure that any particular fraction was completely distilled over. About 1/10 of the original amount of paraflint was left as residue by the end of the fourth distillate. The last fraction was used for coating, other fractions were kept for any eventual use.

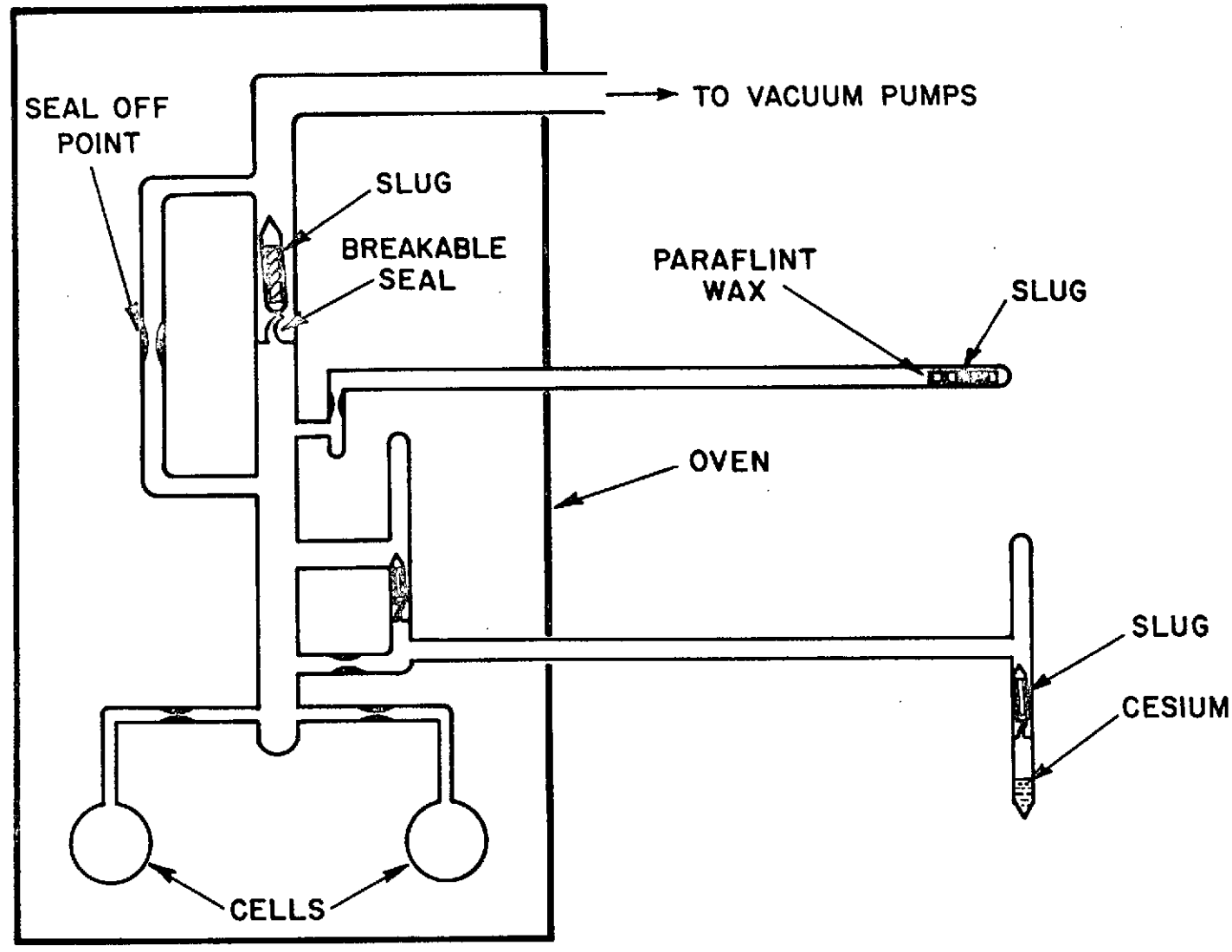

Fig. 18 ARRANGEMENT FOR MAKING PARAFLINT COATED CESIUM VAPOR CELLS

D. Experimental Procedure for Wall Coating.

A very simple procedure for wall-coating with paraflint was developed. It gave excellent, reproducible, thin, and transparent coatings. It was done in the following way: a couple of cells (well cleaned, washed and dried) were attached to the vacuum system (Figure 18). They were baked at about 450°C for 24 hours under vacuum. A small amount of wax (out of the distillate collected in the temperature range 350°C to 375°C) was kept at the farthest end of a 1/2 meter long tube which was connected to the system at its other end. Wax was contained in a glass tube to which a sealed iron slug was attached. After baking and cooling, wax was brought closer to the cells and melted into a previously arranged tube. Wax container with the iron slug and the long tube were removed without breaking the vacuum. The system was sealed off from the vacuum pumps and rebaked for about 8 hours at 365°C. When rebaking, a small temperature gradient was provided in such a direction that it helped in moving some wax into the cells. The system was then cooled slowly. While cooling, attempt was made to have uniform temperature distribution in the oven.

The coatings obtained in this way were very thin and hardly visible. An excessive distillation of wax into some cells could be seen as a deposit of wax at the lowest position of the cell making it slightly translucent. However, this part of the cell surface would be equally effective in inhibiting relaxation of the polarized atoms as the rest of the surface.

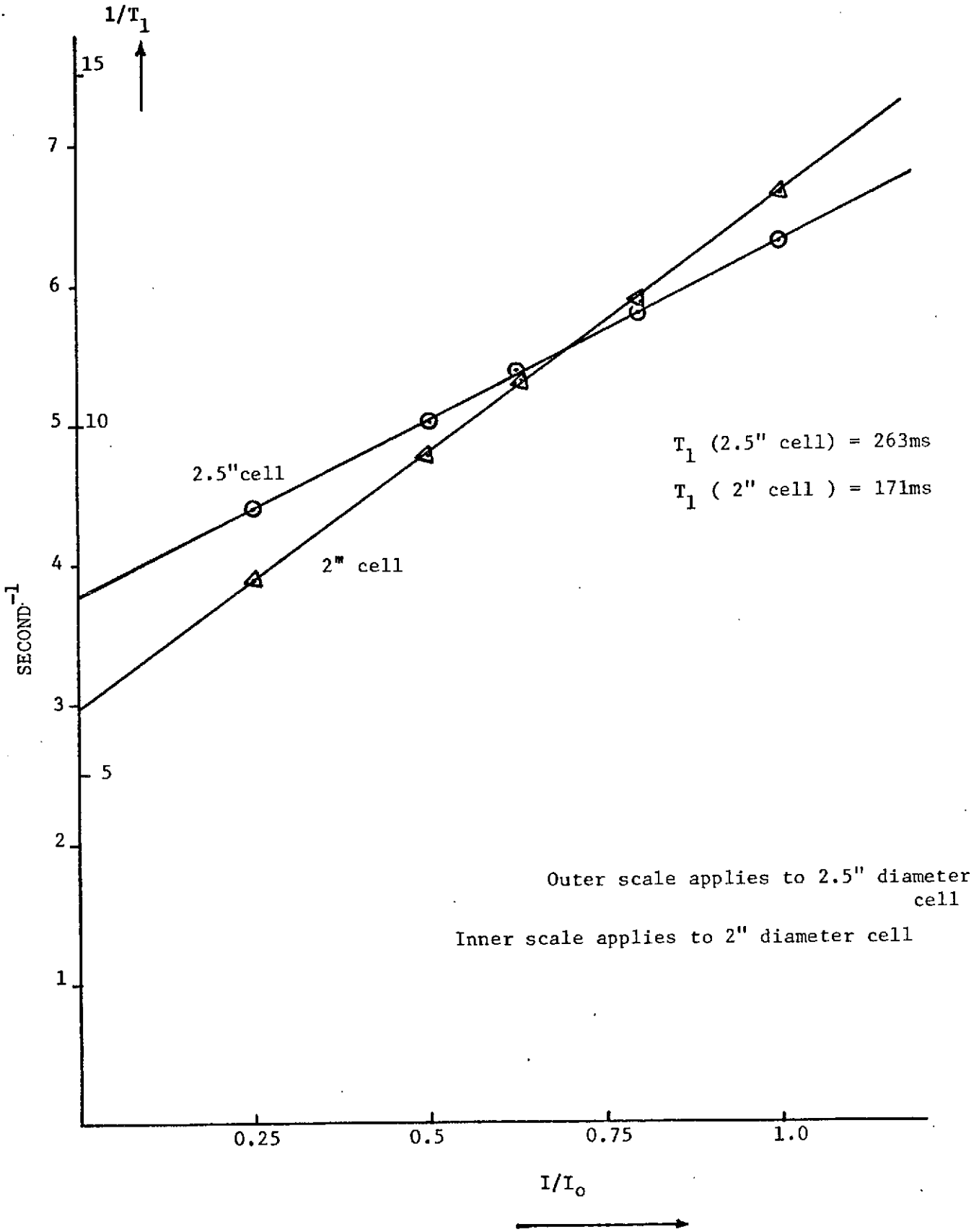

Figure 19. Plot of 'inverse relaxation time' vs light intensity for 2.5" and 2" diameter wall coated cells.

rotated by 180^{o} in a time much shorter than the relaxation time of the atoms. The observed relaxation time (T_{ohs}), thus determined, is related to the longitudinal relaxation time (T_1) and the relative intensity I of the applied resonance light by the relation[48]

$$\frac{1}{T_{ohs}} = CI + \frac{1}{T_1}$$

Thus by plotting $\frac{1}{T_{ohs}}$ against I/I_o, where I is the intensity reduced from the initial intensity I_o by a neutral density filter, the value of T_1 is extrapolated. The values for T_1 thus obtained for the five cells were very good and are given below. A typical relaxation curve is shown in the next chapter (Figure 20a). Figure 19 represents the variation of relaxation times of cells II and V at various light intensities. Behavior of other cells was identical.

Relaxation Time T_1

For

Cell I = 170 ms

Cell II = 263 ms

Cell III = 233 ms

Cell IV = 200 ms

Cell V = 171 ms.

Lower values of the relaxation times in cell I and IV can be attributed to the following accidents with these cells: a drop of cesium fell into the cell IV from its stem (where the cesium is stored). Though much of the cesium was carefully transferred back into the stem, very

fine droplets are still visible. This contamination of the surface is probably responsible for the lowering of its relaxation time. In cell I, somehow, the stem of the cell got overheated when removing the cell from the vacuum system. This might have resulted in an excessive flow of cesium vapors into the cell surface. Settling of cesium on the surface can possibly reduce the relaxation time considerably.

In view of the fact that relaxation time is proportional to the diameter of the cell, the relaxation time of cell V is compatible with that of cell III or II.

In a relaxation time of 263 ms, the atoms make about 1.5×10^3 collisions with the coated wall before their orientation is destroyed. This number of collisions is very close to the one (i.e. 10^3) observed in reference 46 for the case of rubidium atoms in paraffin coated cells.

CHAPTER VIII

DETECTION OF HYPERFINE RESONANCES OF Cs-133 BY THE METHOD OF PHASE DESTRUCTION

A. Preliminary Results

1. Effect of 180^{o}- pulses

It was discussed before that when the vapor cell attains a steady state of polarization, it practically becomes transparent to the pumping light. On the application of a 180^{o} pulse, the polarization is reversed and the cell begins to absorb the pumping light and a decay curve as shown in Figure 20a results. Another 180^{o} -pulse will bring the atoms into the original polarized state and hence a state of no absorption results, except to compensate for the relaxation. This curve was observed and is shown in Figure 20b.

2. Effect of one 90^{o}- pulse

An application of one 90^{o}-pulse will result in a freely precessing state of the atoms. The signal as seen at the detector was not very much different from Figure 20a except for its initial amplitude. In order to check the existence of the freely precessing state, a transverse light beam was used. It is shown in reference 17 that in such an experimental situation, the transverse beam will be modulated at the frequency of the precessing atoms. Such a precession was observed and is shown in Figure 21.

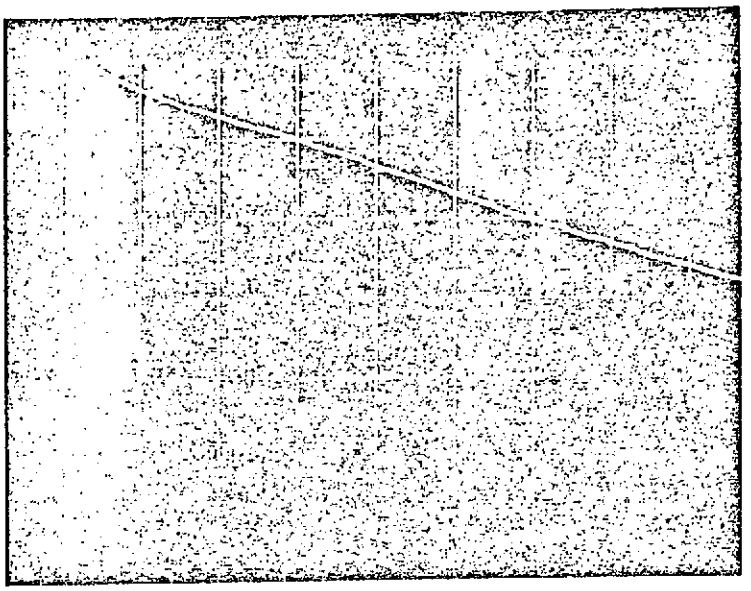

(a)

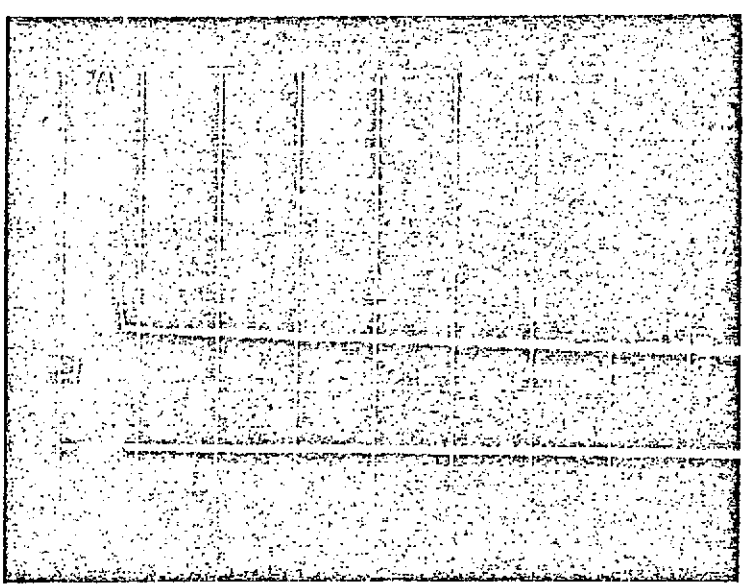

(b)

FIG. 20. ABSORPTION OF THE PUMPING LIGHT VERSUS TIME, AFTER THE LONGITUDINALLY POLARIZED ATOMS ARE ROTATED BY (a) 180° AND (b) 360° . (VERTICAL SCALES: 0.5 v/cm; TIME SCALES: 20 ms/cm IN (a) & 5 ms/cm IN (b).)

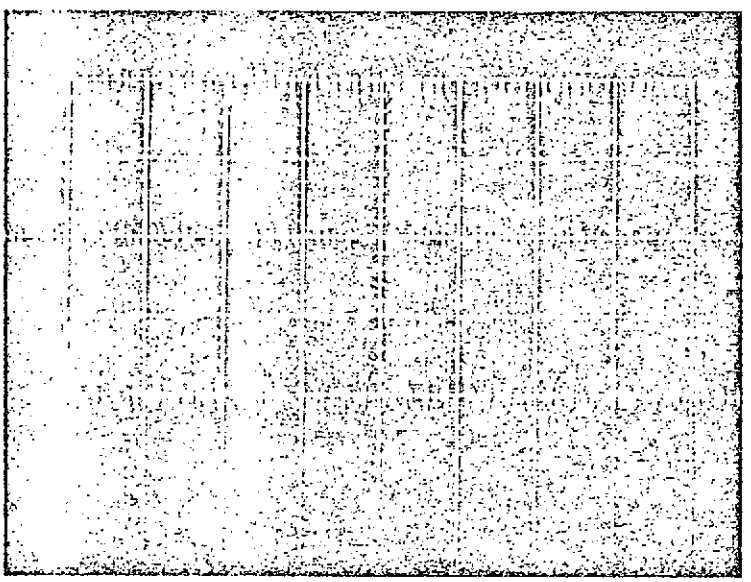

FIG. 21. MODULATION OF THE TRANSVERSE BEAM OF RESONANCE LIGHT BY THE FREELY PRECESSING Cs-133 ATOMS . ATOMS IN THIS STATE HAVE BEEN OBTAINED BY APPLYING A 90^{o}- RF PULSE TO THE LONGITUDINALLY POLARIZED ATOMS. (TIME SCALE : 0.04 ms/cm.)

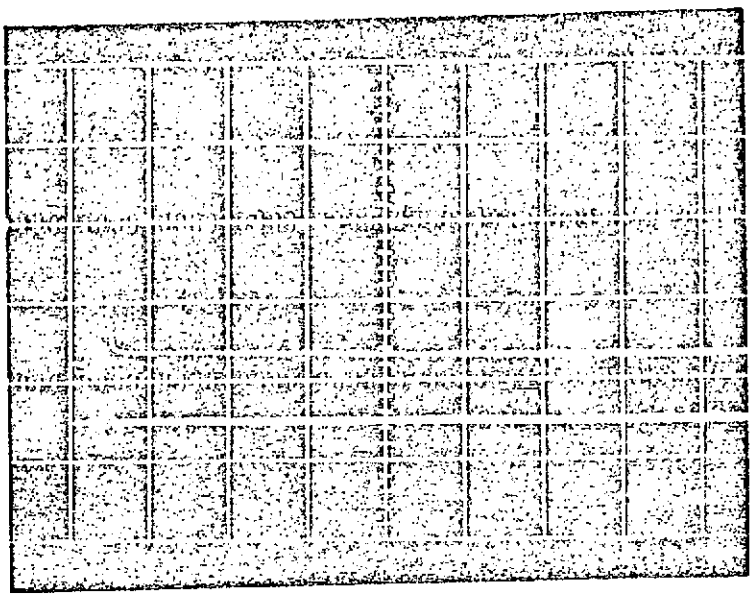

(a) T = 0.0 ms

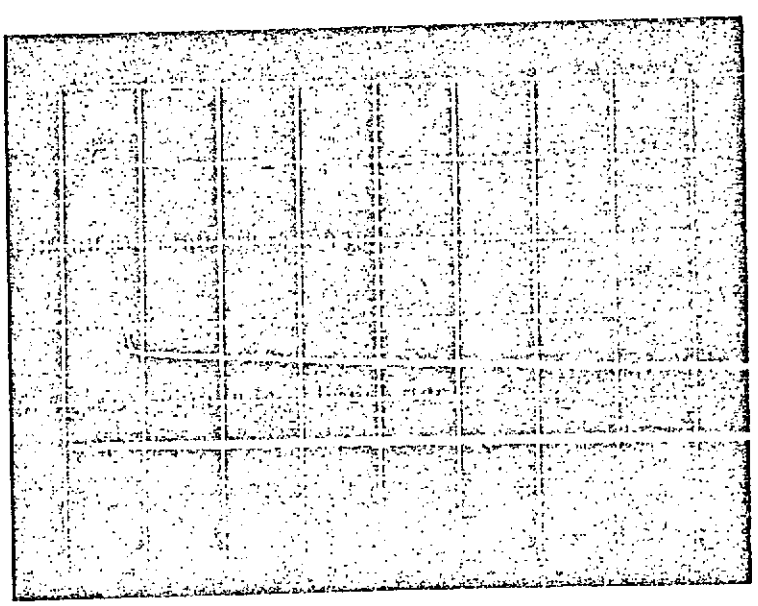

(b) T = 1.6 ms

FIG. 22. ABSORPTION OF THE PUMPING LIGHT INTENSITY FOR DIFFERENT TIME INTERVALS BETWEEN THE END OF THE $+90^{\circ}$- RF PULSE AND THE BEGINNING OF THE -90°-RF PULSE. (a) T =0.0 ms AND (b) T = 1.6 ms. TIME SCALE: 5ms/cm.

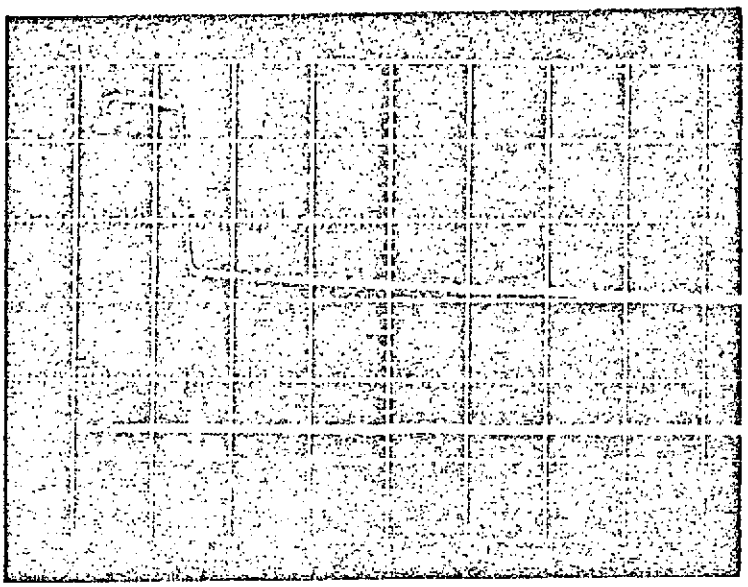

(c)

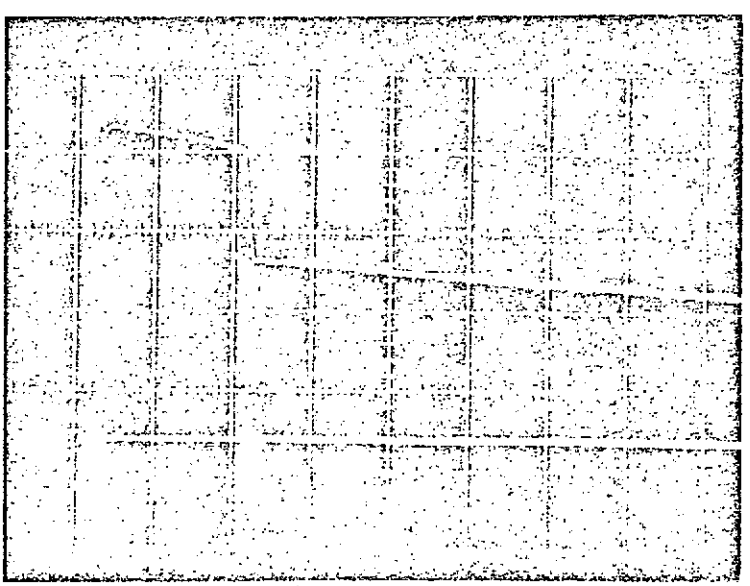

(d)

Figure 22 (c) & (d), Time Scale 5ms/cm.

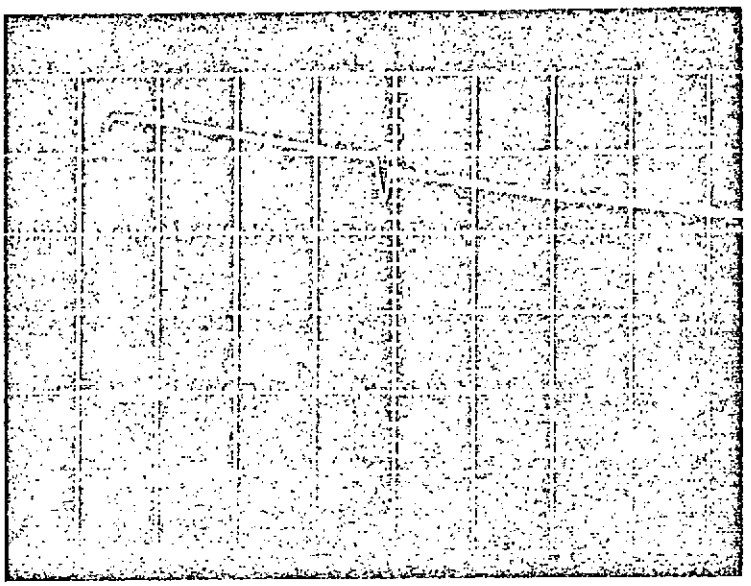

(e)

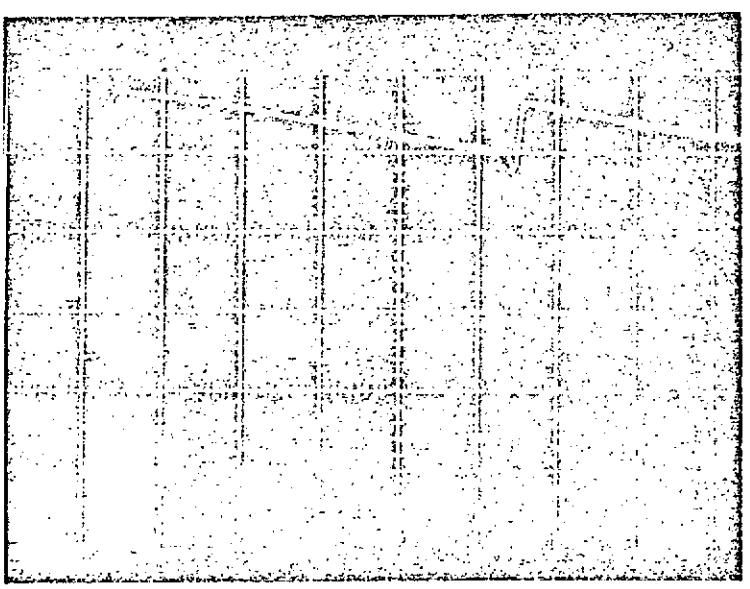

(f)

Figures 22 (e) & (f); Time Scale 5 ms/cm

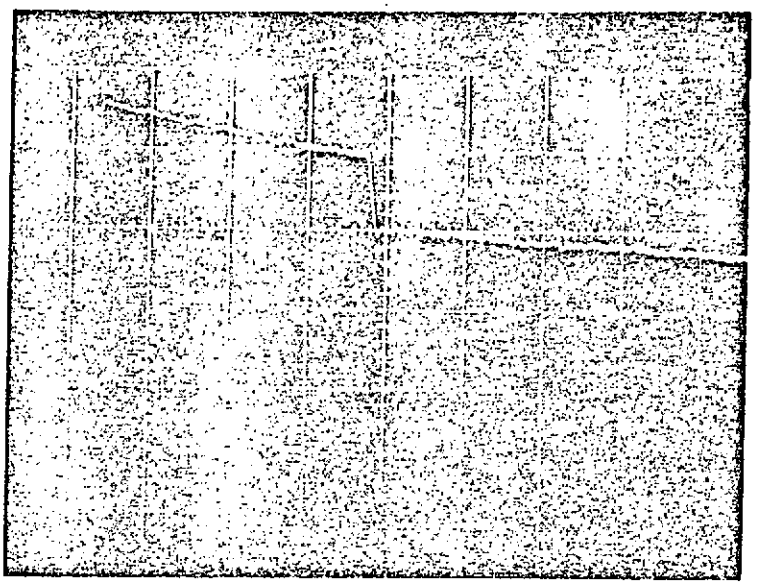

(a)

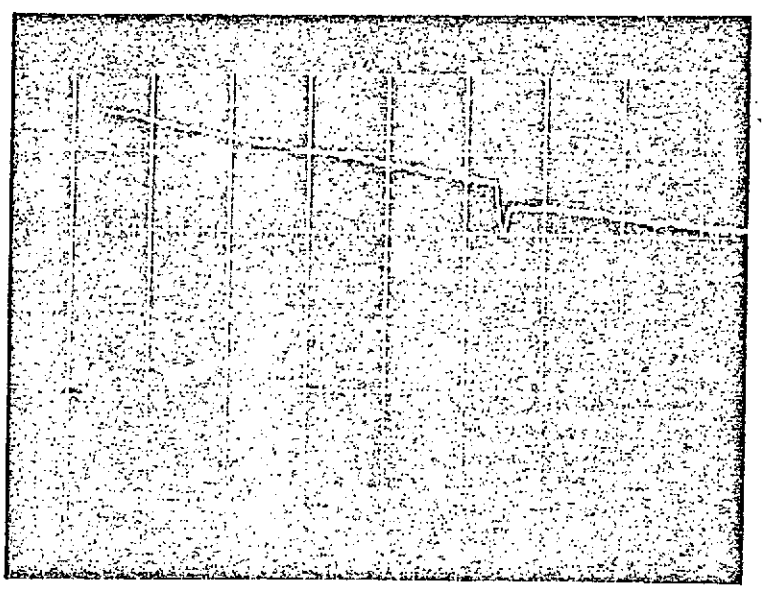

(b)

FIGURES 23 (a) & (b): ABSORPTION OF THE PUMPING LIGHT WHEN ITS INTENSITY IS REDUCED TO $I_o/2$.

TIME SCALE 5 ms/cm

3. Effect of $+90^{o}$-pulse followed by a -90^{o}-pulse

In this part of the observations as well as in previous experiments (A - 1,2;above) the pumping light was kept-on continuously. We shall see next that it pays to keep the pumping light off in between the $\pm 90^{o}$-pulses.

It was shown in Chapter III that a -90^{o} pulse after the $+90^{o}$ pulse will bring the atomic state into its original polarized state of zero absorption except for relaxation. This behavior was observed and is shown in Figure 22a through 22f. These figures were taken at increasing time intervals between the $\pm 90^{o}$ pulses. (This time interval will be denoted by T for future reference.) It is seen in Figure 22e when $T > 16$ ms , that absorption dips to a minimum and then rises again. This behavior is probably due to the fact that some atoms get pumped in the Z-direction during the time T and then get rotated to the freely precessing state by the -90^{o} pulse, whereas the atoms in the freely precessing state are brought into the Z-direction. Optical pumping of the atoms, in effect, results in a loss of coherence in addition to the loss of coherence due to thermal relaxation. As a result,the -90^{o} pulse no longer forms a state of least absorption rather a complicated state results which goes through a minimum in absorption during the time of its formation. This effect can be reduced by reducing the pumping light intensity as shown in Figures 23 a,b.

4. Pumping light off in between the $\pm 90^{o}$-pulses

In this case, the pumping light was turned off 1.6msec before the $+90^{o}$ pulse and was turned-on 1.6msec before the -90^{o}-pulse was

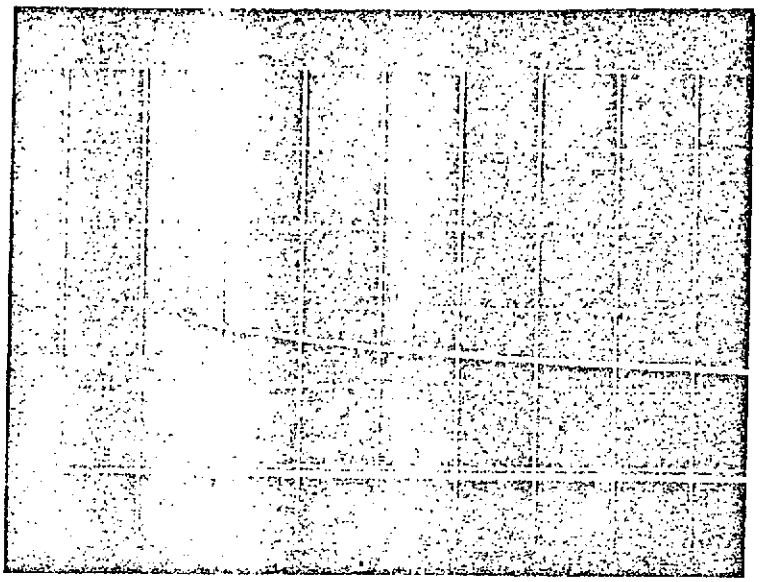

(a)

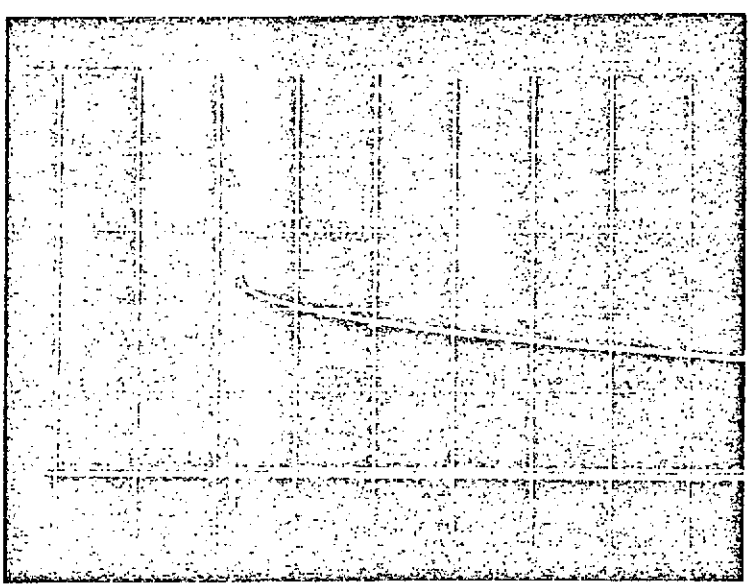

(b)

FIG. 24. ABSORPTION OF THE PUMPING LIGHT FOR DIFFERENT TIME INTERVALS BETWEEN THE $+90^{\circ}$ AND -90° RF PULSES. IN THIS CASE THE PUMPING LIGHT WAS SWITCHED OFF IN THIS INTERVAL, UNLIKE AS IN FIGURES 22 & 23. (SCALES: 1 v/cm & 10 ms/cm)

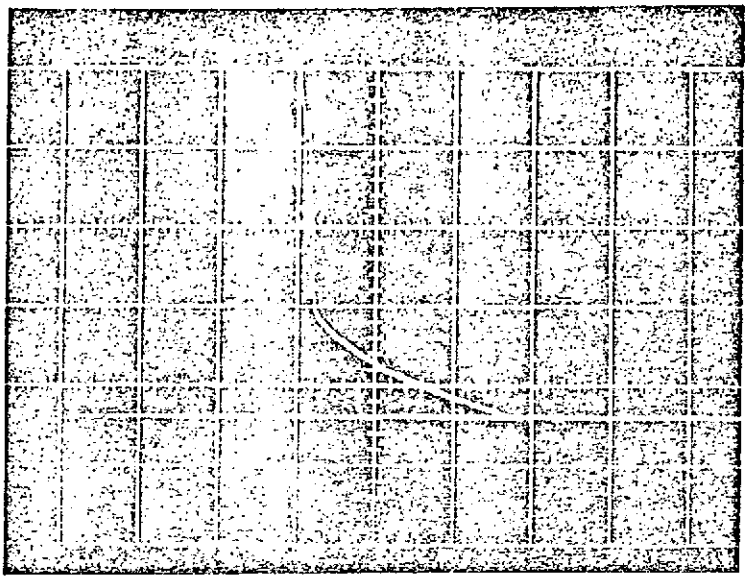

(c)

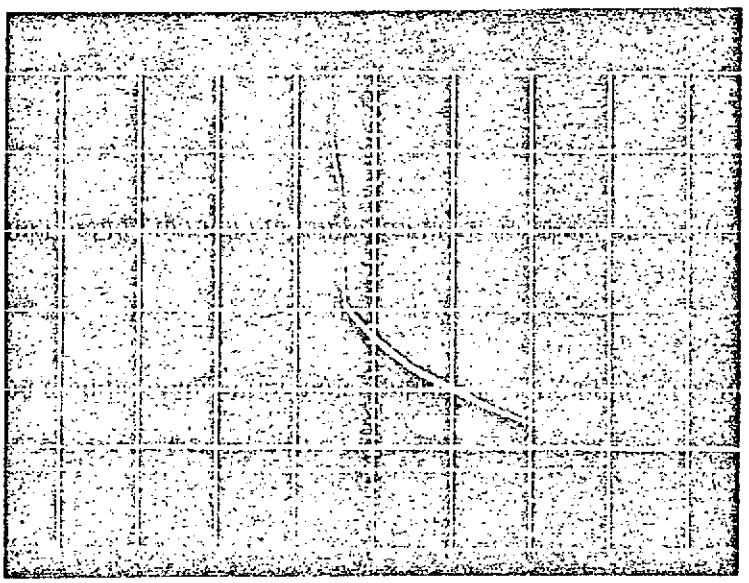

(d)

FIGURES 24 (c) & (d); SCALES: 10 ms/cm, 0.5 v/cm

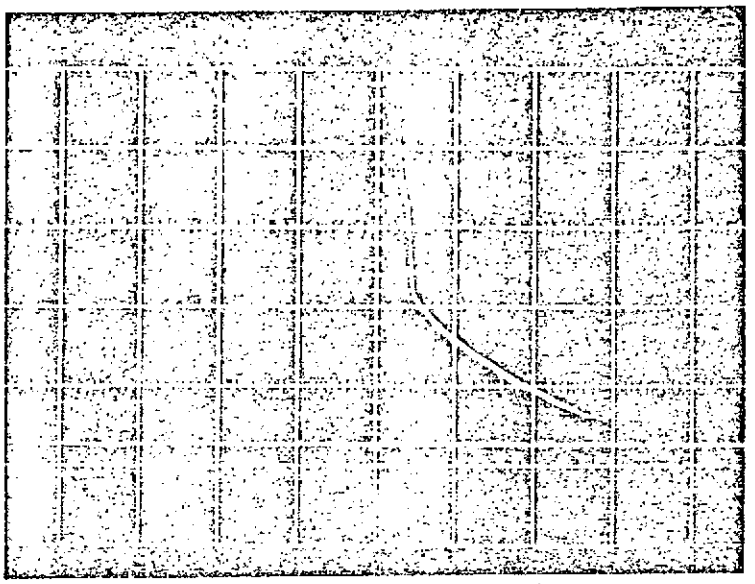

(e)

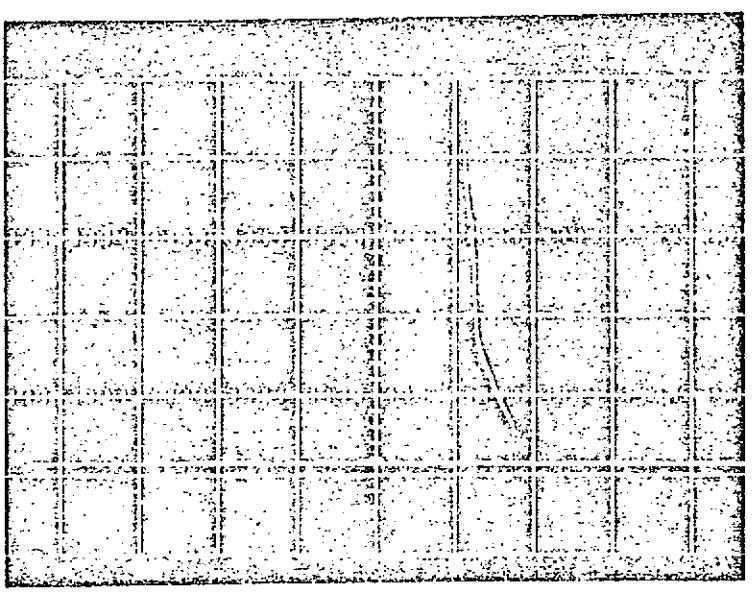

(f)

FIGURES 24 (e) & (f) ; SCALES; 10 ms/cm, 0.5 v/cm IN (e)
& 0.25 v/cm IN (f).

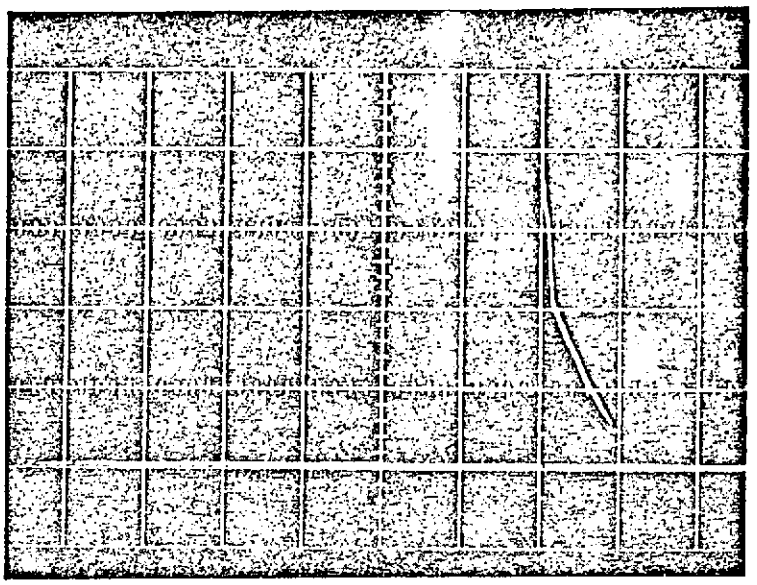

(g)

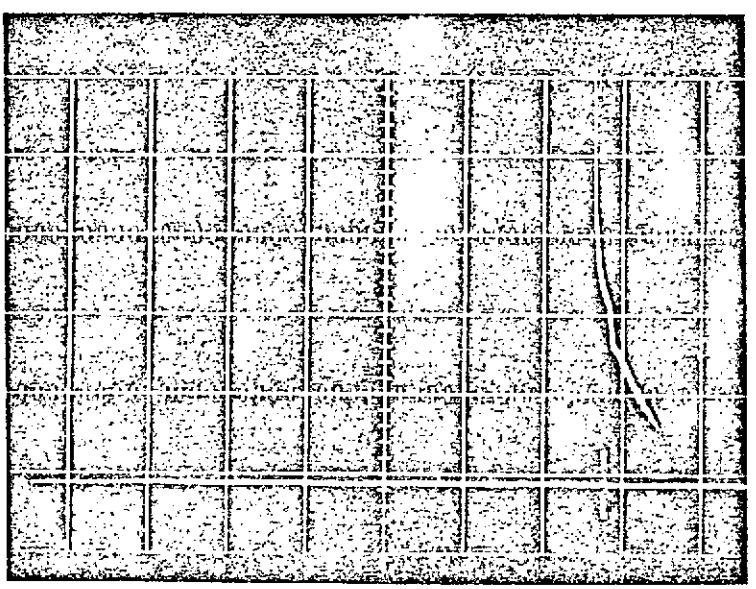

(h)

FIGURES 24 (g) & (h) ; SCALES: 10 ms/cm, 0.25 v/cm.

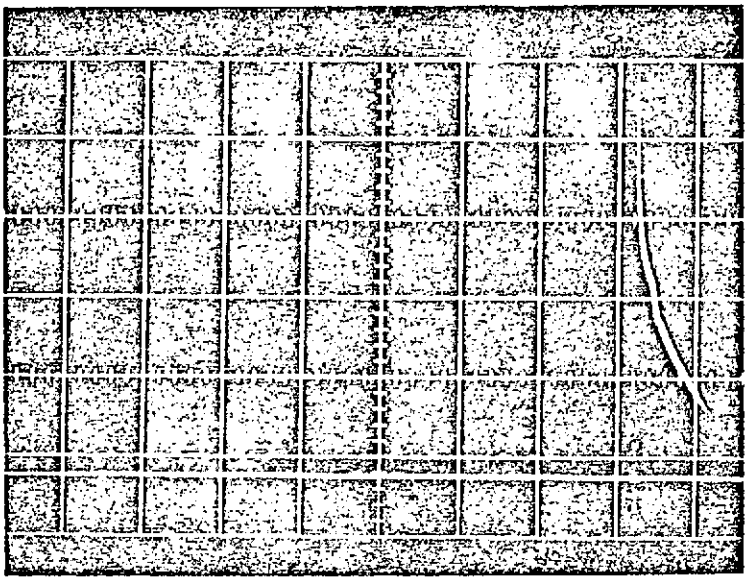

(i)

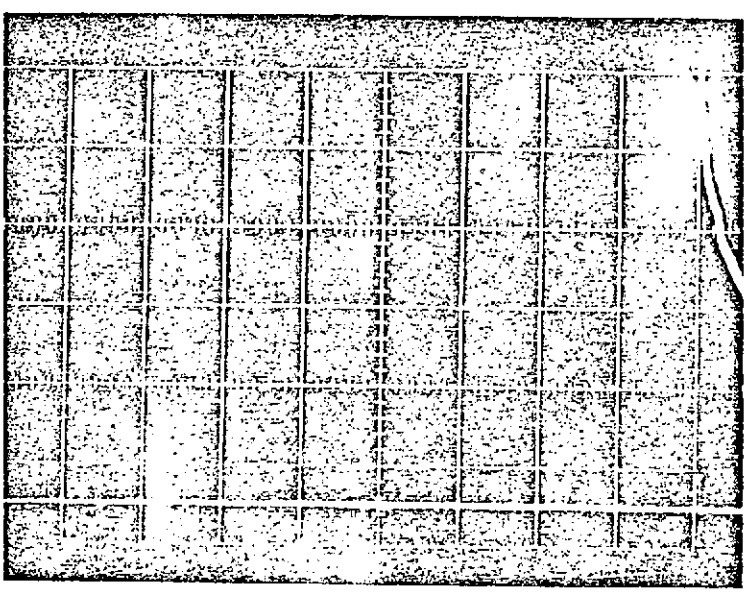

(j)

FIGURES 24 (i) & (j) ; SCALES: 10 ms/cm, 0.25 v/cm

applied. These observations are shown in Figure 24a through 24j. One clearly sees an improvement over the previous case in which the pumping light is kept on during the interval (T) between the $\pm 90^{\circ}$-pulses. We saw in this case that the signal indicative of the formation of the initial polarized state began to be distorted for T larger than 16 ms. On the contrary in Figures 24a through j, the discontinuity in the monitoring signal which is seen when a -90°-pulse is applied, is a clear indication of the recovery of a substantial part of the initial polarized state for the interval T as large as 65 ms. Smaller signals could be seen for the time interval T greater than 80 ms.

B. Observations on the Hyperfine Resonances.

In order to observe the hyperfine resonances, microwaves were pulsed-on for the time interval between the two 90^{0}-RF pulses. The pumping light was switched-off in this interval and was switched on 1.6 ms before the second 90 -pulse in order to monitor the phase destruction caused by the microwave fields. The frequency of the microwaves was varied by tuning the IF-reference frequency to match the $(4,0) \leftrightarrow (3,0)$ transition in the ground state of the cesium sample. The detection of the resonance was noted by observing the variation in the size of the signal following the second 90° -pulse. A typical oscilloscope signal is shown in Figure 25. Figure 25a shows the signal in the absence of any microwave fields whereas Figure 25b displays the signal following the microwave pulse of about 50 ms duration. The lower trace in Figure 25b shows the microwave pulse. To display this pulse a part of the microwave energy was taken from the phase

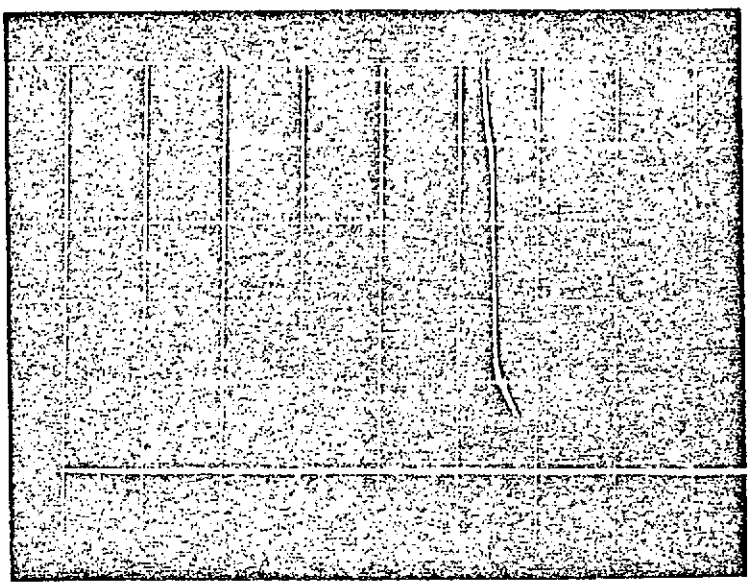

(a)

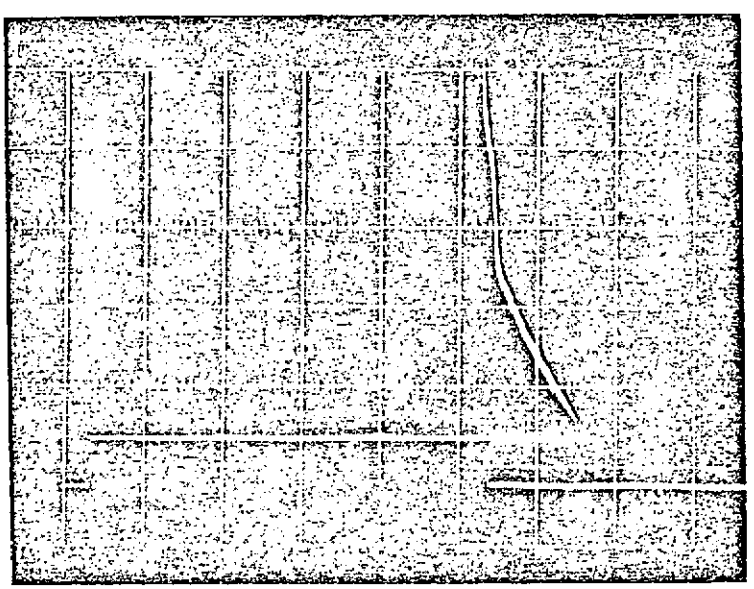

(b)

FIG. 25. DETECTION OF THE 0-0 TRANSITION IN THE GROUND STATE OF Cs-133. (a) SIGNAL IS OBSERVED WITHOUT THE MICROWAVES. (b) SIGNAL IS OBSERVED WHEN THE MICROWAVES AT RESONANCE WITH THE 0-0 TRANSITION ARE SWITCHED ON BETWEEN THE 90°-RF PULSES. (TIME SCALE: 10 ms/cm.) NOTICE THE REDUCTION IN THE SIZE OF THE SIGNAL.

locked klystron source and fed into a crystal detector and its output used. The frequency of the microwaves corresponding to the maximum reduction in the size of the signal determines the resonance frequency. A set of such values found for different cells is given in Table III.

TABLE III

Resonance Frequency Corresponding to the

$(4,0) \leftrightarrow (3,0)$ Transition

Cell No.	Resonance frequency in MHz		Shift from the Free Atom Value (9192.631770 MHz)
I	9192.6314	±450 cps	~ -400 cps
II	9192.6311		~ -650 cps
III	9192.6313		~ -450 cps
IV	9192.6313		~ -450 cps
V	9192.6312		~ -550 cps

in the results of the above mentioned authors is small (~15 cps); whereas, in the present experiment it is large for reasons explained earlier. Large dispersion in the values of the shifts, in the present experiment, can possibly be due to different proportions of residual paraflint wax vapors remaining in the cells after they were sealed off.

APPENDIX I

EFFECT OF A ROTATING MAGNETIC FIELD PULSE ON A PURE QUANTUM STATE $|F,\mu>$

Let the atom under consideration have a magnetic moment μ and be in the quantum state $|F,\mu>$ (Note: the same symbol is used for the magnetic moment and the magnetic quantum number). It is subjected to a constant magnetic field B_o along the Z-axis and a pulsed rotating magnetic field, pulse beginning at t_1 and ending at t_2. Let the magnitude of the ratating be B_1 and be along the Y-axis of a rotating co-ordinate system, rotating with an angular velocity ω_z about the laboratory z-axis. The plane of ratation of Y-axis and hence of B_1 is normal to the laboratory Z-axis. The total magnetic field acting on the atom and hence the wave equation can be written as

$$B_T = \hat{K}B_o + B_1(-\hat{i}Sin\omega_z t + \hat{j}cos\omega_z t) \qquad (1)$$

$$\frac{ih}{2\Pi}\frac{\partial\Psi}{\partial t} = -\vec{\mu}.\vec{B}_T\Psi = -\gamma\vec{F}.\vec{B}_T\Psi$$

$$= -\frac{\gamma h}{2\Pi}\{B_oF_z + B_1(-F_xSin\omega_z t + F_ycos\omega_z t\}\Psi \qquad (2)$$

$$= -\frac{\gamma h}{2\Pi}\{B_oF_z + B_1e^{-i\omega_z tF_z}F_ye^{i\omega_z tF_z}\}\Psi$$

where $t_2 \geq t \geq t_1$

This equation is best solved by transforming it to a co-ordinate system rotating round the Z-axis with an angular velocity ω_z and sense corresponding to the sign of $-\gamma$ (This is essentially the sense of rotation of the rotating magnetic field.) The transformed wave function and the schrodinger equation can be written as

$$\Psi_r = e^{i\omega_z t F_z} \Psi \tag{3}$$

$$\frac{ih}{2\pi} \frac{\partial}{\partial t} \Psi_r = -\{\frac{h}{2\pi}(\omega_z + \gamma B_o) F_z + \frac{\gamma h}{2\pi} B_1 F_y\}\Psi_r \tag{4}$$

It is clear that the time dependence of the magnetic field has been eliminated. In fact equation (4) represents the coupling of the spins with an effective static field

$$B_r = \hat{K}(B_o + \frac{\omega_z}{\gamma}) + \hat{j}B_1 \tag{5}$$

Moreover, the spins will be quantized along the effective field in the rotating frame of reference, the energy spacing being given by $\Delta E = \frac{\gamma h}{2\pi} B_r$. As our rotating frame is coincident with the rotating rf-field which is supposed to be at Zeeman resonance, so

$$\omega_z = -\gamma B_o$$

Therefore the effective field is essentially the rotating field itself. For computation purposes, the effect of this field can also be eliminated

by transforming to a doubly rotating co-ordinate system with a frequency $\omega_1 = -\gamma B_1$ rotating round the Y-axis of the rotating frame of reference. In this doubly rotating co-ordinate system the wave function Ψ_{rr} and the effective field is written as

$$\Psi_{rr} = e^{i\omega_1 t F_y} \Psi_r \tag{6}$$

$$B_{rr} = B_1 + \frac{\omega_1}{\gamma} = 0$$

Obviously in the doubly rotating co-ordinate system the interaction hamiltonian vanishes and the states do not change in time. Therefore one can write

$$\Psi_{rr}(t_2) = \Psi_{rr}(t_1) = \Psi_r(t_1) \tag{7}$$

Since the rf-field has been effective for a time t_2-t_1 and the doubly rotating system has rotated by an angle $-\omega_1(t_2-t_1)$ round the Y-axis of the singly rotating co-ordinate system, therefore , using (6),

$$\Psi_{rr}(t_2) = e^{-i\omega_1(t_2-t_1)F_y} \Psi_r(t_2) \tag{8}$$

$$\Psi_r(t_2) = e^{i\omega_1(t_2-t_1)F_y} \Psi_{rr}(t_2)$$

$$= e^{i\omega_1(t_2-t_1)F_y} \Psi_r(t_1) \tag{9}$$

Using (3) we have

$$\Psi_r(t_2) = e^{i\omega_z t_2 F_z} \Psi(t_2) \tag{10}$$

$$\Psi_r(t_1) = e^{i\omega_z t_1 F_z} \Psi(t_1)$$

Therefore,

$$\Psi(t_2) = e^{i\omega_z t_2 F_z} e^{i\omega_1 (t_2 - t_1) F_y} e^{-i\omega_z t_1 F_z} \Psi(t_1)$$

Let $\Psi(t_1)$ bethe eigen functions of F_z and be denoted by $|F,\mu>$. Then after the 90^o-rf pulse the transition amplitude from state $|F,\mu>$ to state $|F,\mu'>$ can be written as

$$a^F_{\mu\mu'}(t_2) = \langle F,\mu' | e^{i\omega_z t_2 F_z} e^{i\omega_1 (t_2 - t_1) F_y} e^{-i\omega_z t_1 F_z} | F,\mu \rangle \qquad (11)$$

and the new state can be written as

$$\Psi(t_2) = \sum_{\mu'} a^F_{\mu'\leftarrow\mu} |F,\mu'>$$

where

$$a^F_{\mu'\leftarrow\mu} = e^{i\omega_z(\mu' t_2 - \mu t_1)} \langle F,\mu' | e^{i\omega_1 (t_2 - t_1) F_y} | F,\mu \rangle \qquad (12)$$

Here one easily recognizes that $a^F_{\mu'\leftarrow\mu}$ is nothing but the $D^F_{\mu\mu'}(\alpha,\beta,\gamma)$ unitary operator which connects the wave functions in a stationary system to a rotated co-ordinate system. α,β,γ are the Euler angles of rotation. From the definition of the D-Functions one easily recognizes:

$$\langle F,\mu' | e^{i\omega_1 (t_2 - t_1) F_y} | F,\mu \rangle = D^F_{\mu,\mu}(0,-\omega_1(t_2-t_1),0) \qquad (13)$$

$$= D^F_{\mu\mu'}(0,\omega_1(t_2-t_1),0) \qquad (14)$$

Therefore $\psi(t_2) = \sum_{\mu'} e^{i\omega_z(\mu' t_2 - \mu t_1)} D^F_{\mu\mu'}\{0,\omega_1(t_2-t_1),0\}|F,\mu'>$ (15)

which is the desired coherent superposition of the magnetic states.

REFERENCES

1. J. Brossel and A. Kastler, Comptes Rend. 229, 1213 (1949).
2. A. Kastler, J. Phys. et Rad. 11, 255 (1950).
3. J. Brossel, A. Kastler, and J. Winter, J. Phys. et Rad. 13, 668 (1952).
4. J. Brossel, B. Cagnac, and A. Kastler, Comptes Rand. 237 984 (1953).
5. W.B. Hawkins and R. H. Dicke, Phys. Rev. 91, 1008 (1953).
6. W. B. Hawkins, Thesis, Princeton University (1954).
7. W. B. Hawkins, Phys. Rev. 96, 532 (1954); 98, 478 (1955).
8. P. L. Bender, Thesis, Princeton University (1956).
9. C. Cohen-Tannoudji, J. Brossel, and A. Kastler, Comptes Rand. Sci. 244, 1027 (1957).
10. H. G. Dehmelt, Phys. Rev. 105, 1487 and 1924 (1957).
11. W. Franzen and A. G. Emslie, Phys. Rev. 108, 1453 (1957).
12. W. E. Bell and A. L. Bloom, Phys. Rev. 107, 1559 (1957); 109, 219 (1958).
13. M. Arditi and T. R. Carver, Phys. Rev. 109, 1012 (1958); 112, 449 (1958).
14. E. C. Beaty, P. L. Bender, and A. R. Chi, Phys. Rev. 112, 450 (1958); Phys. Rev. Letters 1, 311 (1958).
15. J. P. Barrat, Thesis, Paris (1959); J. Phys. et Rad. 20, 541, 633, and 657 (1959).
16. Carroll O. Alley, Quantum Electronics, ed. C. H. Townes, (1960) p. 146.
17. Carroll O. Alley, "Investigations of the Effect of Gas Collisions and Optical Pumping on the Breadth of Spectral Lines", Unpublished Report, Princeton University (1960) under Contract No. DA-36-039 SC-70147.

18. Carroll O. Alley, "Investigations of the Optical Detection of Hyperfine Resonances in Alkali Vapors, "4th Quarterly Report under Contract No. DA-36-039 SC-87273, DA Project No. 3A99-15-001 w. the U.S. Army Signal Research and Development Laboratory by th Institute of Optics, University of Rochester (May, 1962).

19. C. Cohen-Tannoudji, Thesis, Paris (1962); Ann Phys. 7, 423 and 469 (1962).

20. J. P. Barrat and C. Cohen-Tannoudji, J. Phys. et Rad. 22, 329 and 443 (1962).

21. J. Fricke, J. Haas, E. Lusher and F. H. Franz, Phys. Rev. 163, 45 (1967).

22. M. A. Bouchiat, Thesis, Paris 1964; Publications Scientifiques et Techniques du Ministere de Paris, N.T. 146, 1965.

23. P. Davidovits and R. Novick; Proc. IEEE, 54, 155 (1966).

24. M. Arditi and T. R. Carver; Phys. Rev. 124, 800 (1961).

25. W. Happer and B. S. Mathur; Phys. Rev. 163, 12 (1967).

26. B. S. Mathus, H. Tang and W. Happer; Phys. Rev. 171, 11, (1968).

27. Gurbax Singh, P. DiLavore, C. O. Alley; J. Quantum Electronics, QE-7,#5,p.196,(1971).

28. Carroll O. Alley, Advances in Quantum Electronics, Edited by J. R. Singer, (1961). p. 120.

29. F. A. Franz and J. R. Franz, Phys. Rev. 148, 82, (1966).

30. W. Franzen, 13th Annual Frequency Control Symposium, May (1959). p. 683.

31. M. A. Bouchiat and J. Brossel, Phys. Rev. 147, 41, (1966).

32. R. G. Brewer, J. Chem. Phys. 38, 3015, 2037, (1963).

33. M. Arditi, 15th Annual Frequency Control Symposium, 31, May (1961), p. 181.

34. F. J. Adrian, J. Chem. Phys. 32, 972, (1960).

35. H. M. Goldenberg, D. Kleppner, and N. F. Ramsey, Phys. Rev., 123, 530 (1961), 126, 603, (1962).

36. H. Margenau, P. Fontana and L. Klein, Phys. Rev., 115, 87 (1959).

37. R. Herman and H. Margenau, Phys. Rev., 122 ,1204, (1961).

38. Robert A. Bernheim: J. Chem. Phys., 36, 135 (1962).

39. N. W. Garrett, J. Appl. Phys. 22, p. 1091, 1951.

40. W. Franzen, Phys. Rev. 33, p. 933, 1962.

41. R. J. Hanson and Francis M. Pipkin, Rev. Sci. Inst. 36, p. 179, 1965.

42. Hai-men Lo, M. S. Thesis, 1967, Physics Dept., University of Maryland.

43. W. E. Bell, A. L. Bloom, and J. Lynch, Rev. Sci. Instr. 32, 688 (1961).

44. Gurbax Singh, P. DiLavore, Rev. Sci. Instr. 41 1516 (1970).

45. R. G. Brewer, J. Chem. Phys. 38, 3015, 2037, (1963).

46. M. A. Bouchiat and J. Brossel, Phys. Rev. 147, 41, (1966).

47. This information has been supplied by the manufacturer: Moore & Munger, Inc., 777 Summer Street, Stamford, Conn. 06902.

48. H. G. Dehmelt, Phys. Rev. 105, 1487 (1957).

REPRINTS

Reprinted from:
THE REVIEW OF SCIENTIFIC INSTRUMENTS VOLUME 43, NUMBER 9 SEPTEMBER 1972

A Technique for Preparing Wall Coated Cesium Vapor Cells*

GURBAX SINGH,† PHILIP DILAVORE,‡ AND CARROLL O. ALLEY
Physics Department, University of Maryland, College Park, Maryland 20742
(Received 8 June 1972)

A convenient technique for the preparation of reproducible cesium vapor cells, coated with a thin transparent layer of Paraflint, is described. Cells of 7.5 cm diam showed relaxation times of about 250 msec.

In many radio optical resonance experiments[1] one wishes to put the sample atoms into a particular quantum state and to keep them in that state as long as possible. In evacuated, untreated sample cells, the principal mechanism for relaxation of the sample atoms into unwanted quantum states is in the interaction which occurs when these atoms collide with the cell walls. To prolong the average relaxation time, the sample cell is treated in one

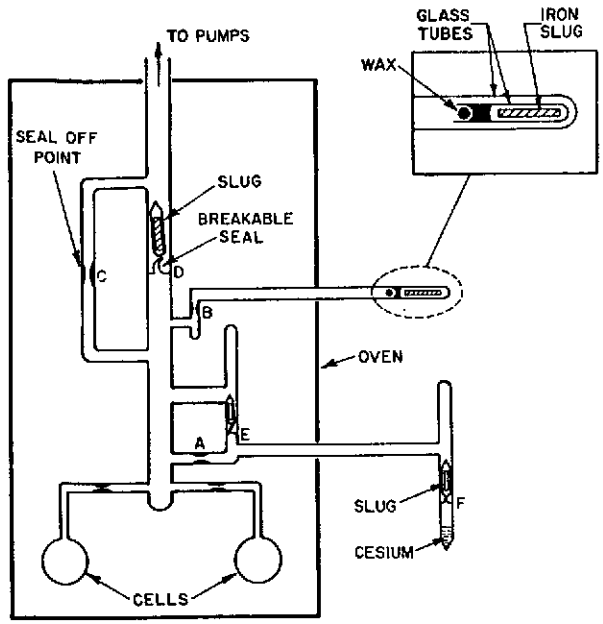

FIG. 1. Arrangement for making Paraffint coated cesium vapor cells.

or both of two ways: It is filled with a buffer gas so that the average atom is many mean free paths away from the cell wall, or the cell wall itself is coated with a material with which the sample atoms can make nonrelaxing collisions. The combination of the two methods can increase the average relaxation time by several orders of magnitude. For alkali metal vapor cells it is common to use the inert gases as buffers and rubidium vapor cells are frequently coated with Paraffint.

Most of the previous work with wall coated alkali vapor cells has been with rubidium; very little has been done with cesium. In addition, previous reports on coated cells have been incomplete in detail and the reproducibility of such coatings is very much open to question. In this paper we give, in sufficient detail for the procedure to be duplicated, a description of a simple method for preparing cesium vapor cells whose interior walls are coated with Paraffint. Following this method carefully, one can produce cesium cells with very long relaxation times of over 250 msec.

Paraffint RG (regular grade),[2] which was used as the coating material for our sample cells, contains volatile components which have a relatively high vapor pressure at room temperature. By performing fractional distillation under vacuum upon the wax (Paraffint), we discovered that the fraction collected in the temperature range 350–375°C had the desired attributes, including a vapor pressure of less than 10^{-6} Torr at 120°C.

A bakable vacuum system was constructed as shown schematically in Fig. 1. It had a number of seal-off points and breakable seals such that the wax and the cesium could be isolated from the main system and introduced, in turn, at the appropriate times. The main portion of the vacuum system could be enclosed in a removable electric oven. The glass components were well cleaned, first with soap and water, followed by several rinses with a 2% solution of hydrofluoric acid, then several rinses with distilled water.

With both the Paraffint and the cesium outside the oven, the system was baked for several hours at 450°C to outgas the glass. Then the system was cooled, the oven removed. The final pressure was about 10^{-8} Torr. The seal-off point at A was closed to prevent wax from getting into the arm containing the cesium. The wax was then moved, by means of a magnet pulling an iron slug encased in glass, to point B, and was melted down into the cup below B by gently heating it with a heating tape. Then the seals at points B and C were closed to isolate the system, which was baked at about 365°C. We discovered that an unavoidable slight temperature gradient, due to the vertical arrangement of the system, was actually helpful in driving the wax into the cells, which were located at the cooler, lower section of the oven. However, the gradient from bottom to top should not be more than a degree or two.

After about two hours of baking, the system was cooled slowly and the breakable seal at D was opened. Using a relatively "cool" gas–air flame, the wax was driven off from the glass through which cesium was to come, including the stems of the cells. It is essential that this be done well, for hot cesium and wax combine chemically into a material which forever fouls up the vacuum system. The seals at E and F were opened and a small amount of cesium was driven, by means of the same "cool" flame, into the stems of the cells. The system was then allowed to pump for a length sufficient to remove any volatile substance possibly produced by breakdown of the wax. The cells were sealed and pulled off the system.

Cesium vapor cells prepared in this manner showed thin, transparent coatings of wax and were highly reproducible. Cells of different diameters and those made at different times had about equal relaxation times when normalized to a unit diameter. The major variation in relaxation times was produced by varying the size of the opening to the cell stem, which acts as a sink for optically pumped atoms. At room temperature in 7.5 cm diam cells, the observed relaxation times were about 250 msec.

* Work supported in part by NASA, under Grants Nos. NGR 21-002-218 and 21-002-022, NSF Grant No. GY-9464, ARPA Contract No. SD-101, and the U. S. Army Research Office, under Contract No. DAHCO 4-67-C-0023.

† Present address, University of Maryland, Eastern Shore, Princess Anne, Md. 21853.

‡ Present address, Indiana State University, Terre Haute, Ind. 47809.

[1] Gurbax Singh, P. Dilavore, and C. O. Alley, IEEE J. Quant. Electron. QE-7, No. 5, 196 (1971).

[2] Paraffint is manufactured by Moore and Munger, Inc., 777 Summer Set St., Stanford, Conn. 06902, and is a mixture of saturated straight chain hydrocarbons with an average molecular weight of about 750 and 50–55 carbon atoms per molecule.

Reprinted by permission from
IEEE JOURNAL OF QUANTUM ELECTRONICS
Vol. QE-7, No. 5, May 1971

GaAs-Laser-Induced Population Inversion in the Ground-State Hyperfine Levels of Cs^{133}

GURBAX SINGH, P. DiLAVORE, AND C. O. ALLEY

Abstract—**This paper describes the achievement of population inversion among the hyperfine levels in the ground state of Cs^{133} by optically pumping these atoms with radiation from a GaAs diode laser. The laser output was used to monitor the populations in the two ground-state hyperfine levels as well as to perform the hyperfine pumping.**

By varying the injection current, a GaAs laser operated CW at about 77°K, was used to scan the 8521-Å line of Cs^{133}. The intensity of the resonance scattering from cesium vapor served as an indicator of the populations of the two levels involved. Experiments were performed both with neon-filled and with paraffint-coated cells containing the cesium vapor.

It was discovered that the diode laser could easily be tuned by manually adjusting the injection current to match either of the hyperfine components of the D_2 optical transition.

Possible future applications, including a restudy of the light shifts, the construction of a cesium maser, and the physics of optical pumping with coherent light are discussed.

Introduction

ONE circumstance that has made possible the operation of rubidium masers is that one of the hyperfine optical transitions of Rb^{87} happens to be nearly coincident with one of Rb^{85}. Thus, the atoms of the one isotope may serve as a hyperfine filter for atoms of the other and it is possible to pump selectively the hyperfine levels of the desired isotope [1]–[3].

In the case of cesium, no such happy coincidence exists in a convenient source, and a cesium maser is yet to be produced. However, since atomic frequency standards, which operate upon a beam of cesium atoms, are capable of a high degree of stability and reproducibility and constitute the present international frequency standard, it would seem highly desirable to operate a cesium maser. In fact, it should now be a matter of the simple optical pumping of cesium vapor contained in a suitably tuned cavity using methods we shall describe here. We have been able to produce population inversions in the hyperfine states of Cs^{133} by using (as pumping radiation) light from a gallium arsenide diode laser operated continuously at about liquid nitrogen temperature. This method holds promise for the development of miniaturized portable and durable frequency standards. The recent achievement of room temperature CW operation of GaAs injection lasers is of particular significance in this connection [4].

The results of this investigation could equally well be applied to operate rubidium masers, pending the development of a suitable diode laser to match the rubidium transition. (This laser would probably be one made of gallium aluminum arsenide.)

Experimental Arrangement

It has only recently been possible to obtain diode lasers that would operate CW. Moreover, GaAs lasers generally emit radiation at roughly 8500 Å when operated at liquid nitrogen temperatures. In order to match the 8521-Å line of Cs^{133}, the laser must be operated at a somewhat higher temperature. We accomplished this by clamping the laser to a copper rod that is thermally connected to a liquid nitrogen reservoir. The thermal resistance of this arrangement is such that it is easy to adjust the temperature, and thus the emitted wavelength, by adjusting the injection current. This can be done with sufficient stability so that the laser can be easily tuned to match the optical transitions $6S_{1/2}$ ($F = 3$ and $F = 4$) to $6P_{3/2}$ (Fig. 1). A simple experimental arrangement for observing the resultant resonance scattering is shown schematically in Fig. 2.

Before the laser was used to produce resonance radiation for a cesium cell, its radiation was examined by means of a Spex Industries model 1400 monochromator. A typical spectrum is shown in Fig. 3. It was found that the strong mode close to 8521 Å had power in excess of 10 mW and could be tuned over a range of a few angstroms by varying the injection current. In order to observe the scattered resonance radiation at 8521 Å from Cs^{133} atoms, the injection current was varied by superposing a slowly varying triangular current pulse on a dc current. Scanning of the 8521-Å line by superposing a fast square pulse on a dc current has been reported [5].

Observations

Fig. 4 shows the resonance radiation scattered at an angle of 90° to the incoming radiation as the laser radiation was swept in frequency decreasing from left to right. The sample was cesium vapor contained in a glass cell of about 2 in diameter, which also contained neon at a pressure of 100 torr as a buffer gas. The transitions involved were $6P_{3/2}$ to $6S_{1/2}$ ($F = 3$ and $F = 4$). These lines were observed as the injection current was increasing. This means that the temperature of the junction was also increasing [6], and that the band gap of the semiconductor

Manuscript received November 30, 1970. This work was supported in part by NASA Grants NGR 21-002-218 and 21-002-022, ARPA Contract SD-101, and the U. S. Army Research Office Contract DAHCO 4-67-C-0023.

G. Singh is with the University of Maryland, Eastern Shore, Princess Anne, Md. 21853.

P. DiLavore and C. O. Alley are with the Department of Physics and Astronomy, University of Maryland, College Park, Md. 20742.

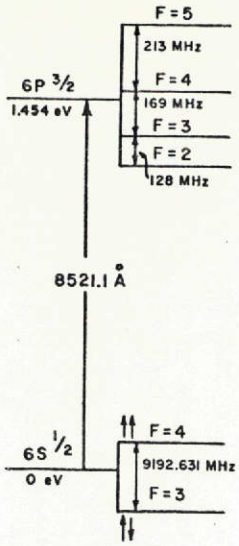

Fig. 1. Relevant energy levels of Cs^{133} ($I = 7/2$).

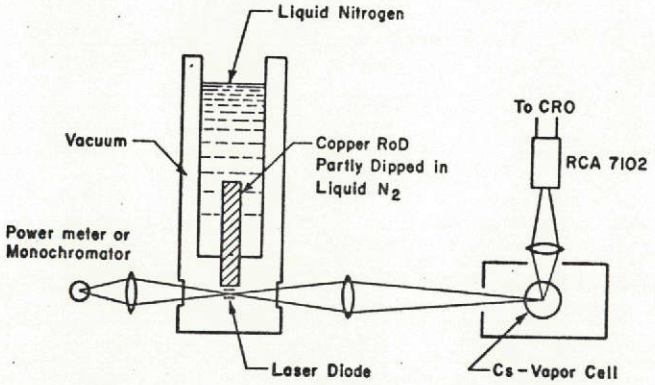

Fig. 2. Block diagram of the experimental arrangement to observe resonance scattering from Cs^{133} vapor cells.

material was decreasing [7]. In other words, the picture was taken during a time of increasing wavelength of the laser radiation. Therefore, the first peak on the left corresponds to the transition ending in the $F = 3$ state, and the second one to the transition ending in the $F = 4$ state. Since the separation of these two transitions is 9192 MHz, and the oscilloscope time base is 50 ms/cm, the laser radiation is sweeping at about 18 GHz/cm in this trial.

The excited-state hyperfine levels are unresolved because the Doppler- and pressure-broadened linewidths are greater than the hyperfine separations. Using the known separation of the two observed peaks, and assuming a linear sweep, the measured linewidth of each of the two lines is approximately 1300 MHz.

The unequal amplitudes of the two peaks would be expected to result from two effects. First, and mainly, the degeneracy of the $F = 3$ level is 7 and that of the $F = 4$ level is 9, so that the strengths of the two lines are in the ratio 7:9. Second, the power output of the laser varies slightly with increasing current. However, an examination of Fig. 4 shows that the ratio of amplitudes is not 7:9 but closer to 1:2. The clue to the reason for this is shown in Fig. 5, in which the left two resonances correspond to

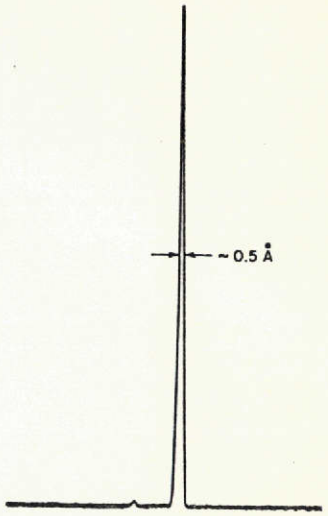

Fig. 3. Mode structure of the GaAs laser used in this investigation (observed mode width is instrument limited).

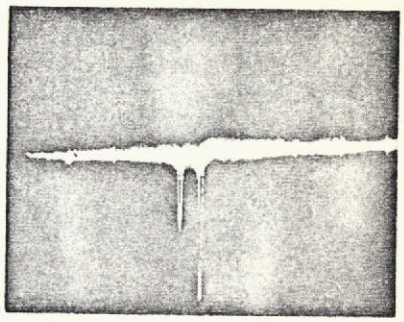

Fig. 4. Resonance radiation scattered by Cs^{133} cell filled with 100 torr of neon. Time scale: 50 ms/cm. Vertical scale: arbitrary.

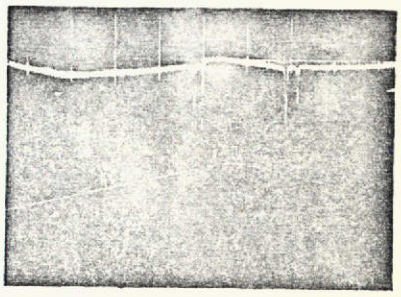

Fig. 5. Resonance radiation scattered by the same cell as in Fig. 4, but at a slower laser sweep rate. The lower trace shows the injection current. Time scale: 200 ms/cm. Vertical scale: arbitrary.

increasing current (and hence increasing wavelength) from left to right and the right two correspond to decreasing current (triangular sweep).

In this case, the ratio of the peak heights for each pair has fallen closer to 7:9. The only difference in these two cases is that, in Fig. 4, the sweep rate is such that the time required to pass from one resonance line to the other is about 25 ms, and in Fig. 5 it is about 40 ms. This indicates that a substantial number of atoms are being pumped into the $F = 4$ level and that the hyperfine relaxation time is long enough so that there is still greater than an equilibrium population in the $F = 4$ state when the laser radiation sweeps through that line 25 ms later but near to

equilibriun population 40 ms later. In the cesium cell being examined, the spin relaxation time was measured (by methods reported in [1]) to be about 18 ms. In the case of atoms for which the hyperfine relaxation time [8], [9] can be measured, for example Rb^{87}, the spin relaxation time and the hyperfine relaxation time are roughly the same at room temperature, so one might reasonably expect the hyperfine relaxation time for cesium in this cell to be close to 18 ms.

Additional evidence in support of the hypothesis of hyperfine pumping is provided by the experiment displayed in Fig. 6. Here the sample cell has been replaced by one with paraflint-coated walls, in which the cesium atoms have a spin relaxation time of about 200 ms. It can be seen in this case that the ratio of the amplitudes of the peaks of the pair on the ascending sweep is different from the ratio on the descending sweep: on the ascending sweep there is pumping of the atoms from the lower hyperfine level into the upper hyperfine level where they can exist for times longer than the sweep time for the pair. On the descending sweep the process is reversed, so that the relative amplitudes are greatly changed. The above-mentioned observations with the buffered and coated cells were consistently repeatable (except for minor variations corresponding to the variations of the laser output) from sweep to sweep and on interchanging the cells back and forth.

It was also encouraging to note that the laser mode could be held for a few seconds on either of the absorption lines by manually controlling the injection current, indicating that automatic locking should be easily possible.

Conclusions

It should now be relatively easy to make a cesium maser. The power available in a single mode from a GaAs laser is considerably in excess of what is required to operate an alkali maser. Since small apertures will suffice to let the resonance radiation from diode lasers into the cavity, it should be easily possible to make a cavity with a high Q value. CW operation of a maser may then be achieved by locking the laser mode to the center of the shorter wavelength hyperfine absorption line.

One also could make a miniaturized cell-type frequency standard by utilizing the selective hyperfine pumping of cesium vapor. With the foreseeable development of appropriate semiconductor lasers, it also should be possible to make a similar rubidium maser and frequency standard.

It will be most interesting to examine experimentally the results of using coherent radiation from lasers in optical pumping experiments. For one thing, it should now be possible to measure the hyperfine relaxation time of cesium atoms. Perhaps even more interesting will be an examination of the effects of using a coherent light source; if coherent radiation is used to perform optical pumping, the behavior of the atomic electric dipoles should be similar to that of magnetic dipoles subjected to a radio-frequency field. A restudy of the light shifts of the ground-state levels of alkali vapors will be worthwhile. One could, for example, study the behavior of the light shifts as the laser line is swept through the Doppler-broadened absorption lines. Nonlinear interactions between microwave and optical transitions exhibited in the light shifts may be useful in relating these regions of the electromagnetic spectrum. It should also soon be possible to eliminate errors due to the light shifts of atomic frequency standards by locking the laser line to the center of the hyperfine absorption line.

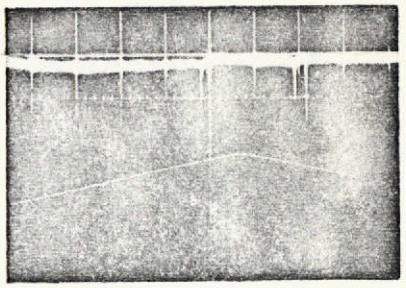

Fig. 6. Resonance radiation scattered by the wall-coated cell without any buffer gas. Time scale: 200 ms/cm. Vertical scale: arbitrary.

Acknowledgment

The authors wish to express sincere thanks to Dr. W. Culver and C. C. Packard of IBM Federal Systems Division, who graciously loaned the GaAs lasers that made this work possible, to K. Cole and R. Ace of the Department of Chemistry, University of Maryland, College Park, who helped to perform the spectral analysis of the laser radiation, and to Dr. H. F. Quinn of the IBM Federal Systems Division, who loaned the diode lasers in the early phases of this experiment. The authors also acknowledge helpful discussions during the early phases of this work with Prof. U. Hochuli of the Department of Electrical Engineering, University of Maryland.

References

[1] C. O. Alley, "Investigations of the effect of gas collisions and optical pumping on the breadth of spectral lines," Princeton University, Princeton, N. J., Contract DA-36-039 SC-70147, Fin. Rep., Sept. 30, 1960.
[2] P. L. Bender, "Atomic frequency standards and clocks," in *Quantum Electronics*, C. H. Townes, Ed. New York: Columbia University Press, 1960, pp. 110–120.
[3] P. Davidovits and R. Novick, "Optically pumped rubidium maser," *Proc. IEEE*, vol. 54, Feb. 1966, pp. 155–170.
[4] I. Hayashi, M. B. Panish, P. W. Foy, and S. Sumski, "Junction lasers which operate continuously at room temperature," *Appl. Phys. Lett.*, vol. 17, Aug. 1, 1970, pp. 109–111.
[5] S. Siahatgar and U. E. Hochuli, "Display of 8521-Å line of cesium utilizing a swept GaAs laser," *IEEE J. Quantum Electron.*, vol. QE-5, June 1969, pp. 295–297.
[6] Wataru Susaki, "Current dependence of junction temperature in C-W operated GaAs laser diodes," *Japan. J. Appl. Phys.*, vol. 6, 1967, pp. 977–981.
[7] H. Yonezu, A. Kawaji, and Y. Yasuoka, "Lasing wavelength of a GaAs injection laser," *Solid-State Electron.*, vol. 2, 1968, pp. 129–134.
[8] M. Arditi and T. R. Carver, "Hyperfine relaxation of optically pumped Rb^{87} atoms in buffer gases," *Phys. Rev.*, vol. 136, 1964, pp. 643–649.
[9] M. A. Bouchiat and J. Brossel, "Relaxation of optically pumped rubidium atoms on paraffin-coated walls," *Phys. Rev.*, vol. 147, 1966, pp. 41–54.

Reprinted from THE REVIEW OF SCIENTIFIC INSTRUMENTS, Vol. 41, No. 10, 1516–1517, October 1970
Printed in U. S. A.

A Pulsed Cesium Spectral Lamp for Optical Pumping Studies*

GURBAX SINGH AND PHILIP DILAVORE

Department of Physics and Astronomy, University of Maryland, College Park, Maryland 20742

(Received 8 May 1970)

ONE can think of a number of optical pumping experiments in which it is desirable to have a spectral lamp which can be accurately switched on and off. We are presently performing such an experiment to study hyperfine transitions in alkali atoms, investigating wall and light shifts of the ground states of these atoms by means of a triple-resonance coherent pulse technique.

For this technique,[1] in which the sample atoms are pumped optically into the highest angular momentum ground state $|F,F>$, it is necessary to switch off the lamp for a time interval during which coherent rotating magnetic field pulses at the Zeeman resonance and microwave pulses at hyperfine resonance are applied to alter the angular momentum state of the atoms. The lamp is then switched on to monitor the remnants of the $|F,F>$ state. The time duration for which it is necessary to have the lamp off may vary from a few milliseconds to over 1 sec, depending upon the relaxation times of the pumped states.

An example of another application of a switchable spectral lamp is an experimental study of the relaxation times of optically polarized atoms in the dark. For such experiments, it is desirable to have a lamp whose switching characteristics are stable and reproducible, with a short switching time and negligible jitter. One might also be concerned with other features like the compactness of the exciting circuit, a high yield of usable radiation, etc.

It is possible, of course, to use mechanical shutters, rotating choppers, or electro-optic devices, but these have one or more of the disadvantages of slow speed, small useful aperture, or high cost. In trying to switch on a conventional lamp, one is hindered by the familiar fact that the discharge begins in an unpredictable way some time after the application of the rf power.

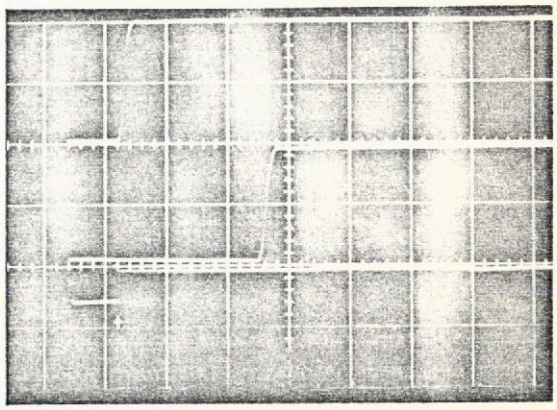

FIG. 2. The bottom trace shows the switching pulse which, at its rising edge (arrow), turns on the primary oscillator. The other two traces show the light output from the switched portion of the lamp. With the secondary discharge off the middle trace results, and with it on the upper trace. The time scale is 1 msec/div.

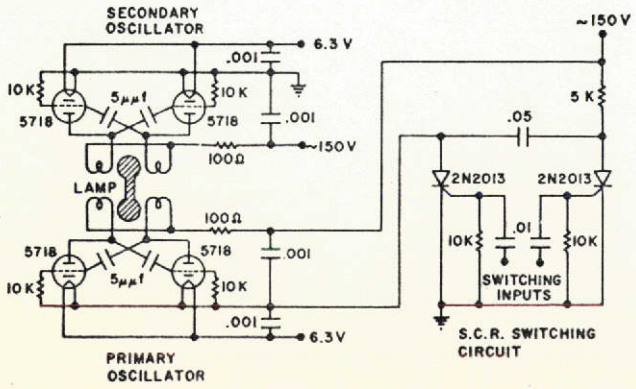

FIG. 1. Schematic of the two identical exciter oscillators, one of which is switched by the SCR circuit.

The lamp we are herein describing is a modification of the electrodeless alkali lamp described by Bell, Bloom, and Lynch[2] (BBL). This modification can easily be applied to the lamp described by Brewer[3] and by Franz,[4] if higher intensity is desired, but the optical pumping signals obtained with the BBL lamp are large enough for most applications.

Our lamp has a dumbbell shape with two 1.2 cm diam

bulbs connected by a 2 cm length of 7 mm Pyrex tubing. The whole thing is blown from a single Pyrex tube and the dimensions are not critical. The lamp is filled with a few milligrams of pure cesium metal distilled in a vacuum of better than 10^{-7} Torr, and is then filled with a few torricelli of xenon gas at room temperature. (Of the inert gases, xenon gives the best results.[4]) Each bulb of the lamp is independently excited by means of an oscillator of the BBL design which combines low noise and compactness. The lamp and both oscillators fit into a 10×5×5 cm aluminum chassis.

In operation, a discharge is maintained continuously in one bulb, while the power supply to the other oscillator is switched by means of an SCR switch. A circuit diagram is shown in Fig. 1. As is shown in Fig. 2, the switching characteristics of the lamp are clean and reproducible. Also, the formerly present time lag no longer exists. Since the switching is done by electrical pulses, the problem of synchronizing the lamp switching with the rest of the apparatus becomes very much simpler. The light output is identical to that of the BBL lamp.

We gratefully acknowledge Carroll O. Alley for his original suggestion for the experiment and his continued support. We also thank Douglas G. Currie for his helpful suggestion for the design of this lamp.

* It is part of a continuing work supported by NASA (Grants NGR 21-002-218, NAS 9-7809, and NGR 21-002-022), ARPA (Contract SD-101), and the U. S. Army Research Office Contract DAHCO 4-67-C-0023.

[1] C. O. Alley, in *Quantum Electronics*, edited by C. H. Townes (Columbia U. P., New York, 1960), pp. 146–155.
[2] W. E. Bell, A. L. Bloom, and J. Lynch, Rev. Sci. Instrum. **32**, 688 (1961).
[3] R. G. Brewer, Rev. Sci. Instrum. **32**, 1356 (1961).
[4] F. A. Franz, Rev. Sci. Instrum. **34**, 589 (1963).